The effect of middle ear pressure on the pressure regulating mechanisms of the inner ear

Robert Feijen

Rijksuniversiteit Groningen

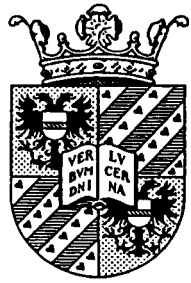

The effect of middle ear pressure on the pressure regulating mechanisms of the inner ear

Proefschrift

ter verkrijging van het doctoraat in de
Medische Wetenschappen
aan de Rijksuniversiteit Groningen
op gezag van de
Rector Magnificus, dr. F. Zwarts,
in het openbaar te verdedigen op
woensdag 7 september 2005
om 14:45 uur

door

Roelof André Feijen
geboren op 2 oktober 1971
te Coevorden

Promotores: Prof. dr. F.W.J. Albers
Prof. dr. ir. H.P. Wit

Beoordelingscommissie: Prof. dr. P. van Dijk
Prof. dr. A.C. Kooijman
Prof. dr. ir. G.J. Verkerke

Acknowledgments

This study is part of the research program of our department: Communication through Hearing and Speech. The program is incorporated in the Sensory Systems Group of the Groningen Graduate School for Behavioural and Cognitive Neurosciences (BCN).

Financial support was provided by:
Abbott b.v., Veenhuis Medical Audio b.v., Oticon Nederland b.v., Stichting Atze Spoor Fonds, Professor Eelco Huizinga Stichting, Carl Zeiss b.v., Electro Medical Instruments b.v. Doesburg (EmiD), Schering-Plough b.v., GlaxoSmithKline b.v., Schoonenberg Hoorcomfort, Medtronic Xomed Benelux, GN ReSound

Print: Ponsen & Looijen b.v., Wageningen
ISBN: 9064643636

Voor Esther en Casper

Contents

Chapter 1

General introduction

Introduction

The development of the *Meniett*™ (figure 1), a small pressure device for therapeutic use in Menière's disease, was in 1999 the reason for the start of the research described in this thesis. In the first section of this introduction a brief overview is given of the characteristics of Menière's disease, pressure therapy in general and the development of the *Meniett*™ in particular. In the second section specific information is given towards inner ear pressure measurements in guinea pigs and towards the anatomic structures of interest. The objectives of the individual studies are subsequently summarized in brief.

figure 1. The Meniett™ (Medtronic Xomed, Inc.; USA). A flexible tube is attached to the device for use in the ear.

Menière's disease and pressure therapy

In 1861 Prosper Menière presented a paper in which he attributed the symptoms of episodic vertigo, hearing loss and tinnitus to a disease of the semicircular canals (Menière 1861). Hallpike and Cairns in 1938 described a distension of the endolymphatic compartment (figure 2 and figure 3) in a postmortem temporal bone study in Menière's disease.

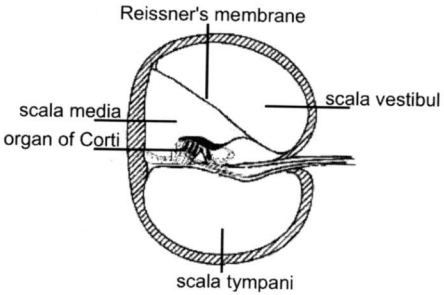

Figure 2. Cross section through the cochlea. Scala vestibuli and scala tympani are filled with perilymph. Scala media is filled with endolymph. In endolymphatic hydrops Reissner's membrane becomes distended and the volume of the scala media increases at the expense of the perilymphatic spaces.

This so-called endolymphatic hydrops was also found in later studies (Rauch et al. 1989, Paparella 1991, Sperling et al. 1993, Okuno and Sando 1987) and it is often associated with raised endolymphatic pressure. However, endolymphatic hydrops can be regarded as an epiphenomenon of Menière's disease since hydrops is also found in temporal bones of subjects who did not show the typical Menière symptoms (Rauch et al. 1989, Merchant et al. 2005).

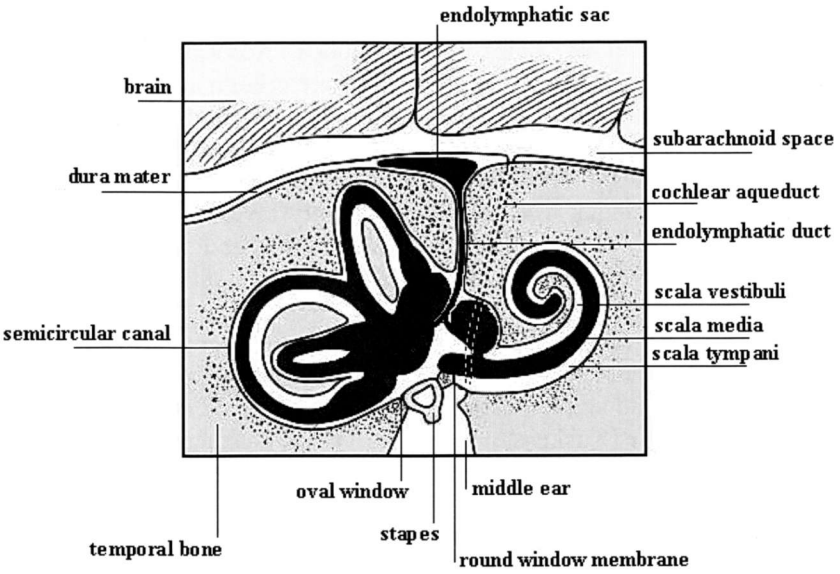

Figure 3. Schematic representation of the labyrinth (modified figure of Baloh RW: The essentials of Neurotology 1984). The endolymphatic compartment (black) is surrounded by perilymph (white). The guinea pig inner ear contains approximately 2 µl of endolymph and 2 ml of perilymph. The cochlear aqueduct (broken lines) ends in the vicinity of the round window membrane in scala tympani.

The cause of the hydrops is unknown. Endolymphatic hydrops can be experimentally induced by obliterating the endolymphatic duct and sac of guinea pigs (Kimura and Schuknecht 1965) and it is thought that hydrops will develop secondary to an imbalance of secretion and absorption of endolymph (Dunnebier et al. 1997).

The prevalence of Menière's disease differs between countries and is estimated between 1 - 100 per 100.000 (Oosterveld 1981, Merchant et al. 1995). The peak

incidence is in the 40 to 60-year age group and a slight female to male preponderance (1.3:1) has been reported (Minor et al. 2004). Menière's attacks are often unpredictable and incapacitating, and may prevent the activities of daily living. The frequency between attacks classically increases over years and approximately after five to ten years vertigo attacks will be absent and sensorineural hearing is seriously damaged (Friberg et al. 1984). In about 30-40% the disease is or will be present in both ears.

Menière's disease is not always easy to diagnose. The American Academy of Otolaryngology - Head and Neck Surgery (AAO-HNS) has determined diagnostic guidelines (Committee 1995). Based on these guidelines the Diagnostic Protocol Groningen (Mateijsen et al. 2002) was developed. According to this protocol Menière's disease is diagnosed if the following three criteria are fulfilled: cochlear hearing loss of at least 20 dB at one of the pure-tone audiogram frequencies, tinnitus and periodic attacks of vertigo (at least two in the past, with a duration of more than 20 minutes). The diagnostic protocol consists of routine ENT examination, audiovestibular tests, routine laboratory investigations, measurement of blood pressure, oto-acoustic emission examination and magnetic resonance imaging (MRI) of the temporal bones and the cerebellopontine angle. With this protocol other pathologies can be ruled out.

Ideally treatment must reduce the number and severity of acute attacks of vertigo, have a positive influence on hearing and prevent progression of the disease. However, up till now no single treatment modality for Menière's disease has been shown to achieve a cure (Ruckenstein et al. 1991). The fluctuating, progressive and unpredictable nature of Menière's disease makes investigation of any treatment effect difficult.

In 1975 Densert et al. used a pressure chamber for the treatment of Menière's disease. They varied the ambient pressure between –100 to 100 cm water and hypothesized that the temporary positive effect on sensorineural hearing was due to a decongesting effect on venous vessels obstructing the endolymphatic duct. After that many positive reports appeared on the subject of hypobaric pressure therapy (Ingelstedt et al. 1976, Tjernstrom 1977, Tjernstrom et al. 1979, Tjernstrom et al. 1980, Younger et al. 1984, Van Deelen and Huizing 1987, Densert 1987, Larsen et al. 1988) which leads, with an intact tympanic membrane, to a relative middle ear overpressure and relief of symptoms.

In parallel to this Krukowski et al. (Krukowski et al.1980) reported experiments in cats in which a mean positive transient perilymphatic pressure shift is found during the application of a low-frequency sinusoidally varying pressure to the ear canal. A few years later Densert et al. (Densert et al.1986) applied complex pressure waves, being the sum of low-frequency pressure waves and a square wave, to the middle ear of cats while simultaneously measuring perilymphatic pressure. Based on their findings and on the results of Carlborg et al. (Carlborg et al. 1982) they suggested that by applying these complex waves the functional patency of the cochlear

aqueduct is influenced and that endolymph instead of perilymph is pressed out of the inner ear.
Subsequently Densert et al. (Densert et al. 1997) presented an interesting clinical study with promising results: after applying multiple complex positive pressure pulses via a transtympanal tube to the middle ear of patients with Menière's disease improvement of possible pathological electrocochleographic parameters was observed. They suggest that an increase in inner ear fluid transport or a change in vascularization of the hydropic inner ear might positively influence endolymphatic hydrops (Densert et al. 1995, Densert et al. 1997). This resulted in the development and production of a small manageable therapeutic pressure device (*Meniett*™; Medtronic Xomed, Inc.; USA), for use by patients with Menière's disease.

Inner ear pressure measurements
A thorough understanding of the hydrodynamic inner ear system can help in understanding the functional properties of the inner ear and its adjacent structures. Inner ear pressure in guinea pigs can be measured with a "servo nulling" micropressure system (Wiederhielm et al. 1964). With this method there is no apparent volume displacement, little damage to vital structures due to the fine tip of the micropipette (± 10 μm) and it is possible to measure electrical potentials (Takeuchi et al. 1990). After opening of the middle ear cavity a bevelled micropipette filled with 2 M NaCl is introduced through the round window membrane into the scala tympani and perilymphatic pressure can be measured with a WPI 900A micropressure system (World Precision Instruments Inc., USA). By inserting the pipette further through the basilar membrane into the scala media inner ear pressure and endocochlear potential can be measured simultaneously.
The inner ear pressure transfer properties are a consequence of the compliance of the inner ear structures (mainly the round window membrane) and the flow conducting properties of the cochlear aqueduct.
In man the compliance of the round window is 5 times that of the oval window (Ivarsson and Pedersen, 1977) and contributes most to the inner ear compliance. The area of the guinea pig round window membrane is 1.2 mm^2 and it separates the middle ear cavity (air) from the scala tympani (perilymph). It has a slight parabolic shape (Ghiz et al. 2001).
The cochlear aqueduct connects scala tympani (containing perilymph) with the subarachnoid space (containing cerebrospinal fluid). Its internal orifice is situated very close to the round window membrane. In 1958 Svane-Knudsen reported that the guinea pig aqueduct is filled with a very loose network of connective tissue, containing small thin-walled vessels. This tissue gradually grows more dense towards the scala tympani opening of the aqueduct and it continues into the connective tissue core of the round window membrane. Also Duckert (1974) describes the aqueduct in guinea pig being filled with a loose connective meshwork, composed of reticular cells and collagen and elastic fibrils. Toriya et al.

(1991a,b) found (using scanning electron microscopy) that the fibroblasts of the connective tissue trabeculae were more compact at the perilymphatic space than in the rest of the duct. In the guinea pig it has a length of approximately 2 mm and its cross-sectional area increases from 0.016 mm^2 at the side of scala tympani to more than 0.20 mm^2 where it joins the subarachnoid space (Ghiz et al. 2001). The smallest diameter of the duct is 0.14 mm. It is generally assumed that the cochlear aqueduct has a function in equalizing inner ear pressure and it is functionally open in guinea pigs (Andrews et al. 1991, Suzuki et al. 1994b) as well as in humans (Gopen et al. 1997).

Objectives

Chapter 2

The aim of the study in this chapter is to measure and describe inner ear pressure changes in normal guinea pig inner ears during application of complex pressure waves to the middle ear produced by the *Meniett*™. A simple model of pressure transfer between the middle and inner ear is introduced.

Chapter 3

The model presented in chapter 2 seems too simple and the complex pressure waves are too complex for an easy interpretation and understanding of the hydrodynamic inner ear system. In this chapter experiments in guinea pigs are described, in which inner ear pressure changes are induced by rectangular middle ear pressure changes. The results are described using a linear physical model.

Chapter 4

The results of the pressure release properties of the guinea pig inner ear in chapter 3 yielded more complicated shapes for inner ear pressure release curves, which is a consequence of the flow conducting properties of the aqueduct and of the compliance of the windows. In order to derive these properties, representative results from two guinea pig ears are selected for further analysis.

Chapter 5

In chapter 5 pressure experiments in guinea pigs are conducted to verify the relation between round window position and aqueduct resistance by keeping the pressure changes that induce fluid flow through the cochlear aqueduct as small as possible. In this way flow resistance can be measured at different constant values of inner ear volume. Because the resistance is measured both for flow in the direction of the cerebrospinal fluid space and for the returning flow, the influence of flow direction on resistance can be determined.

Chapter 6
In chapter 6 experiments are designed to investigate the influence of middle ear pressure on the transfer of periodic CSF pressure fluctuations to the inner ear in more detail. For this purpose middle ear pressure is changed very slowly, in order to allow for equilibration of static inner ear and CSF fluid pressure. In this way the position of the round window changes slowly. During this change CSF pressure is modulated with a small 0.33 Hz pressure signal and both inner ear and middle ear pressure are recorded.

Chapter 7
In a prospective double-blind, placebo-controlled study design the efficacy of intermittent middle ear pressure therapy for Menière's disease, given by the *Meniett*™, on hearing improvement and other clinically relevant parameters is measured.

Chapter 2

Monitoring inner ear pressure changes in normal guinea pigs induced by the *Meniett*™

authors R.A. Feijen
J.M. Segenhout
H.P. Wit
F.W.J. Albers

Acta Otolaryngol (Stockh) 2000; 120:804-809

Introduction

In 1861 Prosper Menière presented a paper in which he attributed the symptoms of episodic vertigo, hearing loss and tinnitus to a disease of the semicircular canals (Menière 1861). In a post mortem study in 1938 Hallpike and Cairns subsequently described endolymphatic hydrops in the temporal bones of patients with Menière's disease during life. This finding is in accordance with later studies (Rauch et al. 1989, Okuno and Sando 1987). Many hypotheses on the aetiology of Menière's disease are based on endolymphatic hydrops (Merchant et al. 1995), thereby often suggesting a disturbance of volume and pressure regulation properties of the inner ear (Claes and Van de Heyning 1997, Gibson and Arenberg 1997, Huang 1999). Subsequently, many therapies are built on this theorem, e.g.diuretics (Van Deelen and Huizing 1986,), salt restriction (Claes and Van de Heyning 1997), endolymphatic sac surgery (Huang 1999, Moffat 1997), endolymphatic fistula procedures and pressure (chamber) therapy (Konradsson et al. 1999). As the aetiology of, and the therapy for Menière's disease remain uncertain, studies of the inner ear and its pressure (transfer) properties are of great interest.

In 1980 Krukowski et al. reported experiments in which a mean positive transient perilymphatic pressure shift is found in cats during the application of a low-frequency sinusoidally varying pressure to the ear canal. A few years later Densert et al. (1986) applied complex pressure waves, being the sum of low-frequency pressure waves and a square wave, to the middle ear of cats while simultaneously measuring perilymphatic pressure. Based on their findings and on the results of Carlborg et al. (1982) they suggested that by applying these complex waves the functional patency of the cochlear aqueduct is influenced and that endolymph instead of perilymph is pressed out of the inner ear. Subsequently Densert et al. (1997) presented an interesting clinical study with promising results: after applying multiple complex positive pressure pulses via a transtympanal tube to the middle ear of patients with Menière's disease improvement of possible pathological electrocochleographic parameters was observed. They suggest that an increase in inner ear fluid transport or a change in vascularization of the hydropic inner ear might positively influence endolymphatic hydrops (Densert et al. 1995, Densert et al.1997). This resulted in the production of a small manageable therapeutic pressure device (*Meniett*™; Medtronic Xomed, Inc.; USA), for use by patients with Menière's disease.

For obvious reasons monitoring the inner ear pressure in humans is still impossible. Therefore the aim of the present study was to measure inner ear pressure changes in normal guinea pig inner ears during application of the *Meniett*™. Results are interpreted using a simple model of pressure transfer between the middle and inner ear.

Materials and methods

Experimental procedure

Female adult albino guinea pigs (Duncan Hartley; HSD Poc) weighing 400 -500 g were used in this study (n = 7). All animals had normal Preyer reflexes and did not show signs of middle ear infection. General anaesthesia was obtained with i.m. administration of ketamine hydrochloride (50 mg/ml) and xylazine (20 mg/ml) at a volume ratio of 2:1 and at a dose level of ≈ 1 ml/kg body weight. Complete muscle relaxation was obtained by i.m. administration of suxamethoniumchloride (5 mg/kg body weight). A screw was fixed upside down on the skull with dental cement after which fixation of the head was possible. The animals were artificially respirated and body temperature was kept between 37 and 38 °C with a heating pad. Heart rate was monitored by means of subcutaneous needle electrodes. A pressure generator was connected to the external meatus via flexible tubing (see figure 1) and ear canal pressure was monitored with an electronic pressure-measuring device (EMA 84; Erwin Halstrup Multur GmbH, Germany).

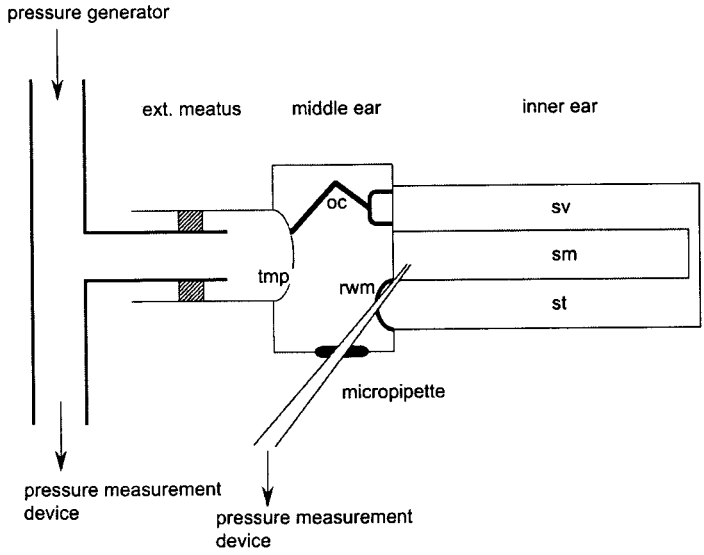

Figure 1. Experimental set-up. oc = ossicular chain; rwm = round window membrane; st = scala tympani; sm = scala media; sv = scala vestibuli; tmp = perforated tympanic membrane.

The middle ear cavity was reached through the bone of the otic bulla using a retroauricular approach. A small hole was cut in the tympanic membrane from the middle ear side without damaging other structures. With a micromanipulator a bevelled micropipette (tip diameter 10 µm) filled with 2 M NaCl was lowered in a

drop of saline onto the round window membrane to measure reference pressure with a "servo-nulling" (Wiederhielm et al. 1964) WPI 900A micropressure system (World Precision Instruments Inc., USA). Subsequently the micropipette was introduced through the round window membrane into the scala tympani, where perilymphatic pressure (PLP) was measured. As endolymphatic and perilymphatic pressure are equal in a normal guinea pig (Takeuchi et al. 1990, Warmerdam et al. 1999) the term "inner ear pressure" will henceforth be used to denote both perilymphatic and endolymphatic pressure. By inserting the pipette further through the basilar membrane into the scala media we could simultaneously measure inner ear pressure and endocochlear potential (Andrews et al. 1991). With the micropipette in situ the hole in the bulla was carefully closed with dental cement to mimic the situation in humans, where *Meniett*™ pressure pulses are applied to the closed middle ear cavity through a tympanic membrane ventilation tube (Densert et al.1997).
The *Meniett*™ generates 3 periods of 12 positive pressure pulses (see figure 2).

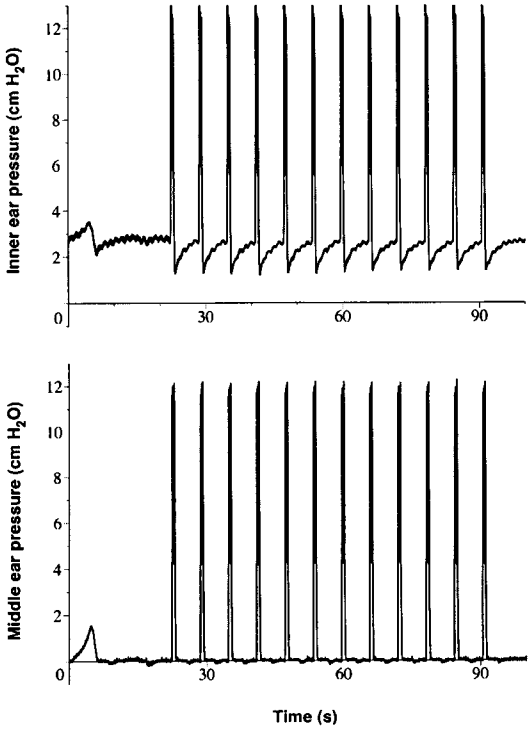

Figure 2. One period of 12 pressure pulses preceded by a built-in airtight test pulse produced by the Meniett™ measured in the guinea pig (middle ear and inner ear simultaneously).

A single pressure pulse is the sum of a static positive component and a component oscillating with a frequency of ≈ 6 Hz (see figure 3a and 3b). A standard series of 3 periods of 12 pulses lasts ≈ 6 min.
The Eustachian tube of the guinea pig was not blocked because the applied pressures were not expected to exceed opening force (Rapport et al. 1975). Calibration of the transducers was performed against a known water column. The output signals of the measuring devices were stored in a personal computer (storage rate of 100 Hz). Animals were sacrificed after the experiment by intracardial pentobarbital injection. The experiment was approved by the Experimental Animal Committee of the Groningen University (protocol number 2439) in accordance with the principles of the declaration of Helsinki.

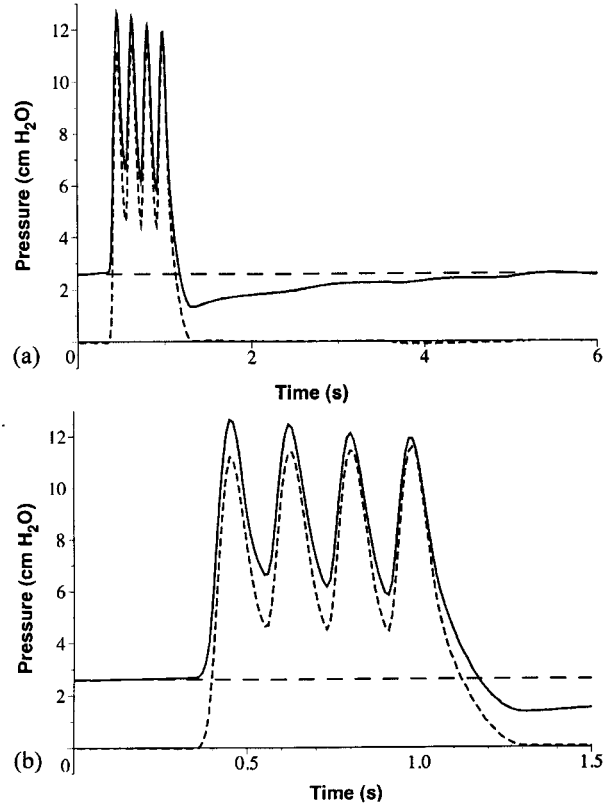

Figure 3. (a) Typical result of experiment in guinea pig ear. Average result of one period of 12 pressure pulses produced by the Meniett™: (——) inner ear; (-----) middle ear;(— —) steady-state value. (b) Detail of figure 3a.

Physical model

During application of a square wave middle ear pressure signal four different stages can be distinguished that will be described with the help of a simple model, shown schematically in figure 4a and 4b.

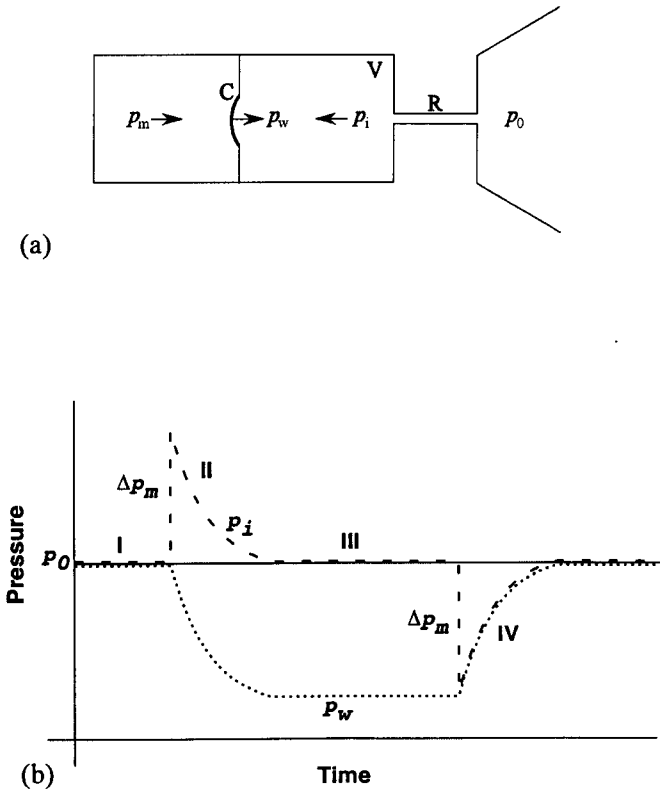

Figure 4. (a) Model for the pressure relations between the middle ear, inner ear and cerebrospinal space during equilibrium: $p_m + p_w = p_i = p_0$. (b) Pressure changes of the windows (p_w), inner ear p_i ,and cerebrospinal space (p_0) induced by middle ear pressure change (Δp_m). (The course of p_i and p_w have been slightly separated from that of p_0 for reasons of clearity. Regions denoted I, II, III and IV correspond to the text.)

I . The inner ear is filled with fluid with a volume V and a pressure p_i, and is assumed to be in open connection with the cerebrospinal space through flow resistance R. As a consequence inner ear pressure (p_i) is equal to cerebrospinal fluid pressure (p_0) at the start of an experiment (t = 0) (Carlborg et al. 1982). Cerebrospinal fluid acts as a buffer reservoir with constant pressure. As the inner

ear is surrounded by bone we may assume that pressure is transferred from the middle ear to the inner ear by the elastic round and oval windows. During pressure equilibrium the following equation holds:

$p_m + p_w = p_i = p_0$

where p_w is the pressure generated by the elastic restoring force of the windows and p_m is the middle ear pressure. Before a pressure signal is applied middle ear pressure (p_m) is zero. This gives $p_w = p_i = p_0$, meaning that the pressure difference between the middle ear and inner ear is maintained by the elasticity of the windows.

II. When middle ear pressure suddenly rises with an amount Δp_m the equilibrium of stage *I* is disturbed:

$p_i = \Delta p_m + p_w > p_0$.

In this situation inner ear fluid escapes through flow resistance R (i.e. the cochlear aqueduct). This results in a decrease in p_w and therefore a decrease in inner ear pressure, with a time constant RC (C = compliance of the windows).

III. When middle ear pressure is maintained at Δp_m for long enough inner ear pressure will return to its equilibrium value p_0 and fluid flow will stop. In this situation:

$\Delta p_m + p_w = p_i = p_0$, meaning that the pressure generated by the elasticity of the windows is smaller (or even negative, depending on the values of Δp_m and p_0) compared to the situation at t = 0.

IV. If after this, middle ear pressure suddenly returns to zero, equilibrium is disturbed again because then $p_i = p_w < p_0$. This creates the undershoot or "bouncing response" (Gyo et al. 1988) in the inner ear, as seen by other researchers (Nishihara et al. 1992, Carlborg et al. 1982, Gyo et al. 1988, Krukowski et al. 1980) and in our experiments. The difference between inner ear pressure and cerebrospinal fluid pressure causes replenishing of inner ear fluid until the steady-state pressure $p_i = p_0$ ($= p_w$) is reached again.

Results

Similar results were obtained from nine ears in which measurements were considered to be successful (see table 1).

The mean value of the inner ear pressure was 2.4 cm water (SD 0.5; Range 1.3) before application of pressure pulses. A typical result of middle and inner ear pressure during Meniett™ pulse application is shown in figure 3 (averaged result of 1 period of 12 pulses after removal of breathing artefacts by digital narrow-band filtering). Middle ear pressure change induced by the Meniett™ was instantly transferred to the inner ear fluid (airtight test included). During delivery of a pressure pulse middle ear pressure slightly increased: averaged over all ears the mean value of the first pressure maximum was 11.0 cm water and of the fourth maximum was 11.5 cm water. Details are given in table 1.

Table 1. Mean pressure values (cm water; SD; range) of 1 averaged period of 12 pressure pulses produced by the Meniett™ for 9 different ears.

		middle ear	*inner ear*
Start pulse		0.0	0.0
Oscillating maximum	I	11.0 (0.6; 2.0)	9.2 (2.5; 8.8)
	II	11.3 (0.5; 1.8)	9.2 (2.3; 8.0)
	III	11.4 (0.6; 1.9)	9.0 (2.2; 7.7)
	IV	11.5 (0.6; 2.0)	9.0 (2.4; 7.9)
Oscillating minimum	I	4.8 (0.3; 0.9)	4.4 (1.6; 5.2)
	II	4.8 (0.3; 1.0)	4.2 (1.5; 5.2)
	III	4.7 (0.3; 0.9)	4.0 (1.5; 4.9)
"Undershoot" after pulse		0.0	-1.0 (0.4; 1.3)

The most important observations of inner ear pressure are:

1. a slight decrease of successive maxima;
2. a somewhat smaller amplitude for the oscillatory part of the signal, compared to the middle ear stimulus (see table I);
3. an undershoot of the signal after application of the stimulus with respect to steady-state inner ear pressure. This undershoot or "bouncing response" (Gyo et al. 1988) had an average value of -1.0 cm water and was released with an average time constant of 1.7 s (SD 0.8; Range 2.7). This time constant was obtained by fitting an exponential curve to the data. It is of the same magnitude as the time constant for pressure recovery after removal of perilymph from the guinea pig inner ear by suction through a micropipette (Wit et al. 1999);
4. no change from its initial value after a complete *Meniett™* session (three periods).

No change in endocochlear potential was observed during or after application of pressure pulses to the middle ear.

Discussion

The WPI 900A uses the servo-nulling principle first described by Wiederhielm (1964) and is designed to measure hydrostatic pressure in limited-volume compartments. Its risetime is (depending on residual volume) < 10 ms according to the specifications. A small ($\approx$ 10 ms) delay in inner ear pressure rise after a sudden change of middle ear pressure was indeed observed and a correction was made for it off-line.

The placement of a micropipette through the round window membrane in our study design carries the danger of interfering with the membrane's mechanical characteristics, possibly affecting the time constant for pressure changes. However, the diameter of the micropipette is relatively small and it was carefully placed near the rim of the round window; therefore we feel that its influence on the results was negligible.

The pressure change in the middle ear cavity induced by the *Meniett™* was transferred instantly to the inner ear of the guinea pig under study. Compared to the oval window the round window membrane is thought to contribute much more to the pressure transfer from the middle ear to the inner ear (Densert et al. 1979, Nishihara et al. 1992). The inner ear pressure course during a *Meniett™* pressure pulse differed only slightly from the pressure course in the middle ear. A small but clear decline in inner ear pressure during a pressure pulse was seen, while middle ear pressure stayed (although oscillating) comparatively stable. This decline in inner ear pressure during constant positive middle ear pressure was first described in cats by Densert et al. (1979) and Krukowski et al. (1980) and was later confirmed by Carlborg et al. (1982) and Nishihara et al. (1988). Inner ear fluid is commonly believed to escape mainly through the cochlear aqueduct, resulting in pressure release whereby the cerebrospinal fluid acts as a buffer (Carlborg et al. 1982, Wit et al. 1999, Nishihara et al. 1992). Other adjacent structures, such as the perineural space, vascular beds, round window membrane and the endocochlear duct and sac, are believed to contribute to the pressure release (Densert et al. 1981, Andrews et al. 1991). If, after a period of time, stable positive middle ear pressure suddenly decreases to atmospheric pressure inner ear pressure will suddenly decrease below its steady-state position, giving rise to the undershoot seen in our experiments. This undershoot phenomenon mainly reflects the elasticity of the round window membrane (Gyo et al. 1988).

In the physical model, as described in the Materials and Methods section, the inner ear is in open connection with the cerebrospinal space through a constant flow resistance R (see figure 4a). In this (linear) model fluid flow through the resistance is obtained by integrating the inner ear pressure response curve. As a consequence the area under this curve above the steady state value pressure (p_0) represents the total volume of inner ear fluid forced to leave the inner ear, while the area below p_0 represents the fluid volume returning into the inner ear from the cerebrospinal fluid space. These two areas should be equal as the inner ear pressure in our experiments always returned to p_0 between two consecutive *Meniett™* pressure pulses (see figure 2) and did not change after a complete series of pulses (see figure 3a), meaning that no permanent change of inner ear fluid volume was attained. However, it can easily be seen from figure 3a that the area under the inner ear pressure curve above the horizontal steady-state pressure line is larger than the area below this line, leading to the conclusion that the assumptions made in the model are too simple. This discrepancy can be solved by assuming that the flow resistance

in our experiments was not constant but depended on flow direction, being higher if fluid was pressed out of the inner ear. This corresponds well to earlier findings in cats in which an asymmetry in pressure-regulating abilities in response to positive and negative pressures was shown (Krukowski et al. 1980, Densert et al. 1981).
In relation to Menière's disease it might be relevant to know wether the *Meniett*™ generated inner ear fluid flow in the vestibular aqueduct as well as in the cochlear aqueduct. In 1997 Gibson and Arenberg postulated that a predisposed narrow vestibular aqueduct silts up with debris in Menière's patients. They stated that this "plugged" vestibular aqueduct could be physiologically overcome by an increased production of endolymph and flow toward the endolymphatic sac, leading to typical attacks of Menière's disease. One might suggest that the *Meniett*™ could contribute to clearing of this supposed debris by flushing the endolymphatic duct towards the sac. When they slowly (1.5 µl/min) injected perilymph into the scala tympani of the normal sealed cochlea of guinea pigs, Salt and DeMott (1998) did not measure any endolymph flow. However, when perilymph was injected into the scala vestibuli, endolymph flow and a related change in endocochlear potential could be measured. When in our experimental situation middle ear pressure is increased by the *Meniett*™, this will move the round and the oval window inward, generating a displacement of perilymph both in the scala tympani and scala vestibuli. Also, because of the greater compliance of the round window (Ivarsson and Pedersen 1977), more perilymph will be moved in the scala tympani than in the scala vestibuli. The perilymph displacement in the scala vestibuli might generate some motion of endolymph, as in Salt and DeMott's experiments, but we did not measure the related change in endocochlear potential.
The present study was designed to gain more knowledge about the *Meniett*™ and its influence on the hydrodynamic inner ear system. The physical model turned out to be too simple and further studies need to be done to elucidate the complex inner ear fluid system and the possible effects on it of the *Meniett*™.

Chapter 3

Change of guinea pig inner ear pressure by square wave middle ear cavity pressure variation

authors R.A. Feijen
J.M. Segenhout
H.P. Wit
F.W.J. Albers

Acta Otolaryngol (Stockh) 2002; 122:138–145

Introduction

In a previous study (Feijen et al. 2000) guinea pig middle ear pressure was changed using complex pressure pulses (Densert et al. 1997) while inner ear pressure was measured simultaneously. Inner ear pressure changes were described by means of a simple (linear) model that will be reviewed below. This model, however, turned out to be too simple. It had to be assumed that flow resistance was not constant and depended on flow direction, being higher if fluid was forced out of the inner ear. This is in accordance with observations in cats (Carlborg et al. 1982) and in guinea pigs (Gyo et al. 1988) and was attributed to specific characteristics of the cochlear aqueduct.

With the knowledge that a thorough understanding of the hydrodynamic inner ear system may elucidate some functional properties of the inner ear and its adjacent structures, the present study describes experiments in guinea pigs, in which an inner ear pressure change was induced by rectangular middle ear pressure changes. In comparison with the complex pressure pulses used in the previous study (Feijen et al. 2000), rectangular pressure changes have the advantage of easier interpretation of the resulting inner ear pressure profiles.

Linear physical model.

The model (illustrated schematically in figure 1) comprises the following assumptions:

1. the inner ear is filled with fluid with a volume V and pressure p_i;
2. the ear is fully enclosed by bone (Andrews et al. 1991);
3. the inner ear is separated from the middle ear cavity by a membrane with constant compliance C;
4. the inner ear is in open connection with the cerebrospinal space through a constant flow resistance R; and
5. cerebrospinal fluid acts as a buffer reservoir with constant pressure p_0.

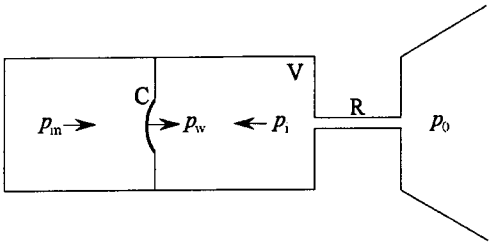

Figure 1. Model for the pressure relations between the middle ear, inner ear and cerebrospinal space during equilibrium: $p_m + p_w = p_i = p_0$.

Inner ear pressure (p_i) is then maintained by the sum of the elastic force of the membrane (p_w) and the middle ear pressure (p_m):

$$p_m + p_w = p_i = p_0$$

In this equilibrium situation no fluid flows in either direction through R. When a positive rectangular pressure step is applied to the middle ear (Δp_m ; figure 2a) the inner ear pressure changes with the same magnitude and p_i becomes larger than p_0 :

$$\Delta p_m + p_w = p_i > p_0$$

This forces fluid out of the inner ear through R, giving rise to an initial positive pressure recovery curve (PIC; figure 2a), until the inner ear pressure equals p_0. In the new equilibrium situation, with a constant positive middle ear pressure, the force that has to be provided by the window has changed (note that p_0 is constant), because the window has moved inwards from its resting position towards the inner ear. With a negative rectangular pressure step applied to the middle ear (figure 2b) the opposite holds:

$$\Delta p_m + p_w = p_i < p_0$$

This forces fluid into the inner ear through R, giving rise to an initial negative pressure recovery curve (NIC) until the inner ear pressure equals p_0. In this equilibrium situation, with a constant negative middle ear pressure, a larger force is generated by the window because it moved outwards from its resting position towards the middle ear. When the middle ear pressure suddenly returns to zero again the inner ear pressure will initially change with the same pressure step, giving rise to a so-called "undershoot" (Gyo et al. 1988, Feijen et al. 2000). After this undershoot volume of inner ear fluid will gradually return to its initial value by an inwardly or outwardly directed movement of fluid through flow resistance R, depending on the sign of the initial middle ear pressure step. The result is an undershoot pressure recovery curve (PUC or NUC, respectively; figure 2). The window will return to its initial position.

The rate of inner ear pressure equalization with cerebrospinal pressure can be characterized by a time constant, T, that depends on flow resistance R and compliance C (Wit et al. 1999). As R and C are assumed to be constant, T will have the same value, RC, for each pressure equalization curve (PIC, PUC, NIC and NUC) as shown in figure 2.

Materials and methods

Seven healthy female albino guinea pigs (Duncan Hartley; HSD Poc) weighing 400 to 500 g were used. They were anaesthetized with ketamine hydrochloride 50 mg/ml and xylazine 20 mg/ml (volume ratio 2:1 at a dose level of ≈ 1 ml/kg body weight), given intramuscularly. Complete muscle relaxation was achieved by i.m. administration of suxamethoniumchloride (5 mg/kg body weight). Body temperature was kept stable at 37–38 °C using a heating pad. Animals were

artificially ventilated by means of tracheal cannulation and heart rate was monitored. The experimental design was grossly the same as that described before (figure 3) (Feijen et al. 2000). Fixation of the animal's head was achieved by means of a screw attached upside down to the skull with dental cement. A flexible tube airtight-glued in the external meatus was connected to a pressure generator (modified WPI 900A micropressure system; World Precision Instruments Inc., USA) controlled by a synthesized function generator (DS345; Stanford Research Systems, USA). Also connected to this tube was an electronic pressure-measuring device (EMA 84; Erwin Halstrup Multur GmbH, Germany) to measure ear canal pressure.

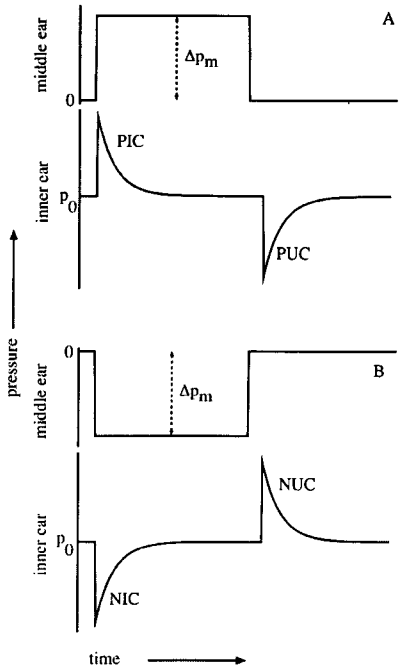

Figure 2. Inner ear pressure change and recovery induced by middle ear pressure change (Δp_m) according to the model shown in figure 1. Note that with constant C and R the inner ear pressure recovery curves (PIC, PUC, NIC and NUC) have equal time constants.

The middle ear cavity was opened via a retroauricular incision. From the middle ear side the tympanic membrane was perforated without damaging other structures. The tip of a bevelled micropipette (tip diameter 10 µm), filled with 2 M NaCl, was lowered in a drop of saline on top of the round window membrane and (atmospheric) pressure was measured with a second WPI 900A system, after which

the micropipette was introduced through the round window rim into scala tympani, making perilymphatic pressure measurements possible. Then, without stirring the micropipette, the hole in the bulla was carefully closed with dental cement.
As a stimulus, two different pressure change profiles were applied through the external ear canal while the resulting perilymphatic pressure changes were recorded. The first type of stimulus consisted of three consecutive positive or negative square wave middle ear pressure changes with an amplitude of 5–6 cm water and a duration of 160 seconds. The second type of stimulus was a 3-step ascending and descending staircase pressure profile, which was applied to the middle ear three times (step size 3 cm water; step duration 80 s). This stimulus was also applied in inverted form.

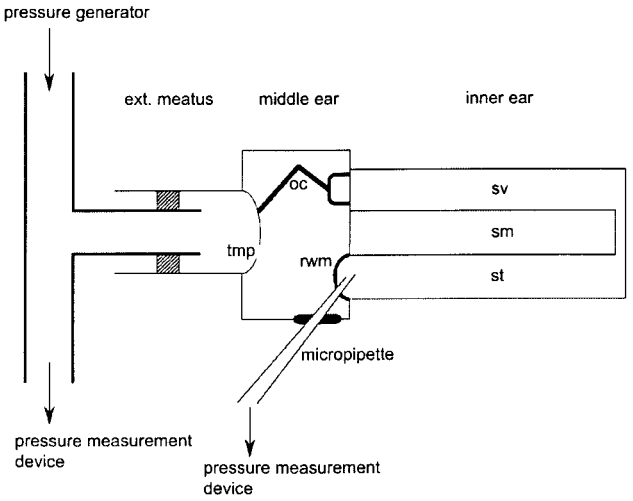

Figure 3. Experimental set-up. oc = ossicular chain; rwm = round window membrane; st = scala tympani; sm = scala media; sv = scala vestibuli; tmp = perforated tympanic membrane.

The stimuli were generated on a personal computer using software for communication with the synthesized function generator (Arbitrary Waveform Composer; version 1.10). The output signals of the pressure-measuring devices were A/D-converted and stored on a hard disk with a rate of 20 Hz. Calibration of the pressure transducers was performed against a known water column. Both ears of the guinea pigs were experimented on and animals were sacrificed after the experiments by intracardial pentobarbital injection. The experiment was approved by the Experimental Animal Committee of Groningen University (protocol # 2439), in accordance with the principles of the declaration of Helsinki.

Statistical calculations

Statistical analysis was performed using a standard software package (SPSS 10.0). Mean values ± standard deviations (SDs) were calculated for the time constants of the pressure recovery curves. A Wilcoxon signed ranks test was used to analyse paired differences and $P < 0.05$ was considered significant.

Results

Measurements were considered successful in 11 ears. Mean perilymphatic steady-state pressure (p_i) was 2.1 cm water (SD 1.0).

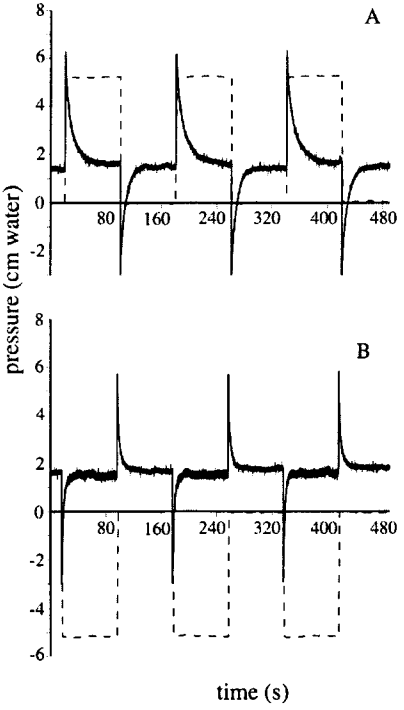

Figure 4. Typical results of inner ear pressure change (solid lines) induced by three consecutive rectangular positive (A) and negative (B) middle ear pressure changes (broken lines).

Rectangular pressure change

Typical results of middle ear and perilymphatic pressure recordings during positive and negative rectangular middle ear pressure change are shown in figure 4a and 4b, respectively. Figure 5a and 5b show the averages of three consecutive periodes of a typical perilymphatic pressure recording, after removal of breathing and heart beat artefacts by off-line digital narrow-band filtering (not the same measurement as figure 4).

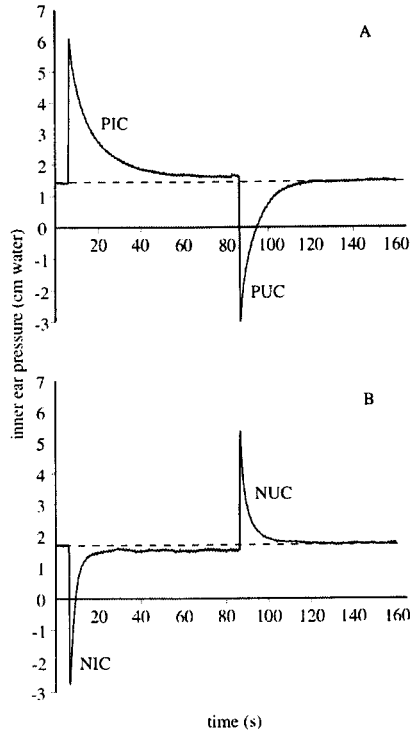

Figure 5. Average of three consecutive inner ear pressure changes after off-line filtering out of heart and breathing artefacts (solid lines). The broken lines show the inner ear equilibrium pressure.

For all 11 ears four time constants were calculated after fitting the pressure recovery slopes ($n = 44$) with the following exponential curves:

$a\,e^{-bt}$ (hereafter called "single exponential").

The "single exponential" gave a good fit (figure 6e) to ten of the eleven negative initial pressure equalization curves (NIC), but was not satisfactory for the remaining curves, where it systematically deviated from the data (figure 5a). Therefore an extra term was added to the fitting formula (Wit el. 1999):

$\frac{a_1 e^{-bt}}{\{1 + a_2(1 - e^{-bt})\}}$ (hereafter called "quotient of exponentials").

This "quotient of exponential" was sufficient for some of the remaining curves (e.g. figure 6d) but not for all (e.g. figure 6b). In that case the following formula was used:

$a_1 e^{-b_1 t} + a_2 e^{-b_2 t}$ (hereafter called "sum of exponentials"; see fits figure 6c and 6d).

The "sum of exponentials" was necessary to obtain a good fit for 21 of 44 curves, mostly for both PIC and PUC.

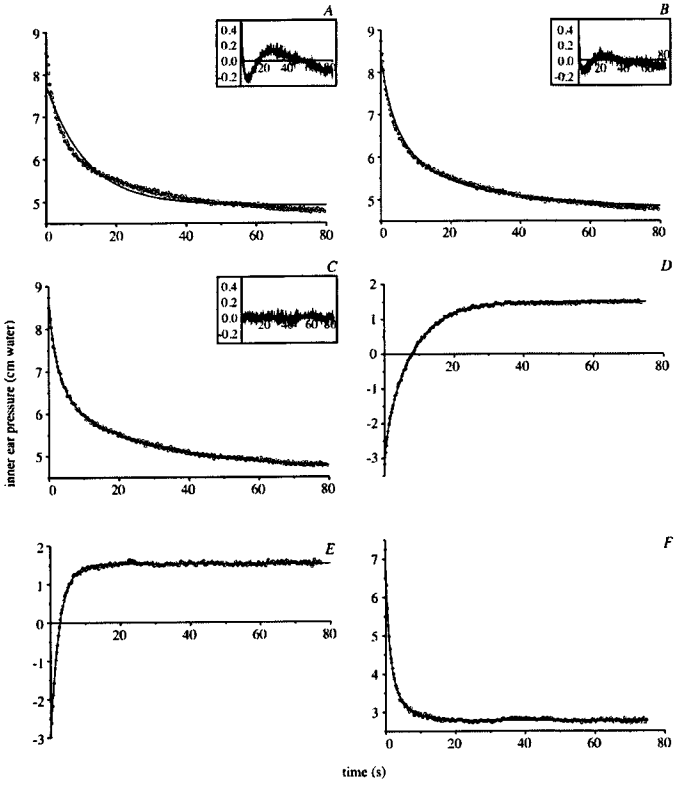

Figure 6. The shape of the pressure recovery curves. (A), (B) and (C) show the same recording of an initial recovery curve after positive middle ear pressure (open circles), fitted (solid line) successively with single, quotient and sum of exponentials. The insets to (A), (B) and (C) give the deviation of the fit from the recorded curves. (D), (E) and (F) show the recovery curves of different recordings (positive undershoot, negative initial and negative undershoot, respectively) and were all fitted with the sum of exponentials.

A time constant was calculated from the fits, defined as the interval of time during which the pressure returns from its maximum value to e^{-1} times this value. The time constants (figure 7) for PIC (mean T_{PIC} = 15.0 s; SD 9.0 s) were found to be larger (p = 0.006) than the time constants for PUC (mean T_{PUC} = 8.6 s; SD 2.7 s).

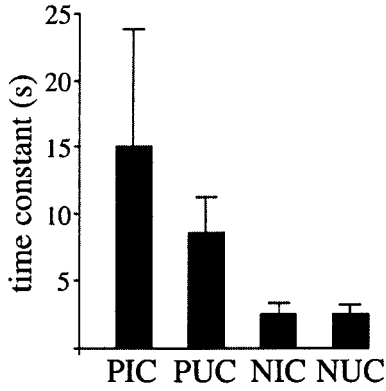

Figure 7. Mean time constants (s) and standard deviations for the different pressure recovery curves. Significant differences in mean (Wilcoxon signed ranks test; $p<0.05$) existed between: (i) PIC, and PUC, NIC and NUC, respectively; and (ii) PUC, and NIC and NUC, respectively. No difference in mean existed between NIC and NUC.

The mean time constants for NIC (mean T_{NIC} = 2.5 s; SD 0.8 s) did not differ (p = 0.821) from the mean time constant for NUC (mean T_{NUC} = 2.5 s; SD 0.8 s). The two mean time constants for the positive pressure recovery curves were significantly larger (p = 0.003) than the two mean time constants for recovery from negative pressure.
It was noted that in all cases inner ear pressure did not fully recover to its initial value. A small difference between initial and final pressure remained after a positive or a negative middle ear pressure step. When middle ear pressure returned to its initial value, inner ear pressure also returned to its value before middle ear pressure change.

Staircase pressure change
A typical result of a three-step ascending middle ear pressure staircase pressure change and simultaneous perilymphatic pressure recording is shown in figure 8a. Time constants for the different pressure recovery curves were calculated (n=6 per

measurement). These T-values increased for each subsequent initial positive pressure recovery curve (figure 8a).

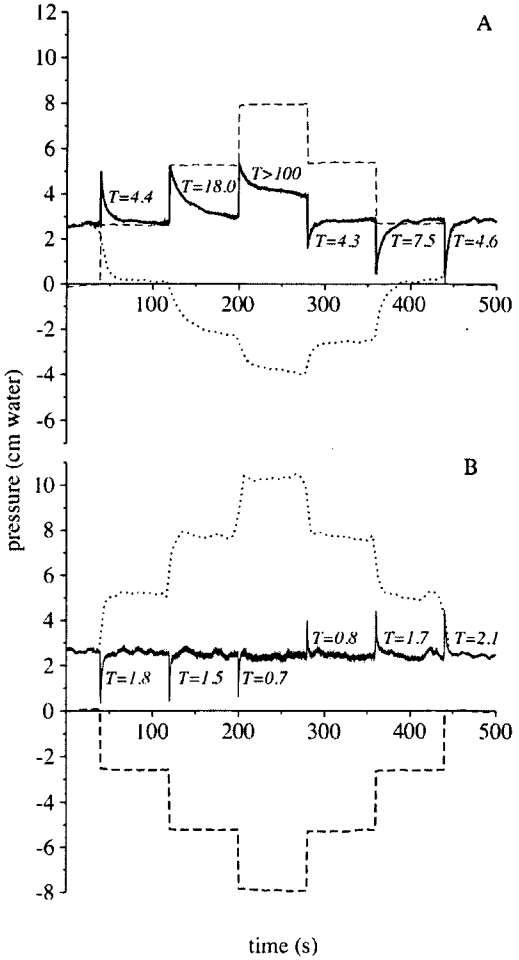

Figure 8. Typical result of inner ear pressure change (solid line) induced by a three-step ascending and descending staircase pressure profile (A) applied to the middle ear (dashed line) and also in inverted form (B). The pressure generated by the windows (p_w; dotted line) was calculated using $p_w = p_i - p_m$.

The value of T even exceeded 100 s after the third middle ear pressure step (when middle ear pressure had reached ≈ 8 cm water). The three time constants for the positive undershoot pressure recovery curves were all shorter compared with the positive initial time constants and did not differ significantly in length.

Figure 8b shows the result of the inverted staircase middle ear pressure change. Separate time constants were calculated (n = 6). Subsequent time constants for the initial negative pressure recovery curves decreased, and increased again when middle ear pressure returned to its initial value in three steps. Both the negative initial and negative undershoot time constants were shorter compared to their positive counterparts.

Discussion

Most of the inner ear pressure recovery curves could not be fitted properly with a "single exponential" function. Therefore (by trial and error) more complicated functions were used to derive a time constant from the fits. These time constants differed significantly for different middle ear pressure steps (figure 7). From this, and the fact that fits with a single exponential curve were not successful, it can be concluded that the linear model presented in the Introduction is too simple. This means that compliance C and/or resistance R (see figure 1) are not constant during inner ear pressure change. That pressure recovery curves deviate from an exactly exponential shape has been noticed before: Densert et al. (1986), when studying inner ear pressure change in cats, distinguished fast and slow recovery phases, with different time constants. In addition, Wit et al. (1999), when injecting artificial endolymph through the round window membrane in guinea pigs, described their results with a model in which inner ear compliance and/or flow resistance depended on inner ear pressure.

During both positive and negative middle ear pressure, inner ear pressure does not completely return to its initial value: a small positive (subsequently negative) pressure with respect to the inner ear equilibrium pressure value remains (figure 5, broken line). Also this observation indicates that the model in the Introduction does not fully describe the results. The model predicts an inner ear end pressure value, during both positive and negative middle ear pressure, equal to the cerebrospinal fluid pressure, which is supposed to remain constant. Suzuki and co-workers (Suzuki et al. 1994b, Suzuki et al. 1998) showed that closing the vestibular or cochlear aqueduct enlarges the difference between the initial and final inner ear pressures after middle ear pressure change. However, in control animals with open aqueducts a (smaller) difference was also measured by these authors.

The difference between the time constants for the recovery curves for a positive middle ear pressure change (figure 7, first two bars) and for a negative pressure change (figure 7, last two bars) is remarkable. The essential difference between these two experimental conditions is that the cochlear windows move further outwards for a negative middle ear pressure, while for a positive middle ear pressure the windows move inwards. Therefore time constants for inner ear pressure recovery are related to window position.

These time constants are the product of flow resistance R and compliance C (figure 1). C is the sum of the compliances of the round and oval window, with the main contribution coming from the round window (Ivarsson and Pedersen 1977, Gopen et al. 1997, Suzuki et al. 1998), which has an area of approximately 1 mm^2 in the guinea pig (Fernández 1952). Ivarsson and Pedersen (1977) showed for the human round window that the relation between inner ear pressure and round window (volume) displacement is not linear. From their results it can be derived (figure 11 in Wit et al. 1999) that for a pressure of a few cm water the round window compliance is two to three times smaller than its maximum value at zero pressure. If the same holds for the guinea pig, then this may explain the much smaller time constants for negative middle ear pressure, when the round window is stretched outwards.

That the flow resistance R also depends on the position of the round window membrane is not an unlikely assumption. The cochlear aqueduct is a funnel-shaped canal between the subarachnoidal and the perilymphatic space (Duckert 1974, Galic and Giebel 1987, Toriya et al. 1991a, Gopen et al. 1997). Its internal orifice is situated very close to the round window. About half a century ago it was thought that this opening was closed by an overlying structure (Waltner 1947), but later studies could not confirm the presence of such a barrier membrane (Gopen et al. 1997, Galic and Giebel 1987, Toriya et al. 1991a, Nishimura et al. 1981). It is now generally assumed that the cochlear aqueduct is normally open and has a function in equalizing inner ear pressure (Andrews et al. 1991, Suzuki et al. 1994b). The inner ear opening of the aqueduct, however, is filled with a meshwork of fibroblasts and loose connective tissue (reticular cells), attached at one side to the round window (Duckert 1974, Nishimura et al. 1981, Toriya et al. 1991a, Galic and Giebel 1987, Gopen et al. 1997, Bergman et al. 1979), as shown schematically in figure 9. It is conceivable that an outward motion of the round window stretches the meshwork, thereby reducing the flow resistance of the aqueduct. This is consistent with the fact that for negative middle ear pressure (outward moving window) considerably smaller time constants for pressure recovery are found than for positive middle ear pressure changes. The staircase pressure change experiment (figure 8) in particular convincingly shows a relation between the pressure exerted by the cochlear windows - which is a monotonic function of window position - and these time constants. If it were a change of window compliance that made the time constants change, than we would not expect to measure the largest time constant for the staircase pressure step leading to the maximum middle ear pressure, because for this situation the windows bulge inwards and have a smaller compliance than for the unstretched situation.

At first sight the findings of Wit et al. (1999) seem to contradict the current results: smaller time constants were found by these authors for pressure recovery after increasing inner ear pressure than for recovery after decreasing inner ear pressure. However, as inner ear pressure was increased (or decreased) by injection

(subsequently withdrawal) of artificial endolymph, leading to a change in window position, those earlier results confirm the present ideas on further consideration.
The significant difference between the time constants for the initial and undershoot pressure recovery curves for positive middle ear pressure change (figure 7, PIC and PUC) cannot be explained by a difference in window position. This position follows the same course (in opposite directions) for both pressure recovery curves, so an additional mechanism must play a role. This could be a dependence of aqueduct resistance on flow direction, as was proposed by Densert et al. (1981) and by Carlborg et al. (1982). Also Krukowski et al. (1980) noticed that the aqueduct reacts differently to positive and negative inputs, producing a non-linear filter effect. However, if aqueduct flow resistance does depend markedly on flow direction, a significant difference in time constants should also be found for the pressure recovery curves after negative middle ear pressure change. It can be seen in figure 7 (NIC and NUC) that such a difference was not measured and therefore additional experiments are needed to resolve this discrepancy.

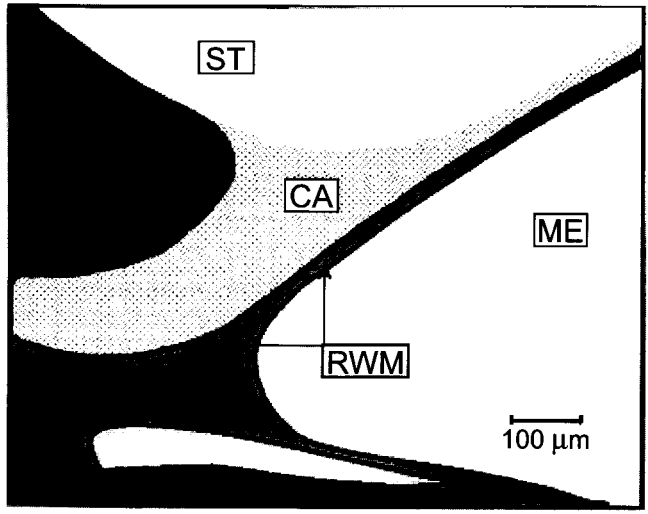

Figure 9. Schematic of the cochlear aqueduct (CA) opening into the scala tympani (ST) [taken from Toriya et al.1991a]. This clearly shows the close relation between the meshwork of fibroblasts and the loose connective tissue filling the CA and the round window membrane (RWM). ME = middle ear space.

Chapter 4

Cochlear aqueduct flow resistance is not constant during evoked inner ear pressure change in the guinea pig

authors H.P. Wit
R.A. Feijen
F.W.J. Albers

Hear Res 2003; 75:190-199

Introduction

The cochlear aqueduct connects scala tympani with the subarachnoid space. In the guinea pig it has a length of approximately 2 mm and its cross-sectional area, when measured with high-resolution magnetic resonance microscopy, increases from 0.016 mm^2 at the side of scala tympani to more than 0.20 mm^2 where it joins the subarachnoid space (Ghiz et al. 2001; figure 5). Under the assumption of a circular cross-section the smallest diameter of the duct is 0.14 mm. The human cochlear aqueduct has the same smallest diameter (0.138 ± 0.058 mm) and an estimated length between 6 and 12 mm (Gopen et al. 1997).

When inner ear fluid pressure is suddenly changed, for instance by a change of ear canal (Krukowski et al. 1980) or middle ear pressure (Densert et al. 1981), or by injection of fluid (Wit et al. 1999), pressure equalization takes place within seconds. The main route for pressure equalization is the cochlear aqueduct (Carlborg et al. 1982). The time constant for pressure release is therefore mainly determined by the flow resistance of the aqueduct, combined with the compliance of the cochlear windows. (Primarily of the round window, with a compliance that is estimated to be one order of magnitude larger than that of the oval window (Ivarsson and Pedersen 1977; Gopen et al. 1997)).

Time constants for inner ear pressure release after middle ear or ear canal pressure increase are different from time constants measured after pressure decrease (Krukowski et al. 1980; Densert et al. 1981, 1986; Carlborg et al. 1982). And smaller time constants are found for pressure release after injection of fluid into the cochlea than after fluid withdrawal (Wit et al. 1999). Furthermore, inner ear pressure recovery curves induced by the upgoing edge of a positive square middle ear pressure wave differ in shape from the curves after the downgoing edge (Densert et al. 1986).

Based on the observed differences in animal studies for the time courses of pressure release after middle ear pressure changes, a device has been developed to diminish complaints of patients with Meniere's disease (Densert et al. 1997; Odkvist et al. 2000). The time course of inner ear pressure changes brought about by this device was studied in the guinea pig (Feijen et al. 2000), but interpretation of the results was difficult because of the complex shape of the applied middle ear pressure profile. Therefore we performed a follow-up study in the guinea pig with square wave middle ear pressure stimuli (Feijen et al. 2002), with results that are comparable to the results that were obtained previously in the cat by Densert et al. (1986).

It was noticed by Densert et al. that inner ear pressure profiles, evoked by square wave middle ear pressure changes, did not have the shape of a single exponential function, as would be expected for a system with constant compliance and flow resistance, but could be described as the sum of two exponential functions with different time constants. Careful analysis of the results that we obtained in the guinea pig (Feijen et al. 2002) yielded even more complicated shapes for inner ear

pressure release curves, which is a consequence of the flow conducting properties of the aqueduct and of the compliance of the windows. In order to derive these properties, representative results from two ears (of different guinea pigs) were selected for extensive further analysis, as presented in this paper.

Theory

The pressure p_w exerted by the elastic window membrane with compliance C (figure 1) on the inner ear fluid is a function of V

$$p_w = g(V) \qquad [1]$$

in which V is the volume bordered by the stretched membrane and the flat plane in which the membrane lies when it is unstretched. (V is positive when the membrane is stretched in the direction of the middle ear cavity.)

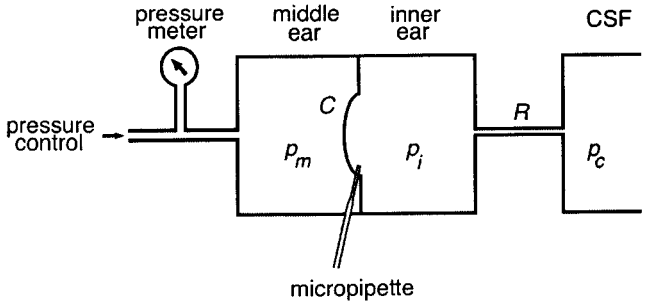

Figure 1. Schematics of experimental set-up. Middle ear pressure p_m is changed with an electronic pressure control system and measured with a solid state pressure meter. Inner ear pressure p_i is measured through a micropipette with a WPI micropressure system. R = flow resistance of cochlear aqueduct; C = compliance of cochlear windows (mainly of round window); p_c =pressure of cerebrospinal fluid (CSF).

The stiffness s of the membrane is the derivative of this function

$$s = \frac{dp_w}{dV} \qquad [2]$$

and

$$C = \frac{1}{s} \qquad [3]$$

Differentiation of [1] with respect to time t and using [2] and [3] gives:

$$\frac{dp_w}{dt} = \frac{dp_w}{dV} \cdot \frac{dV}{dt} = \frac{1}{C} \cdot \frac{dV}{dt} \qquad [4]$$

Inner ear volume change occurs by fluid flow

$$f = -\frac{dV}{dt} \quad [5]$$

through the resistance R, defined by

$$R = \frac{p_i - p_c}{f} \quad [6]$$

Combination of [4], [5] and [6] gives

$$-RC\frac{dp_w}{dt} = p_i - p_c \quad [7]$$

The net pressure on the membrane is $p_i - p_m$. This net pressure is equal to p_w, when the membrane does not move. So

$$p_w = p_i - p_m \quad [8]$$

It is reasonable to assume that this relation also holds when the membrane moves.

General case

If both p_i and p_m are known as a function of time,

$$\frac{dp_w}{dt}$$

can be calculated with

$$\frac{dp_w}{dt} = \frac{dp_i}{dt} - \frac{dp_m}{dt}$$

(see Eq. 8). This relation reduces to

$$\frac{dp_w}{dt} = \frac{dp_i}{dt} \quad [9]$$

if p_m is constant.

If $f = 0$, inner ear pressure p_i is equal to intracranial pressure p_c, which is assumed to be constant. This means that $p_c = \lim_{t\to\infty} = p_i$, for a situation where p_i returns to a constant value.

And if the time course of p_i and

$$\frac{dp_w}{dt}$$

are known, RC can be calculated as a function of time with Eq. 7.

Simple case R, C and p_m constant

Substitution of Eq. 9 in Eq. 7 gives the differential equation

$$RC\frac{dp_i}{dt} = p_c - p_i \quad [10]$$

in which R, C and p_c are constants. The solution for Eq. 10 is:

$$p_i = p_0 e^{-t/RC} + p_c \qquad [11]$$

in which p_0 is the initial pressure difference between inner ear and cerebrospinal fluid space.

This means for instance that a square wave change of middle ear pressure induces a sudden change in inner ear pressure, that recovers following an exponential curve with time constant $\tau = RC$, as shown in figure 2.

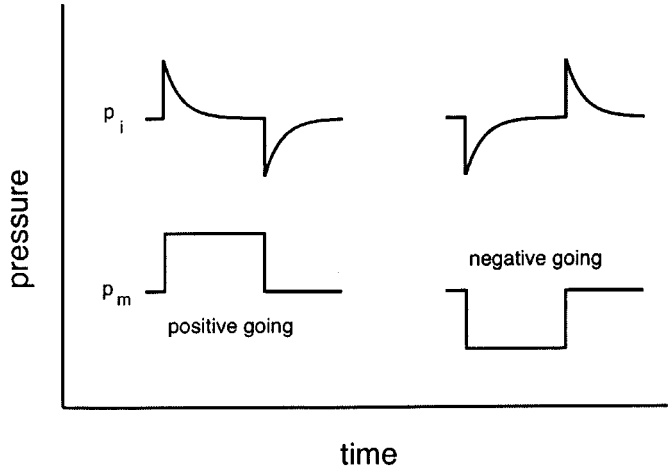

Figure 2. Predicted inner ear pressure (p_i) profile induced by square wave middle ear pressure (p_m) change, for constant compliance C and resistance R.

Method

A detailed description of materials and methods has been given elsewhere (Feijen et al. 2002). For the present purpose the description is limited to the following: A flexible tube was glued in the external auditory meatus of the guinea pig and connected to a pressure generator (modified World Precision Instruments type 900A micropressure system) and a solid state pressure measuring device. The pressure generator was controlled by a synthesized function generator (Stanford Research Systems, type DS345), producing square waves with a duration of 80 seconds. The middle ear cavity was opened via a retroauricular incision and from the cavity side a large perforation was made in the tympanic membrane. The bevelled tip of a micropipette (tip diameter 10 μm), filled with 2 M NaCl, was introduced in scala tympani through the rim of the round window, to measure inner ear pressure with a second WPI micropressure system. After this the round window membrane was carefully inspected for leakage of fluid along the pipette tip and the

hole in the bulla was carefully filled up with dental cement, to close the middle ear cavity again. The experimental set-up is schematically shown in figure 1.
The output signals of the middle ear and the inner ear pressure measuring devices were stored on hard disk with a rate of 20/s. Inner ear responses were digitally filtered off-line to remove breathing artefacts, and responses to three consecutive middle ear square wave stimuli were averaged. All calculations were performed with a Mathematica 3.0 software package.
Measurements were done in female albino guinea pigs, anaesthetised with a mixture of ketamine hydrochloride (33 mg/kg) and xylazine (7mg/kg). The experiment was approved by the Experimental Animal Committee of Groningen University (protocol # 2439), in accordance with the principles of the Declaration of Helsinki.

Analysis of results
The rise and fall time of the recorded middle ear square wave pressure profile were approximately 0.05 s and pressure stability was better than 0.5 mm water (5 Pa).
The results given in figures 3 through 6 are for the same ear. Figure 3 shows inner ear pressure change in response to a negative going square wave middle ear pressure. The rising and the falling part of the inner ear pressure recovery curve could reasonably well be fitted with the same single exponential curve with a time constant of 1.7 s, as shown with the dashed lines.

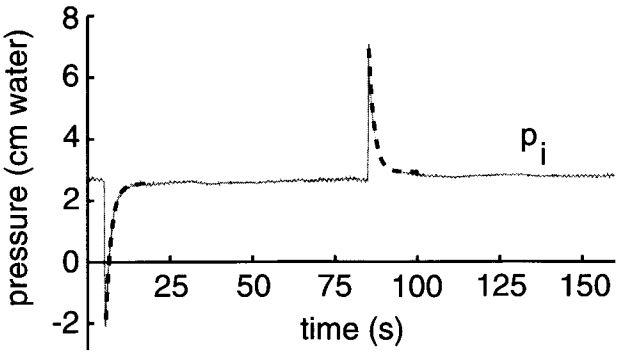

Figure 3. Inner ear pressure profile, measured in a guinea pig, induced by a square wave middle ear pressure change of 35 cm water and 80 s duration. The thick dashed line segments are exponential curves $p_i = ae^{-t/\tau} + p_c$, *with* $\tau = 1.7$ *s.*

For a positive going square wave middle ear pressure change the situation is quite different, as can be seen in figure 4: the falling part of the curve has a longer time constant than the rising part, and both time constants are much longer than the time

constant in figure 3. Furthermore, fits with a single exponential curve gave unsatisfying results.

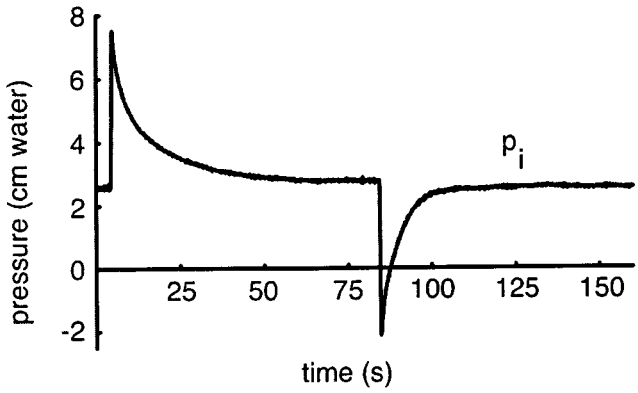

Figure 4. Inner ear pressure profile induced by a square wave middle ear pressure change of +5 cm water and 80 s duration. Results are from the same ear as the results shown in figure 3.

To further analyse the shape of the curve in figure 4 high frequency fluctuations were removed by numerical low-pass filtering, and after this analytical expressions were sought to fit the sloping parts of it. These expressions were found as sums of first and second order (Gaussian) exponential curves. (The choice of these curves has no special meaning; they were obtained by trial and error to give good fits.) The fitting curves (apart from a constant term) are given in the upper panels of figures 5 and 6; respectively for the falling and the rising part of the inner ear pressure recovery curve of figure 4. These fitting curves differ nowhere systematically from the measured curves; the only difference is a noise-like signal with a standard deviation of 0.03 cm water.

Window pressure p_w as a function of time was derived from the fitted curves for inner ear pressure p_i, by using relation Eq. 8 of the theory section. The results are given in figures 5b and 6b. And by differentiating these curves with respect to time the curves as shown in figures 5c and 6c were obtained.

The product of flow resistance R and window compliance C can then be obtained as a function of time with relation Eq. 7, by dividing $p_i - p_c$ (as shown in figures 5a and 6a) by

$$-\frac{dp_w}{dt}$$

(shown in figures 5c and 6c).

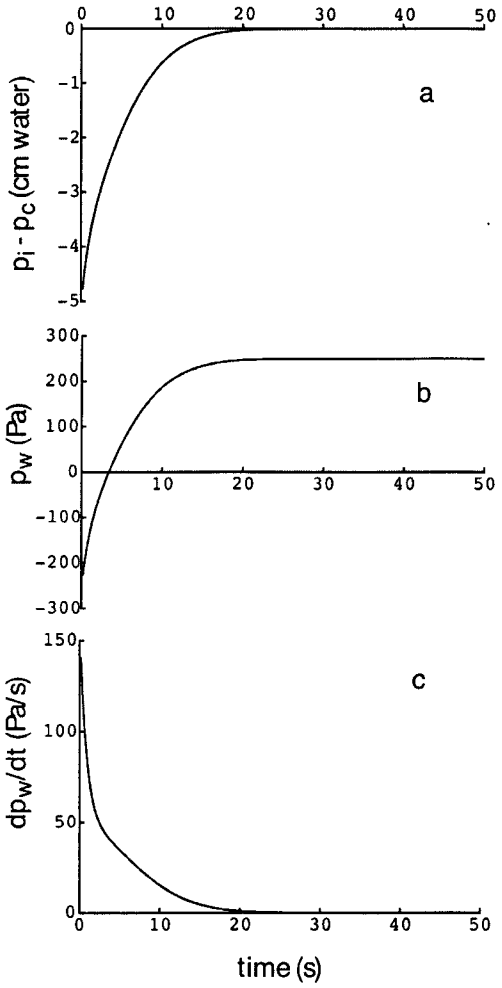

Figure 5. (a) Smoothed first 50 s of down-going part of inner ear pressure curve, as shown in figure 4. (b) Window pressure change, calculated from curve a, using Eq. 8 in Section 2. (c) Time derivative of curve b.

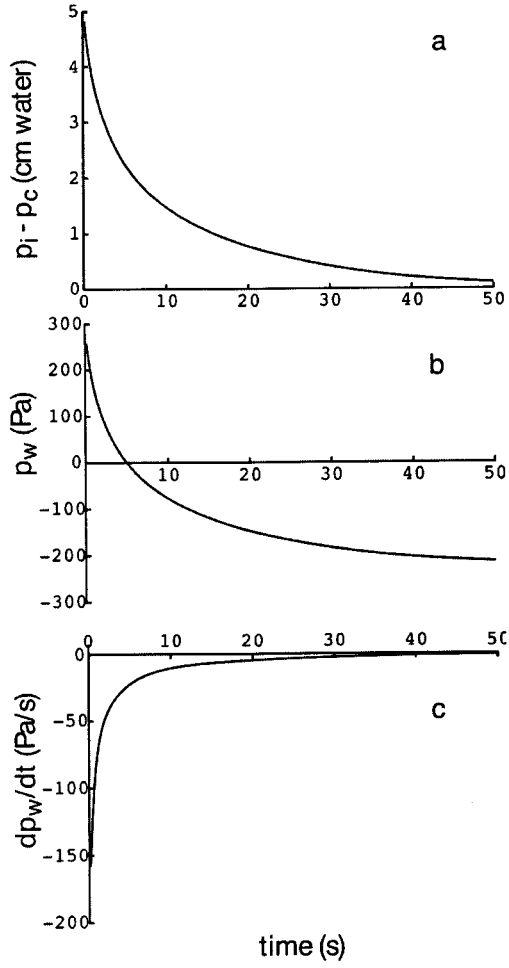

Figure 6. (a) Smoothed first 50 s of up-going part of inner ear pressure curve, as shown in figure 4. (b) Window pressure change, calculated from curve a, using Eq. 8 in Section 2. (c) Time derivative of curve b.

Results of this calculation, for the same ear as for which results are given in figures 3 through 6, are shown in figure 7. Also given in this figure (with dashed lines) are *RC* curves calculated with the same procedure for another ear (from another guinea pig). For this ear the time constant for pressure recovery after a negative going

middle ear pressure step was 2.4 s. It is clear from figure 7 that *RC* is not constant during inner ear pressure recovery.

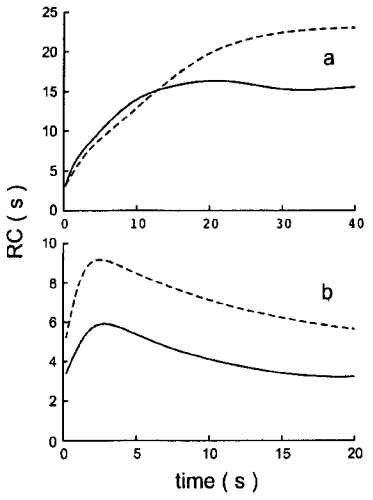

Figure 7. Product of flow resistance R and window compliance C, calculated with $-RC\frac{dp_w}{dt} = p_i - p_c$, *during inner ear pressure recovery after a sudden middle ear pressure change from (a) 0 to +5 cm water, and (b) +5 to 0 cm water. Solid lines are for the same ear as for which results are given in figures 3 - 6. Dashed lines are results from another guinea pig.*

Because middle ear pressure p_m is kept constant after a stepwise change, window pressure p_w and inner ear pressure p_i differ only by a constant value during inner ear pressure recovery, according to Eq. 8. If it is further assumed that the pressure of the cerebrospinal fluid p_c is constant (apart from "high" frequency fluctuations caused by breathing and heartbeat), $p_i - p_c$ and p_w also only differ by a constant value, as can be seen by comparing figures 5a and 5b and figures 6a and 6b (1 cm water = 100 Pa). Using this presumption *RC* is plotted as a function of $p_i - p_c$ as well as p_w in figure 8.

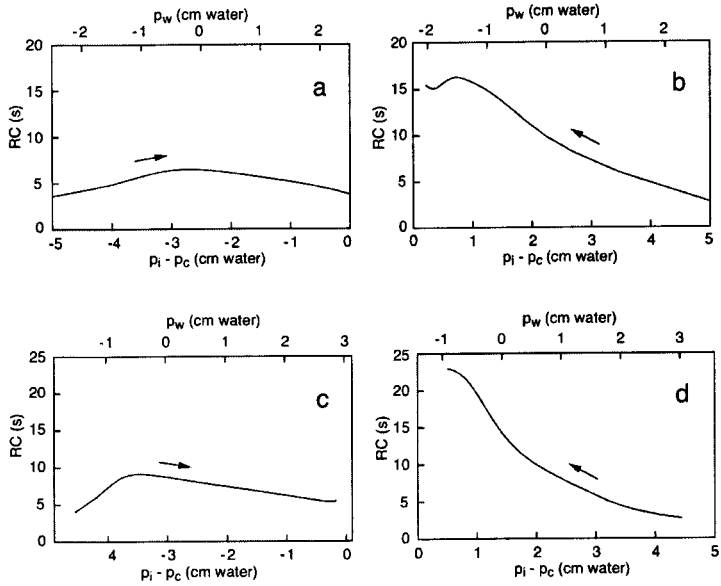

Figure 8. Change of product of flow resistance R and window compliance C during inner ear pressure recovery, plotted as a function of window pressure (upper horizontal axis) as well as the difference between inner ear and CSF pressure (lower horizontal axis). The curves in b and d are the same as the solid and the dashed curve, respectively, in figure 7a (after middle ear pressure change from 0 to +5 cm water). The curves in a and c are the same as in figure 7b (after middle ear pressure change from +5 to 0 cm water). The arrows indicate the direction of RC change.

Discussion

To calculate the flow resistance R of the cochlear aqueduct, it is needed to know window compliance C, because figures 7 and 8 only give information on the product RC.

C is a function of window stretch, which is a function of inner ear volume V (defined in the theory section). Figure 9a gives the relation between window pressure and volume for the human round and oval window (Ivarsson and Pedersen 1977). The dashed line in figure 9b gives compliance as a function of pressure, derived from this relation, for the p_w range as used in our measurements. Also given in figure 9b, with a filled square, is the value for the compliance of the guinea pig round window (0.14 nl/Pa), as given by Décory et al. (1990); plotted at a pressure value of 2.6 cm water, which is the average normal inner ear fluid pressure of the guinea pig (Wit et al. 1999; table 1).

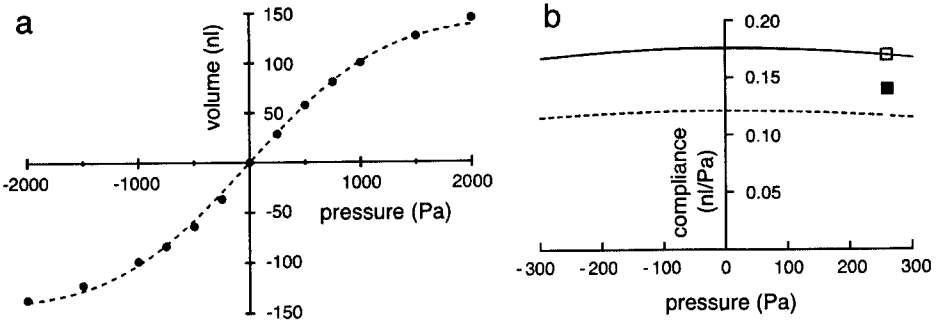

Figure 9. (a) Relation between pressure p exerted on human inner ear fluid by the (round and oval) windows and inner ear volume V (as defined in the text). Filled circles were taken from Ivarsson and Pedersen (1977, figure 2). The dashed line is a least squares fit with $V=a \cdot Erf[bp]$;
$a = 143.5$, $b=0.0007463$. *(b) Calculated relation between window compliance C and pressure* p_w *, for a pressure range that corresponds to the maximum change in the experiment (see e.g. figure 8). The dashed line is for the human ear (=Gaussian-shaped derivative of the curve in a); the solid line is the assumed relation for the guinea pig ear. The open square gives a value for the guinea pig round window compliance, taken from Déccory et al. (1990). The filled square is the assumed value for the compliance of round and oval window together.*

In man the compliance of the round window is 5 times that of the oval window (Ivarsson and Pedersen 1977; figures 4 and 5). Assuming the same ratio for the guinea pig gives the open square in figure 9b for the compliance of round and oval window together. The solid curve in figure 9b is a scaled-up version of the dashed line. This curve will be taken for the value of C as a function of p_w in the guinea pig.
Figure 10 was constructed by dividing RC (as shown in figure 8) by this function for C. It is not surprising that figure 10 resembles figure 8 to a large extent, because C only changes a few percent for the range of window pressure variation during an experiment.
For a negative going middle ear pressure change the time constant $\tau = RC$ for inner ear pressure recovery, as shown in figure 3, was found to be 1.7 and 2.4 s for the two investigated ears. An analysis in 7 guinea pigs, including the two described in this paper, gave on average a slightly higher value of 2.5 s for τ, both for an initially negative going middle ear pressure and for its subsequent return to zero (Feijen et al. 2002). So for negative going middle ear pressure changes τ is constant and has a value of a few seconds. Comparable values for τ were found for inner ear pressure release after fluid injection (0.5-1.9 s) or withdrawal (2.1-4.2 s) by Wit et al. (1999), also in the guinea pig. Values for τ of 1.7 and 2.4 s, divided by a

compliance of 0.17 nl/Pa (figure 9; open square), give values of 10 and 14 Pa.s/nl subsequently for the flow resistance *R*.
For a positive going square wave middle ear pressure change the situation is quite different, as is shown in figure 10: the resistance changes during inner ear pressure release and it reaches higher values after the onset of middle ear pressure change (maximum 94 and 132 Pa.s/nl; in figure 10b,d subsequently), than after the offset (maximum 33 and 53 Pa.s/nl; figure 10a,c).

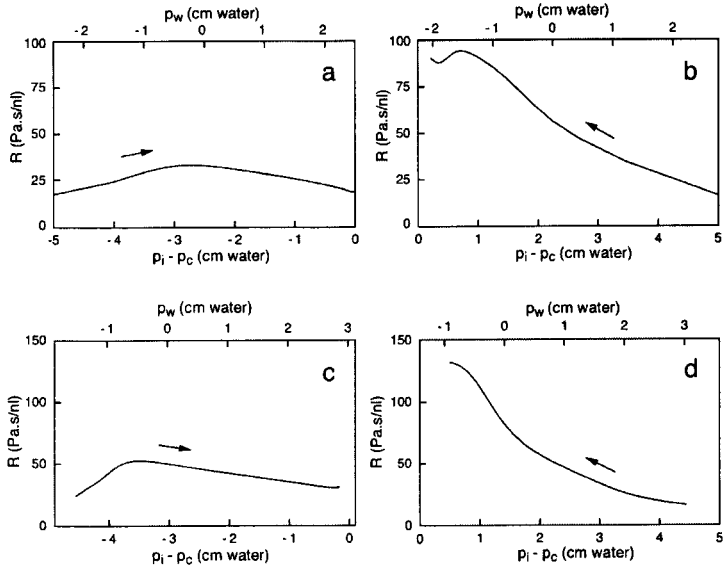

Figure 10. Change of flow resistance R during inner ear pressure recovery, plotted as a function of window pressure (upper horizontal axis) as well as the difference between inner ear and CSF pressure (lower horizontal axis). The curves in b and d show the change of R after a middle ear pressure change from 0 to +5 cm water. The curves in a and c give R after a middle ear pressure change from +5 to 0 cm water. The arrows indicate the direction of R change.

If τ is defined as the time in which inner ear pressure returns to e^{-1} times its maximum change, τ = 7.7 s for the situation in figure 5a and τ = 5.3 s for pressure recovery as shown in figure 6a. In 7 guinea pigs - as mentioned above - these values were on average 15.0 s and 8.6 s (Feijen et al. 2002), with a rather large spread in values.
The narrow portion of the cochear aqueduct has a length of approximately 1 mm (Ghiz et al. 2001). As the flow resistance of a cylindrical duct depends on the fourth power of its diameter (Poiseuille's formula, see e.g. Allen 1987), it is this

portion that determines the flow resistance of the cochlear aqueduct. Duckert (1974) gives a value of 0.15 mm for the diameter of the narrow portion of the aqueduct. This value is in accordance with the value of 0.14 mm that can be derived from the minimal fluid filled cross-sectional area given by Ghiz et al. (2001). Toriya et al. (1991a) give a diameter of 0.06 mm for the narrowest segment of the aqueduct. In our opinion the latter value is too small, because we observed that a metal wire with a diameter of 0.1 mm easily passes through a guinea pig aqueduct preparation, after removal of soft tissue.

For a tube with a length of 1 mm and a diameter of 0.1 mm the resistance is 0.3 Pa.s/nl. This follows from the relation $R = 8\eta l/(\pi r^4)$ (Wit et al. 2000), if η is taken as 6.9×10^{-4} Pa.s, the value for saline at body temperature, and l and r are length and radius of the duct.

Thus, the resistance values, as derived above from the pressure release experiments, are two orders of magnitude larger than the calculated value of 0.3 Pa.s/nl. This must be because the resistance of the aqueduct is not determined by its dimensions, but because it is filled with material with a high resistance for fluid flow.

About half a century ago it was thought that the internal orifice of the aqueduct was closed by a "barrier membrane" (Waltner 1947), but in later studies the presence of such a structure could not be confirmed: Svane-Knudsen (1958) reported that the (guinea pig) aqueduct is filled with a very loose network of connective tissue, containing small thin-walled vessels. This tissue gradually grows more dense towards the scala tympani opening of the aqueduct and it continues into the connective tissue core of the round window membrane. Also Duckert (1974) describes the aqueduct in guinea pig being filled with a loose connective meshwork, composed of reticular cells and collagen and elastic fibrils. Toriya et al. (1991a,b) re-examined the fine structure of the pores at the opening of the aqueduct to the perilymphatic space, using scanning electron microscopy. They found that the fibroblasts of the connective tissue trabeculae were more compact at the opening to the perilymphatic space than in the rest of the duct. Moreover, the arrangement of the fibroblasts at the opening of the perilymphatic space was found to be perpendicular to the long axis of the aqueduct, whereas the fibroblasts in the main duct were parallel to the long axis.

Because the pressure $p_i - p_c$ across the aqueduct and the pressure p_w exerted on the inner ear fluids by the windows change simultaneously during inner ear pressure release, the behaviour of R as a function of p_w and $p_i - p_c$, as shown in figure 10, can not straightforwardly be explained. For instance: If R would not depend on $p_i - p_c$ and be a function of p_w only, the curves in figures 10a and 10b (and in c and d) would have the same shape.

During inner pressure recovery after a negative going square wave middle ear pressure change, as shown in figure 3, R has a value in the order of 10 Pa s/nl, and a good fit to the data is obtained with the assumption that RC is constant. The

situation after a positive going middle ear pressure change (figure 4) is quite different: R attains values in the order of 100 Pa.s/nl (figure 10) and RC is far from constant (figure 8). This different behaviour of R can only be a consequence of the fact that the range for p_w change is different in these two cases. After a negative going middle ear pressure change the windows move further outward, after a positive change they move inward. The ranges for change of $p_i - p_c$ are the same in both cases (0 to +5 and -5 to 0 cm water).

It is not unlikely that the flow resistance of the aqueduct depends on window position, considering the shape of the round window. Based on a two-dimensional electron microscopic image, shown in figure 11 (Toriya et al. 1991a), and on (unpublished) light microscopic images obtained in our laboratory, this shape was reconstructed as drawn in figure 12. The pouch-like extension of the membrane possibly obstructs the aqueduct opening when the membrane has moved inward, explaining a high value for the flow resistance; and it could stretch the meshwork inside the opening of the aqueduct when moving outward, giving a lower resistance. This meshwork is attached to the membrane, as can be seen in figure 11.

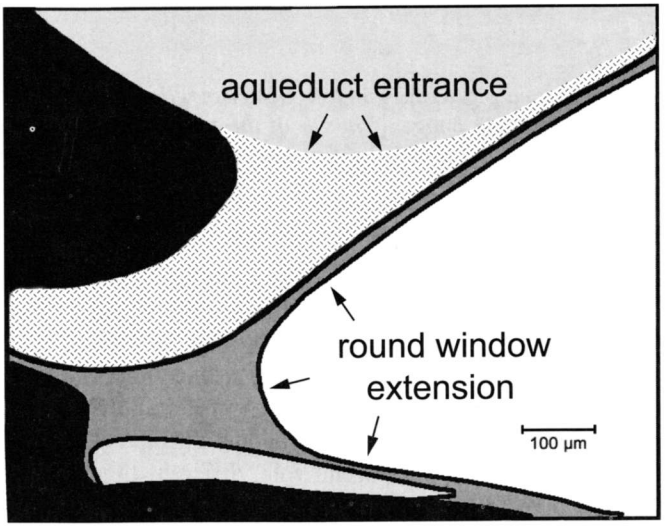

Figure 11. Cross-sectional view of pouch-like round window membrane extension adjacent to cochlear aqueduct entrance. This figure is an adaptation of a low power electron microscopic view of the opening of the aqueduct to scala tympani, obtained by Toriya et al. (1991a, figure 3). The aqueduct entrance is filled with a meshwork of fibroblasts and loose connective tissue (reticular cells), attached at one side to the window membrane.

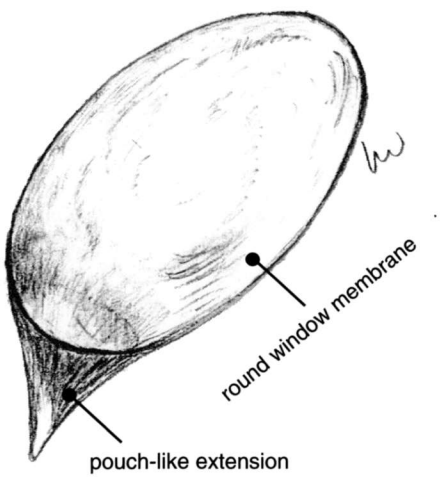

Figure 12. Shape of guinea pig round window membrane, derived from two-dimensional electron and light microscopic images. The tip of the pouch-like membrane extension is adjacent to and partly enters the opening of the cochlear aqueduct in scala tympani, as can be seen in figure 11.

It has been explained above (comparing figures 10a and 10b) that this can not be the whole story; also the pressure difference across the aqueduct plays a role. An influence of pressure difference was also found by Thalen et al. (2001), when comparing time constants for inner ear pressure release for different values of the initial pressure difference across the aqueduct. And it could furthermore be that R depends on the flow direction through the aqueduct (Thalen et al. 2002). But if the direction of flow would play an important role, different time constants would be measured for the two recovery curves in figure 3 (dashed lines), which is not the case.

Starting from figure 9b, an inner ear volume change of 83 nl can be calculated for a p_w change from +250 Pa to -250 Pa, as occured after positive going middle ear pressure changes (see figures 5 and 6). Because of the 5:1 ratio assumed for the compliance of the round and the oval window, the position change of the round window contributes 69 nl to the total volume change. The area of the guinea pig round window membrane is 1.2 mm^2 (Ghiz et al. 2001). By assuming a spherical shape for the round window membrane, a displacement of 115 μm of its center can

be calculated to correspond to this volume change of 69 nl. When this displacement is compared with the dimensions of the structures in figure 11, it must be concluded that the measured changes in R are caused by relatively small displacements of the round window membrane.
Figure 13 was constructed in an attempt to explain the shape of the resistance curves in figure 10a and 10b.

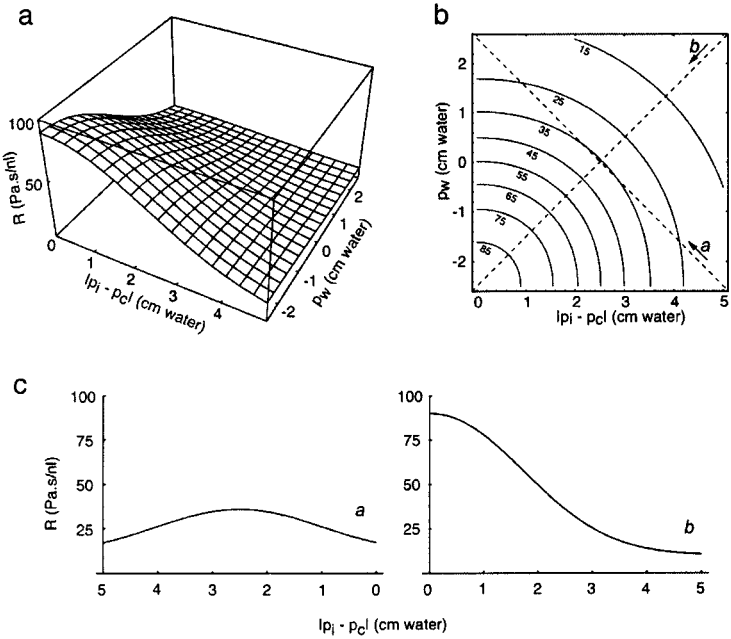

Figure 13. (a) 3D plot for the flow resistance R of the cochlear aqueduct as a function of both the pressure exerted on the inner ear fluids by the windows and (the absolute value of) the pressure difference across the aqueduct. The equation for the curved surface is

$$R = 80e^{-\left[\left(\frac{\Delta p}{\alpha}\right)\beta + \left(\frac{p_w + 2.5}{\alpha}\right)\beta\right]} + 10,$$

with $\Delta p = |\, p_i - p_c \,|$, α*=3.3,* β*=2.1. Surface parameters* α *and* β *were obtained by trial and error. (b) Contour plot for the figure shown in panel a. The dashed lines correspond with the trajectories along which* p_w *and* $|\, p_i - p_c \,|$ *change simultaneously after a sudden middle ear pressure change from 0 to +5 (trajectory b), or from +5 to 0 cm water (trajectory a). (c) Change of flow resistance R along the trajectories shown in panel b.*

The basic assumption is that R is a function of both window pressure p_w and the magnitude $|\ p_i - p_c\ |$ of the pressure difference across the aqueduct. The shape of this function is plotted in figure 13a. Figure 13a is replotted in figure 13b as a contour plot, and the dashed lines, denoted by b and a in this figure, are the trajectories along which p_w and $|\ p_i - p_c\ |$ change after a middle ear pressure change from 0 to +5 or from +5 to 0 cm water respectively. The change of R along these trajectories is plotted in figure 13c; which resembles the upper panels in figure 10. In a similar way it is possible to obtain curves that resemble those in the lower panels of figure 10 by deforming the curved surface in figure 13a somewhat.
After a sudden middle ear pressure change from 0 to -5 cm water and the subsequent return to 0 after 80 seconds, RC for inner ear pressure recovery is constant (see figure 3) and has a low value compared to the situation after a positive middle ear pressure change. Combining the value for $\tau = RC$ in figure 3 (1.7 s) with $C \approx 0.17$ (see figure 9b) gives $R \approx 10$ Pa s/nl. This value for R and the fact that R is nearly constant is well predicted by the assumption in the foregoing paragraph about the dependance of R on both window pressure p_w and the magnitude $|\ p_i - p_c\ |$ of the pressure difference across the aqueduct. This can be concluded from figure 14: after a middle ear pressure change from 0 to -5 cm water p_w changes from +2.5 to +7.5 cm and $|\ p_i - p_c\ |$ from +5 to 0 cm water. Along this pressure trajectory R hardly changes. The same holds after a middle ear pressure change from -5 to 0 cm water.
Whether the model presented in figures 13 and 14 gives a good description of the depence of aqueduct flow resistance on different middle and inner ear variables will be the subject of future research.

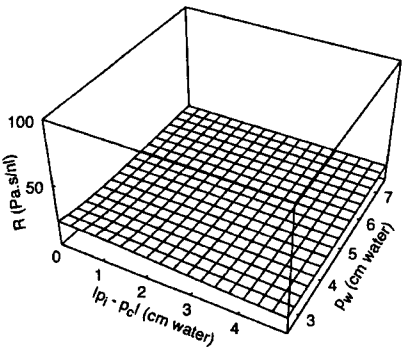

Figure 14. Continuation of the surface shown in figure 13a in the direction of larger positive values for window pressure pw, explaining the (nearly) constant low value for flow resistance R after a sudden
middle ear pressure change from 0 to 35, or from 35 to 0 cm water. The figure has the same vertical scale as figure 13a for better comparison.

Chapter 5

Cochlear aqueduct flow resistance depends on round window membrane position in guinea pigs

authors R.A. Feijen
J.M. Segenhout
H.P. Wit
F.W.J. Albers

JARO 2004; 5:404-410

Introduction

The common explanation for the symptoms of Menière's disease is an increase in endolymphatic volume ("hydrops") and, as a consequence, a pressure difference between endolymph and perilymph. Manipulation of middle ear pressure through a ventilation tube inserted in the tympanic membrane, which influences inner ear fluid pressure, is the mechanism applied by the *Meniett*™. This is a small therapeutic device, designed for the relief of symptoms in patients suffering from Menière's disease (Ödkvist et al. 2000).

The inner ear pressure change profile created by application of the *Meniett*™ has a complex shape (Feijen et al. 2000). This makes it difficult to derive the relation between the resulting inner ear pressure changes and the producing middle ear pressure changes from experiments in which the *Meniett*™ is the pressure generator. Therefore we studied inner ear pressure changes in the guinea pig induced by middle ear pressure changes with a simple rectangular profile (Feijen et al. 2002). One of the outcomes of this study was that the resistance for fluid flow through the cochlear aqueduct, which connects scala tympani with the cerebrospinal fluid space, is not constant but depends on both inner ear volume and pressure. The dependence on inner ear volume was explained by round window membrane position influencing aqueduct flow resistance (Wit et al. 2003). The study also indicated that aqueduct flow resistance does not depend on flow direction, in contrast with evidence from earlier research (Densert et al. 1981; Carlborg et al. 1982; Thalen et al. 2001, 2002).

The present study was designed to verify the relation between round window position and aqueduct resistance by keeping the pressure changes that induced fluid flow through the aqueduct as small as possible. In this way flow resistance could be measured at different (almost) constant values of inner ear volume.

Because the resistance was measured both for flow in the direction of the cerebrospinal fluid space and for the returning flow, the influence of flow direction on resistance could also be determined.

Materials and Methods

The experimental design was grossly the same as described before (Feijen et al. 2002). The head of the guinea pig was fixated and a flexible tube, glued airtight in the external meatus, was connected to a pressure generator (modified WPI 900A micropressure system (World Precision Instruments Inc., USA)) controlled by a synthesized function generator (DS345; Stanford Research Systems, USA). Also connected to this tube was an electronic pressure-measuring device (EMA 84; Erwin Halstrup Multur GmbH, Germany), to measure ear canal pressure. Via a retroauricular incision the bulla was opened. The tympanic membrane was perforated and the tip of a bevelled micropipette (tip diameter 10 μm), filled with 2 M NaCl, was introduced through the round window rim into scala tympani.

Through this tip perilymphatic pressure was measured with a second WPI 900A system. Finally the hole in the bulla was carefully closed with dental cement. The experimental set-up is schematically shown in figure 1.
A pressure change profile was applied to and monitored in the external ear canal, while the resulting perilymphatic pressure change was recorded. This stimulus consisted of a small positive pressure step of 0.5 cm water, followed after 60 seconds by a returning pressure step of –0.5 cm water, superposed on a constant pressure p_{mc}. This stimulus was repeated every 120 seconds and inner ear pressure responses to 10 successive stimuli were recorded and averaged off-line. The complete procedure was carried out for 4 values of p_{mc}: –2.5, 0, 2.5 and 5 cm water.

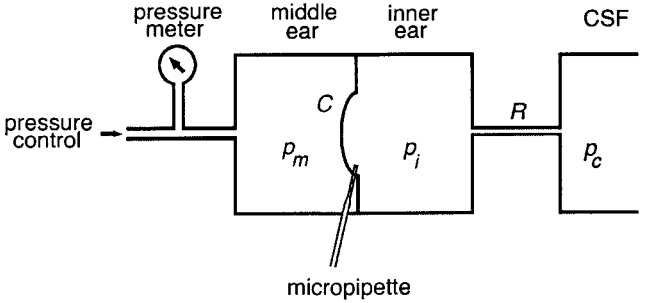

Figure 1: Experimental representation of measurement set-up. Middle ear pressure p_m is changed with an electronic pressure control system and measured with a solid state pressure meter. Inner ear pressure p_i is measured through a micropipette with a WPI micropressure system. R = flow resistance of cochlear aqueduct; C = compliance of cochlear windows (mainly of round window); p_c = pressure of cerebrospinal fluid (CSF).

Stimuli were generated on a personal computer with software for communication with the synthesized function generator (Arbitrary Waveform Composer; version 1.10). The output signals of the pressure measuring devices were A/D converted and stored on hard disk with a rate of 20 Hz. "High-frequency" fluctuations caused by breathing and heartbeat were removed off-line from the inner ear pressure recordings by digital filtering. Calibration of the pressure transducers was performed against a known water column.
This study used 4 healthy female albino guinea pigs (Duncan Hartley; HSD Poc) weighing 400 to 500 g. They were anaesthetised with ketamine hydrochloride 50 mg/ml and xylazine 20 mg/ml (in the volume ratio 2:1, at a dose level of approximately 1 ml/kg body weight), given intramuscularly. Complete muscle relaxation was obtained by intramuscular administration of suxamethonium-

chloride (5 mg/kg body weight). Body temperature was kept stable between 37 to 38 °C with a heating pad. Animals were artificially ventilated through tracheal canulation and heart rate was monitored. Both ears of the guinea pigs were experimented on and animals were sacrificed after the experiments by intracardial pentobarbital injection. The experiment was approved by the Experimental Animal Committee of Groningen University (protocol number 2439), in accordance with the principles of the declaration of Helsinki.

Analysis of results

Measurements were considered successful in 5 ears. At p_{mc} = 0 (atmospheric pressure) mean inner ear pressure was 3.4 (± 1.4) cm water.

An illustrative result of a complete series of measurements in one ear is given in figure 2.

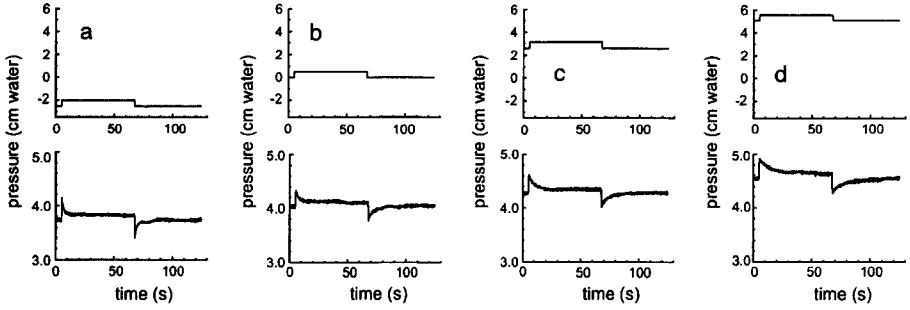

Figure 2: Middle ear air pressure (upper panels) and inner ear fluid pressure (lower panels) profiles. Small positive pressure steps of 0.5 cm water, followed after 60 seconds by small negative steps with the same magnitude, were superimposed on constant middle ear pressures of -2.5, 0, 2.5 and 5 cm water (panels a, b, c and d respectively).

The upper panels show the pressure profiles applied to the middle ear, while the resulting inner ear pressure profiles are shown in the corresponding lower panels. It is noticeable that the time constants τ for the exponentially shaped inner ear pressure recovery curves increase with increasing equilibrium middle ear pressure (from –2.5 to 5 cm water in panels a to d).

The product of the flow resistance R of the aqueduct and the compliance C of the cochlear windows was derived from the slope of these recovery curves in the following way:

R is defined as:

$$R = \frac{\Delta p}{f}, \qquad [1]$$

in which Δp is the pressure difference across the cochlear aqueduct and f is the fluid flow through it. This flow is not directly measurable. It is equal to the change of inner ear volume with time:

$$f = \frac{dV}{dt} \qquad [2]$$

Combining [1] and [2] gives:

$$R.\frac{dV}{dt} = \Delta p \qquad [3]$$

Inner ear (excess) volume V (see figure 3a) is related to the pressure p_w exerted on the inner ear fluids by the cochlear windows:

$$V = F(p_w) \qquad [4]$$

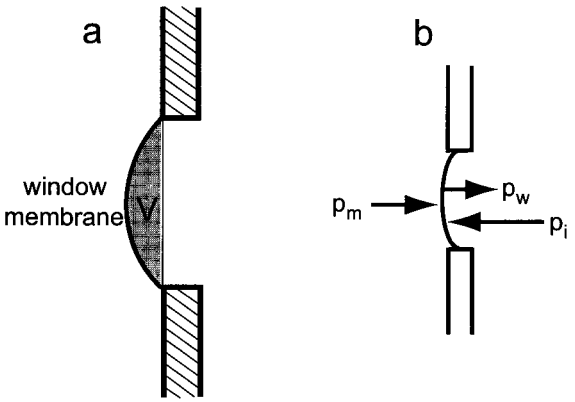

Figure 3: a. Definition of excess inner ear volume V (grey area). b. Inner ear pressure (p_i) counteracts the sum of middle ear pressure (p_m) and the pressure (p_w) exerted on the inner ear fluid by the elastic membrane: $p_i = p_m + p_w$.

Differentiating this function with respect to time gives

$$\frac{dV}{dt} = \frac{dV}{dp_w} \cdot \frac{dp_w}{dt} \qquad [5]$$

Because the compliance C of the cochlear windows is defined by $\frac{dV}{dp_w}$, the foregoing expression can be replaced by:

$$\frac{dV}{dt} = C \cdot \frac{dp_w}{dt} \qquad [6]$$

The relation between inner ear pressure p_i , middle ear pressure p_m and window pressure p_w is:

$p_i = p_m + p_w$ (see figure 3b).

So in general:

$$\frac{dp_i}{dt} = \frac{dp_m}{dt} + \frac{dp_w}{dt} \qquad [7]$$

If p_m is constant, which is the situation right after a stepwise middle ear pressure change, this relation reduces to:

$$\frac{dp_i}{dt} = \frac{dp_w}{dt} \qquad [8]$$

Combining [6] and [8] gives

$$\frac{dV}{dt} = C \cdot \frac{dp_i}{dt} = C \cdot p_i^* \ , \qquad [9]$$

And finally, from [3] and [9], the relation

$$RC = \frac{\Delta p}{p_i^*} \qquad [10]$$

is obtained.

Because it was found that *RC* is not constant during inner ear pressure recovery after a change of inner ear pressure (Thalen et al. 2002), we restricted our analysis to the first part of the recovery curves, immediately following a middle ear pressure step (at t_0). A horizontal line was fitted to the part of the measured p_i-curves preceding t_0, to obtain a value for p_1 (see figure 4). Then a sloping line (first or second order; depending on the curvature) was fitted to the part of the p_i-curves right after t_0, to obtain p_i^* at t_0 and a value for p_2 (figure 4). The difference $p_1 - p_2$ gives Δp. From the values for p_i^* and Δp the product *RC* was calculated with [10.]

The results for 4 ears are compiled in figure 5 (Results from the 5th ear were incomplete). Open circles in this figure give *RC* for a flow direction out of the ear and open squares for the returning flow. The 4 different pairs (circle + square) in one figure correspond to the equilibrium values +5, +2.5, 0 and –2.5 cm water for p_m. Fits with exponential curves were made to the data points in figure 5, both for outgoing and returning fluid flow (long and short dashes respectively). It can be

seen that the fits do not differ systematically for the two directions of flow. Averaging of the 8 fitted lines gives the relation

$$RC = 11.93 \exp(-0.285\, p_w) \qquad [11]$$

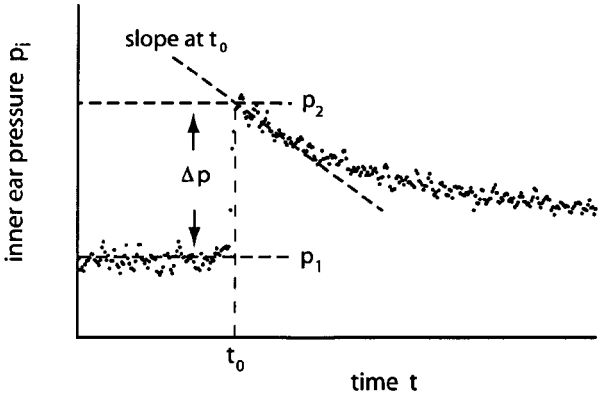

Figure 4: First part of inner ear pressure recovery curve after a middle ear pressure step. This pressure step increases inner ear pressure by Δp. The sloping dashed line is a fit to the first part of the decaying pressure curve.

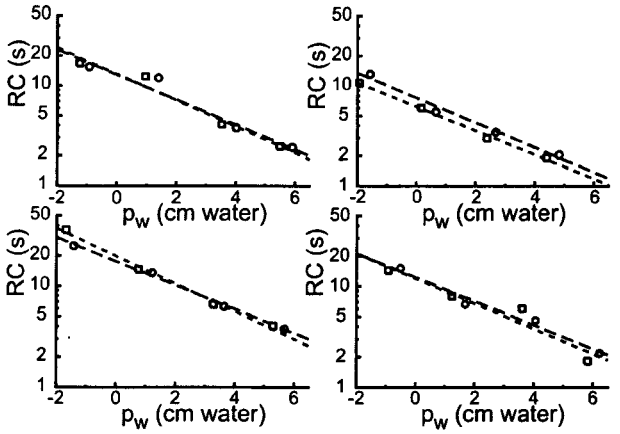

Figure 5: The product RC of aqueduct flow resistance and window compliance for different values for window pressure p_w, for 4 different ears. Circles are for fluid flow out of the inner ear, squares for the returning flow. Dashed lines are linear fits to logRC as a function of p_w (long dashes for the circles; short dashes for the squares). Window pressure p_w is inner ear pressure p_i just after a pressure step (= p_2 in figure 4 for a positive going step) minus middle ear pressure after this pressure step.

An average value of 21 Pa.s/nl was obtained for R in a direct measurement of flow resistance (Thalen et al. 2004), at a pressure of 2.8 cm water (= 280 Pa). Substituting these two values in [11] gives a value of 0.26 nl/Pa for C at p_w = 2.8 cm water. The compliance of the human cochlear windows as a function of inner ear pressure has a gaussian shape (Ivarsson and Pedersen 1977, Wit et al. 2003). If we suppose the same to be true for the guinea pig and combine this assumption with the above given value for C at p_w = 280 Pa, figure 6 can be constructed.

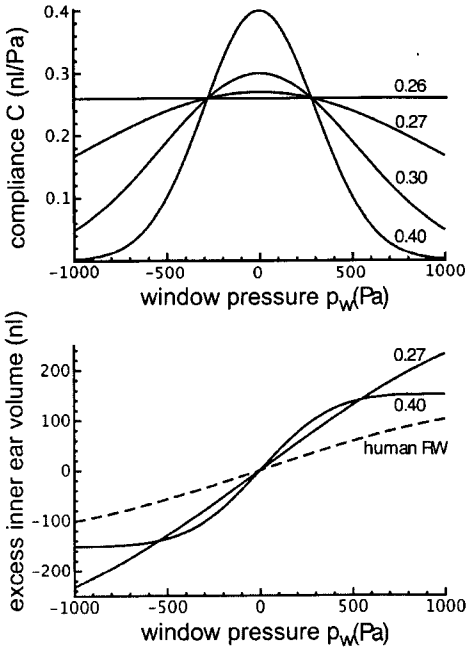

Figure 6: Upper panel: assumed gaussian shape for window compliance as a function of window pressure for 4 different values for C at p_w = 0. The curves intersect at C = 0.26 nl/Pa for p_w = 280 Pa. Lower panel: Integrals of two curves in the upper panel and, for comparison, the relation between inner ear excess volume and window pressure for the human round window.

This figure gives C as a function of p_w for different values C_0 of C at p_w = 0 in the upper panel, and the derived relation between inner ear volume V and window pressure p_w in the lower panel. The curves in the lower panel are the integrals of the gaussian curves in the upper panel. For comparison the relation is also given for the human round window (Ivarsson and Pedersen 1977).

Figure 7 gives the derived relation between excess inner ear volume V and cochlear aqueduct flow resistance R. This figure was constructed by using the relation between C and p_w as given in the upper panel of figure 6 and the relation between V and p_w as given in the lower panel of this figure. The values given by these relations were substituted in [11], for a p_w-range between –200 and +600 Pa.

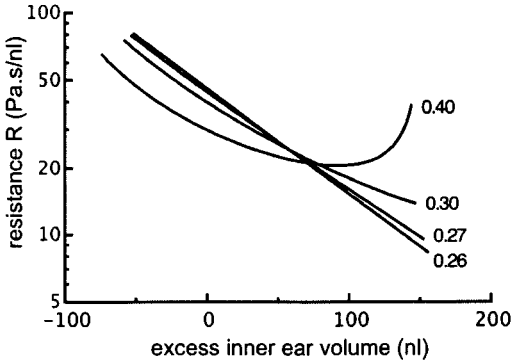

Figure 7: Derived aqueduct flow resistance R for 4 different values for C_0, as given in the upper panel of figure 6.

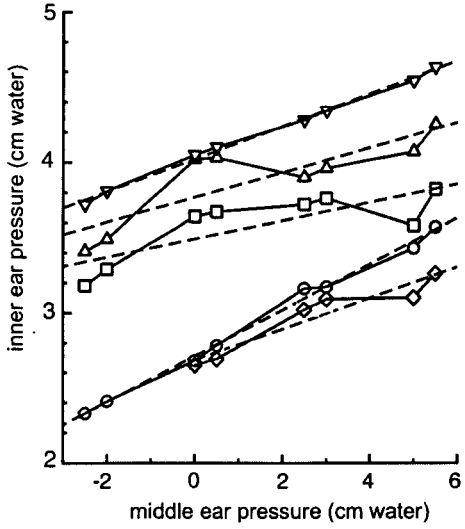

Figure 8: Permanent change of inner ear pressure for 5 ears (different symbols) for different (constant) values of middle ear pressure. Dashed lines are linear least squares fits to the data from these 5 ears. The average slope of these lines is 0.10.

It can be seen in figure 2 that the equilibrium value to which p_i returns after a pressure step slightly changes with different equilibrium values for p_w (from 3.8 cm water in panel a to 4.6 cm water in panel d). This effect was observed in all 5 investigated ears, as can be seen in figure 8. The average slope of the dashed line in this figure is 0.10.

Discussion

The value for the compliance of the guinea pig cochlear windows is not exactly known. In a previous paper we took a value of 0.17 nl/Pa (Wit et al. 2003; figure 9b), which was based on a value that was indirectly obtained by Décory et al. (1990). In the present paper we take somewhat larger values for the compliance (figure 6), to match the value for R from Thalen et al. (2004) and the product of R and C as given in [11].

Figure 7 shows that the flow resistance of the cochlear aqueduct depends on excess inner ear volume (as defined in figure 3a). This can be explained by the influence of the position of the round window on the conducting properties of the aqueduct: if the round window bulges outward (positive volume) it stretches the meshwork inside the opening of the aqueduct and lowers the flow resistance. If the window bulges inward (negative volume) the meshwork collapses and the resistance increases (Wit et al. 2003).

With this explanation the curve for C_0 = 0.40 nl/Pa in figure 7 has an unlikely shape. This gives an upper limit for C_0 that must be somewhat lower. The same conclusion can be drawn from figure 6: for C_0 = 0.40 nl/Pa the cochlear windows behave as almost completely stiff for pressures above 500 Pa ($\approx$ 5 cm water).

It can be seen in figure 5 that the time constant (τ = RC) for pressure recovery after a small pressure step changes by about a factor 10 for the applied range of pressure values. This large difference in τ -values is clearly observable in figure 2: pressure recovery is much faster in panel *a* than in panel *d*.

The relation between excess inner ear volume and the displacement of the center of the round window is given in figure 9. It was assumed that the round window has a parabolic shape with an area of 1.2 mm^2 (Ghiz et al. 2001), and that the contribution of the round window displacement to the inner ear volume change is 5 times that of the oval window (Ivarsson and Pedersen 1977).

No systematic difference exists for the relation between RC and p_w for fluid flow out of the inner ear through the cochlear aqueduct (circles in figure 5) and the returning flow (squares in the same figure). Because it is very unlikely that C depends on the direction of motion of the cochlear windows, this means that R does not depend on the direction of flow through the cochlear aqueduct. That is to say, for the flow values that occurred. With formulas [2] and [9] this range of flow values (immediately after the middle ear pressure step) was calculated to be between 0.5 and 5 nl/s. Although the possibility that R depends on flow direction

could not be excluded in earlier experiments (Thalen et al. 2001), it was concluded later that flow direction has no influence (Wit et al. 2003), which is in accordance with the present results.

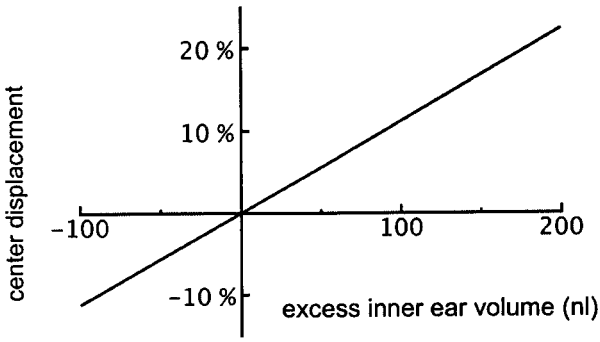

Figure 9: Calculated displacement of round window center as a function of excess inner ear volume (as defined in figure 3a), expressed in percentage of its diameter.

The pressure profile applied to the ear canal of Menière-patients by the *Meniett*™ is the sum of a "DC" pressure shift of 8 cm water during 1 second and an "AC" pressure modulation with an amplitude of 3 cm water and with a frequency of 6 Hz. This profile is repeated every 6 seconds. The DC pressure shift will move the round window inward and increase the flow resistance of the cochlear aqueduct. In this situation the AC pressure modulation will create fluid flow with changing direction, possibly mainly in the endolymphatic duct, which is the connection between the inner ear and the endolymphatic sac. Why this is beneficial to Menière-patients is unclear.

When the vestibular or cochlear aqueduct was obstructed, Suzuki et al. (1994a,b) found marked effects on the neural vestibular response to middle ear pressure changes, most probably caused by a permanent change in inner ear fluid pressure. And, contrary to what would be expected, inner ear pressure did not return to the value it had before middle ear pressure was changed in their control measurements (Suzuki et al. 1994b, no aqueduct obstructed; figures 1 and 2), both after a positive and a negative middle ear pressure change.

We observed the same effect, as is shown in figure 8. This means that in a static situation (middle ear pressure constant) inner ear pressure depends on middle ear pressure. The permanent change of inner ear pressure is about 10% of the (permanent) change in middle ear pressure. This means that the model that we proposed earlier for the relation between inner and middle ear pressure (Wit et al. 2003; figure 1) is too simple. In this model it is assumed that the CSF-space, to

which the inner ear is connected through the cochlear aqueduct, has an infinitely large compliance, making inner ear pressure always to return to the (constant) CSF-pressure in a static situation. The present results can be explained by modelling the exit of the cochlear aqueduct in the CSF-space as a closed volume, surrounded by a membrane, as schematically shown in figure 10. The compliance C_2 of this membrane must be about 9 times that of the cochlear windows (Appendix1), because the permanent change in inner ear pressure is one tenth of the change in middle ear pressure.

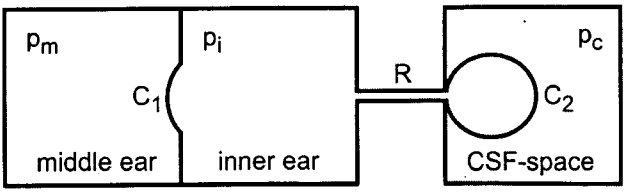

Figure 10: Schematic representation of model to explain the relation between static middle ear and inner ear pressures (mathematical formulation in Appendix 1).

However, an unsolved discrepancy remains: when fluid is injected into the inner ear, inner ear pressure rapidly returns to its pre-injection value (e.g. Takeuchi et al. 1991, Wit et al. 1999) after termination of the injection. No permanent shift of inner ear pressure was reported, although substantial amounts of fluid (a few µl) were injected. An increase in inner ear fluid volume with 1 µl in figure 10 gives an increase of p_i of about 3 cm water for the estimated values of C_1 and C_2. Such a pressure increase would have been easily observable.

Appendix 1

Starting from the situation as shown in figure 10 middle ear pressure p_m is increased by an amount Δp. This will move the membrane with compliance C_1 inward and displace a fluid volume ΔV through flow resistance R. The volume surrounded by the membrane with compliance C_2 will then expand by an amount ΔV, causing the pressure exerted by this membrane on the inner ear fluids to increase with $\frac{\Delta V}{C_2}$. Because the pressure in the CSF-space p_c is supposed to remain constant, this pressure increase is equal to the increase of inner ear pressure: $\Delta p_i = \frac{\Delta V}{C_2}$. On the other hand, Δp_i is also equal to the increase in middle ear pressure minus the decrease of the pressure exerted by the membrane with compliance C_1. In formula: $\Delta p_i = \Delta p_m - \frac{\Delta V}{C_1}$. Combining the two relations for p_i by removing ΔV gives, after some rewriting: $\frac{\Delta p_i}{\Delta p_m} = \frac{C_1}{C_1 + C_2}$.

Chapter 6

Transfer of CSF pressure fluctuations to the inner ear depends on middle ear pressure in the guinea pig

authors R.A. Feijen
J.M. Segenhout
F.W.J. Albers
H.P. Wit

submitted for publication

Introduction

When doing experiments in cats on the relation between fluid pressure in the cerebrospinal fluid (CSF) space and the inner ear Beentjes (Beentjes 1972) and also Carlborg (Carlborg et al. 1982, Carlborg and Farmer 1983) noticed that pressure variations due to breathing discontinued to be transferred from the CSF space to the inner ear, as soon as the cochlear aqueduct was blocked.
In earlier experiments (Feijen et al. 2002, Wit et al. 2003, Feijen et al. 2004) we have shown that the flow resistance of the cochlear aqueduct depends on middle ear pressure. This finding was explained by a relation between round window position and the permeability of mesh-like structures in the aqueduct.
The present experiment was designed to investigate the influence of middle ear pressure on the transfer of periodic CSF pressure fluctuations to the inner ear in more detail. For this purpose middle ear pressure was changed very slowly, in order to allow for equilibration of static inner ear and CSF fluid pressure. In this way the position of the round window changes slowly. During this change CSF pressure was modulated with a small 0.33 Hz pressure signal and both inner ear and middle ear pressure were recorded.

Materials and methods

Animal preparation

Female adult albino guinea pigs (Duncan Hartley; HSD Poc) were used in this study (n = 4). General anaesthesia was obtained with i.m. administration of ketamine hydrochloride (50 mg/ml) and xylazine (20 mg/ml) at a volume ratio of 2:1 and at a dose level of $\approx$ 1 ml/kg body weight. Complete muscle relaxation was obtained by i.m. administration of suxamethoniumchloride (5 mg/kg body weight). The animals were artificially respirated and body temperature was kept between 37 and 38 °C with a heating pad. Heart rate was monitored by means of subcutaneous needle electrodes. A screw was fixed upside down on the skull with dental cement after which fixation of the head was possible.
Animals were sacrificed after the experiment by intracardial pentobarbital injection. The experiment was approved by the Experimental Animal Committee of the Groningen University (protocol number 2439) in accordance with the principles of the declaration of Helsinki.

External ear canal pressure measurement and manipulation

A flexible tube was glued in the external auditory meatus of the guinea pig and connected to a pressure generator (modified World Precision Instruments type 900A micropressure system) and a solid state pressure measuring device (EMA 84; Erwin Halstrup Multur GmbH, Germany). The pressure generator was controlled by a synthezised function generator (Stanford Research Systems, type DS345),

producing triangular waves with a duration of approximately 16 minutes. The experimental set-up is schematically shown in figure 1.

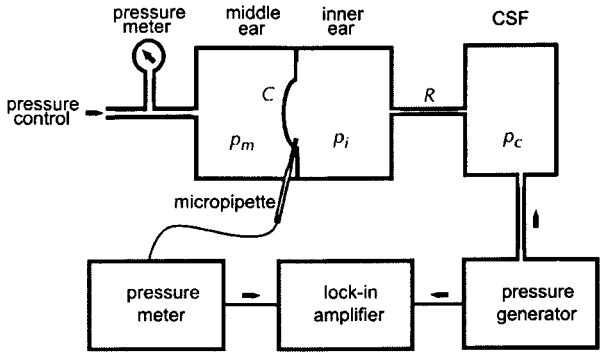

Figure 1. Schematic of experimental set-up. (p_m = middle ear pressure, p_i = inner ear pressure, p_c = cerebrospinal fluid pressure, C = compliance of the windows, R = flow resistance of the cochlear aqueduct).

Inner ear pressure measurement

The middle ear cavity was opened via a retroauricular incision. From the cavity side a large perforation was made in the tympanic membrane. The bevelled tip of a micropipette (tip diameter 10 μm), filled with 2 M NaCl, was introduced in scala tympani through the rim of the round window, to measure inner ear pressure with a second WPI 900A micropressure system. After this the round window membrane was inspected for leakage of fluid along the pipette tip. The hole in the bulla was closed carefully with dental cement around the micropipette.

Intracranial pressure measurement

A hole was drilled in the cranium of the guinea pig without damaging the dura. In this hole a stainless steel tube was fixed with dental cement. The tube was connected to a pressure generator (another modified WPI micropressure system). The pressure generator was controlled by a second synthezised function generator (Stanford Research Systems, type DS345), producing sinusoidal waves with a frequency of approxamitely 0.33 Hz. The amplitude of the evoked 0.33 Hz component in the inner ear pressure signal was measured with a lock-in amplifier (Stanford Research Systems, type SR830).

Data

Calibration of the transducers was performed against a known water column. The output signals of the middle ear and the inner ear pressure measuring devices as well as the output signal of the lock-in amplifier were stored on hard disk with a

rate of 20 Hz. Off-line calculations were performed with a Mathematica 3.0 software package.

Results

Successful experiments could be performed in 6 ears of 4 guinea pigs.
Figure 2 is a typical result of the simultaneous recording of middle ear pressure p_m and inner ear pressure p_i in a guinea pig ear. The insert in this figure shows "fast" periodic changes of the p_i-signal.

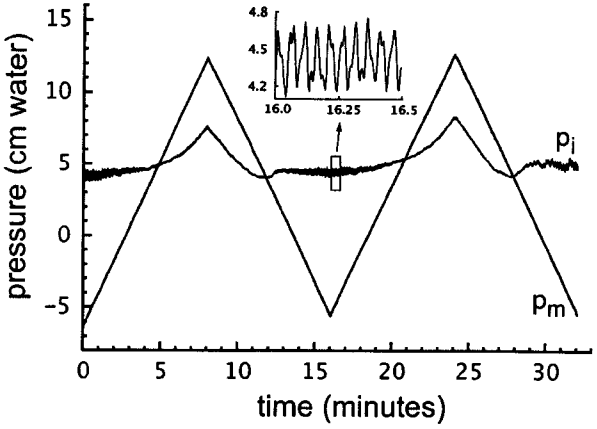

Figure 2. Change of middle ear pressure (p_m) and inner ear pressure (p_i) during very slow variation of p_m. The insert shows periodic "high" frequency components in p_i, caused by artificial ventilation of the animal and by 0.33 Hz variation of CSF pressure.

Frequency analysis of the p_i-signal - as shown in figure 3 - reveals two components: one at 0.33 Hz and one at 0.75 Hz. The first component is caused by the periodic variation of CSF pressure with an external pressure generator; the second component is due to artificial ventilation of the animal with a rate of 45 strokes per minute. The envelopes in the time-domain of both components were obtained by digital filtering and Hilbert-transformation.
These two envelopes are given in figure 4. In figure 5 the envelope of the 0.33 Hz component is compared with the output signal of the lock-in amplifier.

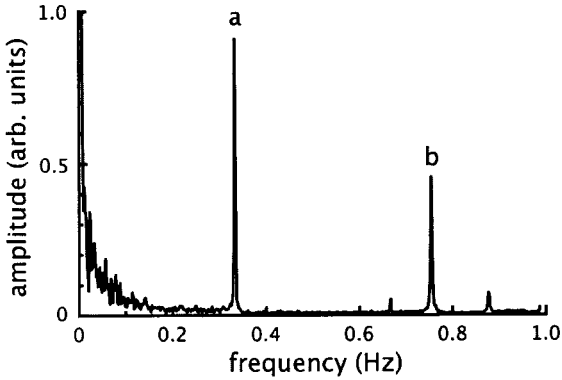

Figure 3. Frequency spectrum of the "high" frequency components in inner ear pressure at 0.33 Hz (peak a) and at 0.75 Hz (peak b). This spectrum was obtained by fast Fourier transformation (FFT) of the p_i-signal in figure 2.

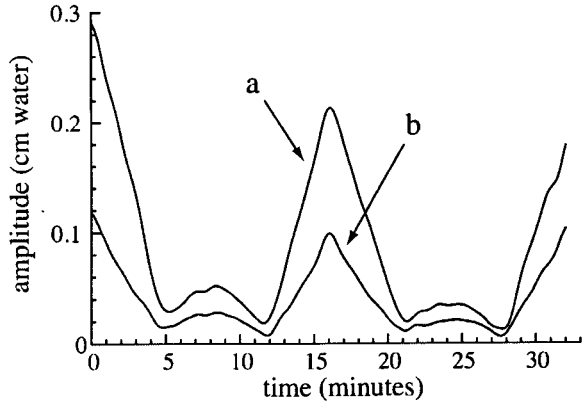

Figure 4. Amplitudes of the 0.33 Hz component (a) and the 0.75 Hz component (b) in the inner ear pressure signal in figure 2.

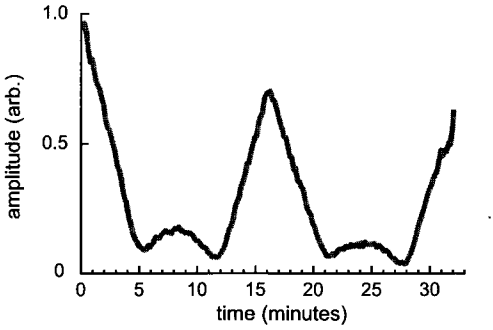

Figure 5. Dashed line: same as curve a in figure 4. Thick gray line: Output signal of lock-in amplifier. Vertical scale of both curves have been normalized.

The four half periods of the two envelopes in figure 4 were averaged and plotted against the pressure exerted on the cochlear fluids by the cochlear windows in figure 6. This window pressure was derived from figure 2 as p_i - p_m.

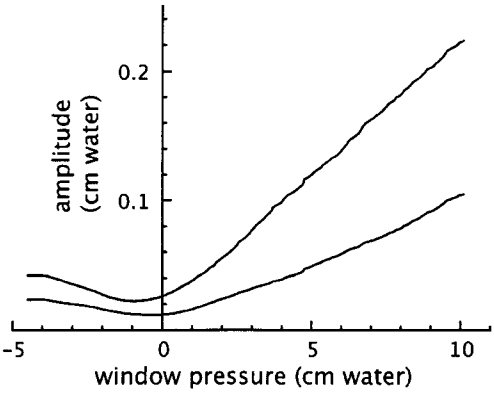

Figure 6. Amplitude of the 0.33 Hz and 0.75 Hz components in the inner ear pressure signal in figure 2 as a function of window pressure, which is the difference between inner ear and middle ear pressure.

For this purpose the "high" frequency components were removed from the p_i-recording by digital filtering. Because the envelopes of the "high" frequency components and the lock-in amplifier recording have the same shape (see figure 5), the latter recording was used to construct figure 7 from the results obtained in 6 different ears. For these 6 ears p_i (with "high" frequencies removed) is plotted against p_m in figure 8, both for increasing and decreasing middle ear pressure.

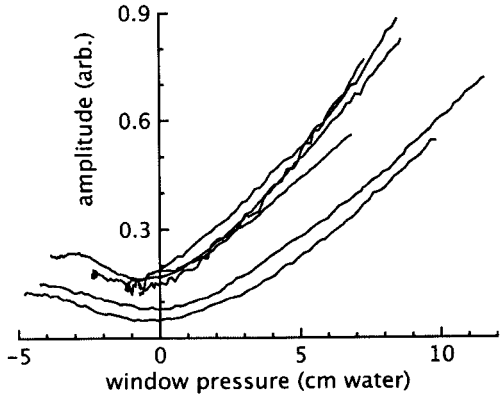

Figure 7. Amplitude of 0.33 Hz component in inner ear pressure signal as a function of window pressure for 6 different ears.

Discussion

Window pressure p_w is a measure for the position of the cochlear windows. A positive pressure corresponds with outward bulging windows. In this position the windows exert a positive pressure on the inner ear fluids, caused by elastic forces. A negative p_w means that the windows have moved inward.

Figure 7 shows that the amplitude of the 0.33 Hz component in the inner ear pressure recording, caused by manipulation of CSF pressure, depends on window pressure for all 6 investigated ears. Changes in CSF pressure reach the inner ear mainly through the cochlear aqueduct. This means that figure 7 most easily can be explained by assuming that the flow resistance of the cochlear aqueduct depends on window pressure. For negative pressure (inward bulging windows) this resistance is large. For positive pressures (outward bulging windows) this resistance is much lower.

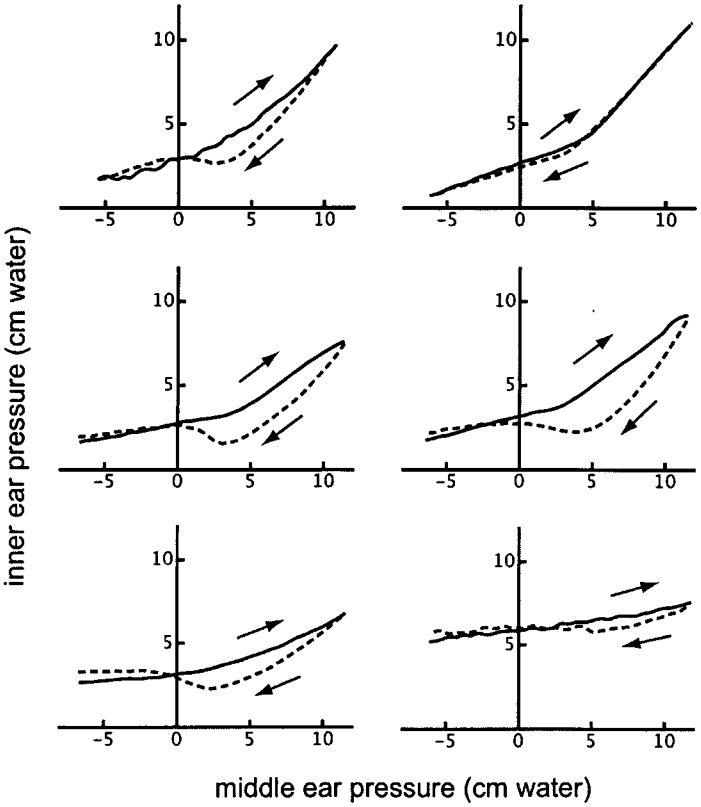

Figure 8. Change of inner ear pressure (with "high" frequency components removed) during very slow variation of middle ear pressure. Solid lines: upward change of middle ear pressure. Dashed lines: downward change of middle ear pressure.

A similar relation between window pressure and aqueduct resistance was found in earlier work (Wit et al. 2003, Feijen et al. 2004) and explained as follows: The opening of the cochlear aqueduct in scala tympani is adjacent to a pouch-like extension of the round window. This opening is filled with a fibrous structure (periotic duct) that is connected to the window extension. Change of window position changes the traction force on the fibrous structure and (assumably) influences the flow resistance of the aqueduct opening.
In a previous paper (Feijen et al. 2004) we reported a relation between middle ear and inner ear pressure. Such a relation is confirmed in the present experiment (see figure 8). For al 6 investigated ears inner ear pressure follows middle ear pressure, if middle ear pressure changes slowly. And the shape of the change curves in figure

8 depends on the direction of middle ear pressure change, as indicated by arrows. The time constants for pressure recovery after a sudden change of inner ear pressure is a few seconds (Thalen et al. 2002). In the present experiment the time course of middle ear pressure change is two orders of magnitude slower. It was therefore expected that inner ear pressure would remain constant, because the inner ear is connected to the CSF reservoir with constant pressure through the aqueduct.
Up to now we have not found a plausible explanation for the relation between middle ear pressure and inner ear pressure as observed in the present experimental set-up. It might be that the inner ear is not directly connected with a large reservoir with constant pressure, but this is contradictory to the results of experiment in which fluid is injected into the inner ear (Takeuchi et al. 1991, Wit et al. 1999). In the latter experiments inner ear pressure returns quickly to its equilibrium value (which is supposed to be CSF pressure). So this problem needs further experiments.

Chapter 7

Treatment of Menière's disease with intermittent middle ear pressure
a randomized controlled trial

authors R.A. Feijen
H.P. Wit
F.W.J. Albers

submitted for publication

Introduction

Menière's disease is characterised by the triad of symptoms: fluctuating neurosensory hearing loss, tinnitus and vertigo and is often accompanied by the feeling of aural fullness. Menière's attacks are often unpredictable and incapacitating, and may prevent the activities of daily living. The cause of the disease remains unknown (in spite of the relatively frequent incidence of the inner ear disease) and therapy is often symptomatic.

Endolymphatic hydrops, secondary to an imbalance of secretion and absorption of endolymph, is commonly accepted to be the histopathological epiphenomenon of Menière's disease (Merchant et al. 1995). So it is no surprise that many therapeutics options (more or less experimental) focus on influencing a possible endolymphatic hydrops and/or endolymphatic overpressure.

In 1997 Densert et al. (Densert et al.1997) presented a study in which pathologic electrophysiological inner ear parameters improved immediately after intermittent increase of middle ear pressure. They suggested that an increase of inner ear fluid transport or a change in vascularization of the hydropic inner ear could give a transient decrease of endolymphatic hydrops, but the exact therapeutic mechanism remains elusive. This gave rise to the development of a commercially available pressure device (*Meniett*™; Medtronic Xomed, Inc.; USA) for the treatment of Menière's disease. In later studies benefit of middle ear pressure therapy was found for respectively hearing loss (Ödkvist et al. 2000) and vertigo (Gates et al. 2004, Tomsen et al. 2005).

Aim of the present study was to evaluate the efficacy of middle ear pressure therapy for Menière's disease on hearing improvement and other clinically relevant parameters in a double-blind, placebo-controlled study design.

Patients and Methods

Population, Enrolment and Assignment

This study was conducted at the University Hospital Groningen from 2002 until 2004. Informed written consent was required from all patients before inclusion in the study. Patients received a letter with a short explanation about the aim of the study and with the request to contact the researchers by telephone if they were interested. The study was approved by the Medical Ethics Committee of the University Hospital Groningen.

Inclusion criteria included Menière's disease in one ear and a minimum age of 18 years. Menière's disease was diagnosed if the following three criteria were fulfilled: cochlear hearing loss of at least 20 dB at one of the pure-tone audiogram frequencies, tinnitus and periodic attacks of vertigo (at least two in the past, with a duration of more than 20 minutes). The diagnosis Menière's disease was established by means of the Diagnostic Protocol Groningen (Mateijsen et al. 2002). This diagnostic protocol consists of routine ENT examination, audiovestibular

tests, routine laboratory investigations, measurement of blood pressure, oto-acoustic emission examination and magnetic resonance imaging (MRI) of the temporal bones and the cerebellopontine angle. With this protocol other pathologies could be ruled out and the diagnosis Menière's disease was affirmed. Patients were ineligible for entry in this study for any of the following reasons: Menière's disease in both ears, endolymphatic sac surgery in history, former pressure therapies, medication for Menière's disease within 4 weeks prior the start of the study or a dysfunctional middle ear ventilation tube.

Study design

The study was designed as a prospective, randomized, double-blind, placebo-controlled clinical trial. Randomization was performed by an external office. One group was randomized for pressure therapy and one group for placebo therapy. Stratification for age took place (as hearing deteriorates with increasing age). Patients and evaluators were unblinded after all patients had fulfilled the study.
Patients were seen three times at the outdoor clinic, in a period of six weeks (figure 1). At the first visit (t_1) a ventilation tube (Aero-Tymp®, Entermed b.v.; The Netherlands) was placed during local anaesthetics. Measurements took place immediately before and after the placement. Two weeks later (t_2) the patency of the ventilation tube was checked and randomization was performed. During that visit the assigned device was used under supervision of the also blinded researcher (author R.A.F., MD). Again measurements took place before and directly after the use of the device. After this the patients used the assigned device at home three times a day for a period of four weeks. At the last visit (t_3) the patency of the ventilation tube was checked again and final measurements were done.

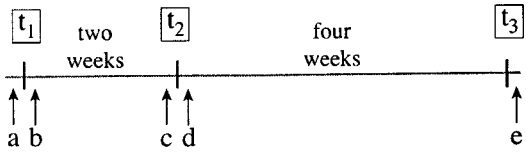

Figure 1. Schematic time window of study. t_1 = placement of ventilation tube; t_2 = first time therapy; t_3 = end of study; $t_2 - t_3$ = four weeks of therapy; a, b, c, d and e indicate the measurements.

Therapy

A *Meniett*™ generates 3 periods of 12 positive pressure pulses, after a built in air-tight test (Feijen et al. 2000). One period lasts approximately 75 seconds and a whole series lasts approximately 6 minutes, after which the device turns of automatically. A single pressure pulse is the sum of a static positive component

(≈ 8 cm water) and a component oscillating with a frequency of approximately 6 Hz (amplitude ≈ 3 cm water).
The placebo device is a *Meniett*™ look-a-like. It also starts with a built in air-tight test which is repeated every 30 seconds. However, in between these tests the device is inactive. After a period of 6 minutes it will turn of automatically.
The pressure pulses are transmitted to the middle ear cavity via a tubing and a fitting earplug through the middle ear ventilation tube. Patients were instructed how to insert an earplug in their ear canal and a written information guide was given to them for use at home.

Measurements: Audiometric and subjective parameters
Change in hearing levels was evaluated with Von Bekesy audiometry (Clinical Audiometer AC40, Interacoustics, Inc.; USA) at 500, 1000, 2000 and 4000 Hz, with a pulsed tone.
Emission measurements were performed in a sound-proof chamber with the Madsen Cochlear Emissions Analyzer (GN Otometrics; Denmark; software Noah 2.0a). Click evoked oto-acoustic emissions were measured using the nonlinear mode with 80-μs pulses. The stimulus level was about 80 dB SPL. The criteria for a valid click evoked oto-acoustic emission were a successful probe fit and a reproducibility of 70% or higher (Lutman 1993). In case of a reproducibility between 40% and 70% visual inspection was used to decide whether a click evoked oto-acoustic emission was present or not.
Patients were asked to grade hearing loss, vertigo, tinnitus and aural fullness using a standard visual analogue scale (VAS), which ranges from 0 – 10 cm (0 = no symptoms, 10 = maximal complaints).
Patients were asked to register their typical Menière's attacks during the four weeks therapy period.

Data analysis
A subject record form was used for data collection. Storage and statistical analysis was performed using a standard software package (SPSS 10.0). A parametric test (T-test,) or a non-parametric test (Mann-Whitney U test (MWU)) was used to analyse the effects, regarding the distribution of the analysed parameters. $P \leq 0.05$ (two-tailed) was considered significant.

Results
Population characteristics
59 Menière patients who met the criteria were included in the study. Two patients were excluded for analysis during the study; one patient because of an acute otitis media three weeks after placement of the ventilation tube and one patient withdrew because of experiencing too overwhelming Menière's symptoms (both in therapy group). No patients experienced user or technical problems when using the device.

Of the 57 patients who finished the study (see table 1) 29 patients were randomized for placebo therapy (11 female, 18 male; mean age 55.0 years) and 28 patients for pressure therapy (12 female, 16 male; mean age 52.7 years). Average duration of symptoms of the disease was 87.3 months for the control group and 80.8 months for the therapy group. The average frequency of Menière attacks in the placebo group was 28.3 times a year and 13.0 times a year in the therapy group. All above mentioned characteristics were equally distributed between groups (MWU).

Table 1. Patients and Characteristics

	Control (N =29)	*Therapy (N = 28)*	P-value†
Age (year; mean ± SE)	52.7 (1.8)	55.0 (1.9)	0.354
Sex	11 F, 18 M	12 F, 16 M	0.707
Affected ear	13 AD, 16 AS	12 AD, 16 AS	0.882
Duration of symptoms (month; mean ± SE)	87.3 (11.4)	80.8 (8.1)	0.917
Frequency attacks (a year; mean ± SE)	28.3 (12.9)	13.0 (5.0)	0.681
Last attack (days; mean ± SE)	306.1 (79.8)	406.8 (114.8)	0.631

(†Mann-Whitney U test; $P \leq 0.05$ is considered significant different)

Table 2 gives the audiometric parameters and he VAS scores at the beginning of the study.

Table 2. Parameters at start of study

		Control	*Therapy*	P-value	N
Bekesy audiometry (dB HL; mean ± SE)	500 Hz	46.8 (4.2)	52.3 (3.8)	0.338 t	55
	1000 Hz	41.9 (4.0)	50.7 (3.1)	0.096 t	55
	2000 Hz	41.3 (3.9)	43.2 (3.7)	0.723 t	55
	4000 Hz	49.7 (3.4)	52.4 (3.4)	0.586 t	53
Visual analogue scale (cm; mean ± SE)	vertigo	1.1 (0.3)	1.2 (0.4)	0.872 m	57
	tinnitus	6.0 (0.4)	6.1 (0.6)	0.994 t	57
	hearing	6.2 (0.5)	7.0 (0.4)	0.223 t	57
	aural fullness	4.9 (0.6)	3.6 (0.7)	0.181 t	57

(t = T-test; m = Mann-Whitney U test; $P \leq 0.05$ is considered significant different)

Figure 2 gives the average Extended Fletcher Index (EFI; mean HL (dB) for 500, 1000, 2000 and 4000 HZ) for both groups. These parameters did not differ between groups (MWU). Nine patients did have a measurable click evoked oto-acoustic emission at the beginning of the study. Figure 3 gives the level of click evoked oto-acoustic emissions (for both groups) and the corresponding EFI.

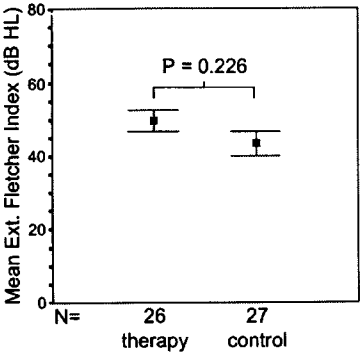

Figure 2. The average (SE) Extended Fletcher Index (EFI = mean HL (dB) for 500, 1000, 2000 and 4000 HZ) at start of study. Control group = 43.4 dB HL (SE 2.9); therapy group = 49.6 dB HL (SE 2.9). Note that the number of measured EFIs does not correspond with the total number of patients; for one patient in the control group hearing levels could not be determined for 2000 and 4000 Hz, as it was for one patient for 4000 Hz, hearing levels could not be determined for all the frequencies for two patients in the therapy group.

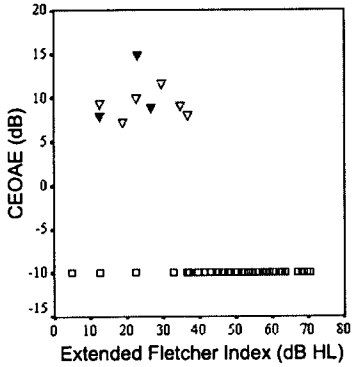

Figure 3. Amplitudes of click-evoked oto-acoustic emissions as a function of the Extended Fletcher Index at the beginning of the study. The triangles indicate the subjects from which an emission was measured (open triangles randomised for placebo therapy (n=6), filled triangles randomised for placebo therapy n=3). The open squares indicate the subjects from which no emission could be measured (the amplitude is consequently meaningless).

Outcome after the first time therapy

Outcome after the first time therapy was defined as a change in parameter after using the device for the first time (see figure 1; direct outcome = d – c, thus a positive number indicates a negative effect and the other way around).

Figure 4 gives the mean change in hearing level (dB) for 500, 1000, 2000 and 4000 Hz. These changes did not differ significantly between groups.

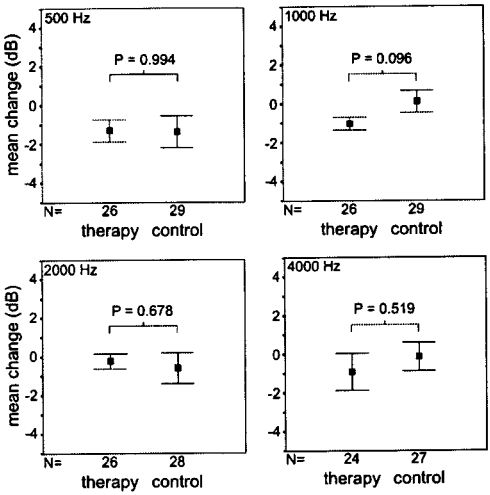

Figure 4. Mean change in hearing level (dB) directly after therapy once for respectively 500, 1000, 2000 and 4000 Hz. Control group: –1.4 dB (SE 0.81), 0.1 dB (SE 0.58), –0.6 dB (SE 0.81) and –0.1 dB (SE 0.73); Therapy group: –1.3 dB (SE 0.58), –1.0 dB (SE 0.34), –0.2 dB (SE 0.39) and –0.9 dB (SE 0.96). $P \leq 0.05$ was considered significant (T-test).

Figure 5 gives the mean change in VAS score for respectively vertigo, tinnitus, hearing loss and aural fullness. These changes did not differ significantly between groups.

Two weeks after placement of the ventilation tube click evoked oto-acoustic emissions could be measured in eight subjects. Two of the nine patients with a measurable click evoked oto-acoustic emission at the beginning of the study lost their click evoked oto-acoustic emission and by one patient a click evoked oto-acoustic emission became measurable after placement of the tube. Of these eight subjects six were in the control and two in the therapy group. No systematic changes could be observed directly after the first time therapy. No click evoked oto-acoustic emission appeared after therapy.

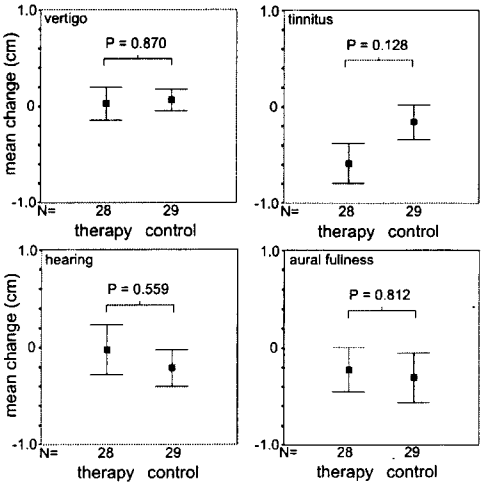

Figure 5. Mean change in VAS (cm) directly after therapy once for respectively vertigo, tinnitus, hearing loss and aural fullness. Control group: 0.1 cm (SE 0.11), –0.2 cm (SE 0.18), –0.2 cm (SE 0.19) and –0.3 (SE 0.25); Therapy group: 0.0 cm (SE 0.17), –0.6 cm (SE 0.21), 0.0 cm (SE 0.26) and –0.2 cm (SE 0.22). P ≤ 0.05 was considered significant (T-test).

Outcome after four weeks therapy

Outcome after four weeks of therapy was defined as a change in parameter after using the device for four weeks at home (see figure 1; direct outcome = e – c, thus a positive number indicates a negative effect and the other way around).

Figure 6 gives the mean change in hearing level for respectively 500, 1000, 2000 and 4000 Hz. These changes did not differ significantly between groups.

Figure 7 gives the mean change in VAS score for respectively vertigo, tinnitus, hearing loss and aural fullness. These changes did not differ significantly between groups.

Of the eight patients with a measurable click evoked oto-acoustic emission the emission could no longer be measured after four weeks of therapy in two subjects (both in the control group). No overall systematic change in emissions could be observed. No click evoked oto-acoustic emission appeared after four weeks of therapy.

There was no difference in the mean number of attacks during the four weeks of therapy between the therapy group (2.36; SE 1.14) and the placebo group (0.93; SE 0.38); P = 0.611 (MWU).

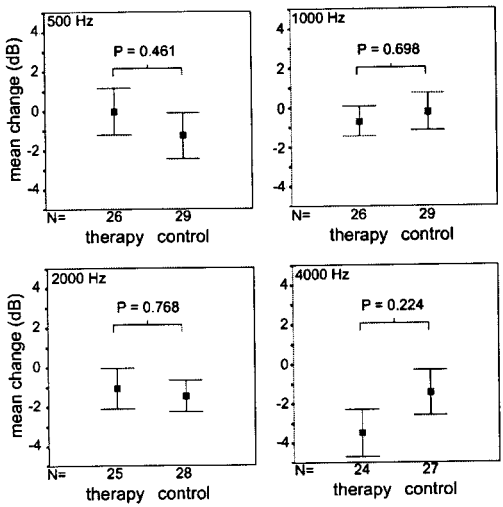

Figure 6. Mean change in hearing level (dB) after four weeks of therapy for respectively 500, 1000, 2000 and 4000 Hz. Control group: –1.3 dB (SE 1.17), –0.2 dB (SE 0.96), –1.5 dB (SE 0.81) and –1.4 dB (SE 1.16); Therapy group: –1.3 dB (SE 1.17), –0.7 dB (SE 0.77), –1.1 dB (SE 1.03) and –3.5 dB (SE 1.19). $P \leq 0.05$ was considered significant (T-test).

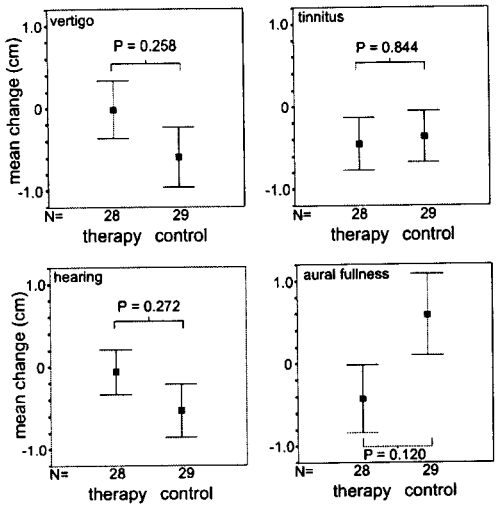

Figure 7. Mean change in VAS (cm) after four weeks of therapy for respectively vertigo, tinnitus, hearing loss and aural fullness. Control group: –0.6 cm (SE 0.36), –0.4 cm (SE 0.31), –0.5 cm (SE 0.32) and 0.6 (SE 0.49); Therapy group: 0.0 cm (SE 0.35), –0.5 cm (SE 0.32), –0.1 cm (SE 0.27) and –0.4 cm (SE 0.41).

Side Effects
Figure 8 gives the mean change in VAS score, for the whole study population, two weeks after the placement of a ventilation tube (see figure 1; c – a). Both vertigo and tinnitus worsened statistically significant (+0.7 cm). Hearing and aural fullness did not change statistically significant (respectively –0.1 and –0.2 cm).

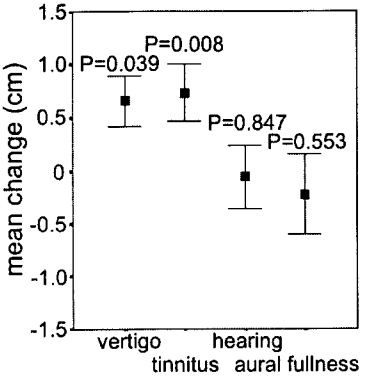

Figure 8. Mean change in VAS (cm) two weeks after placement of the ventilation tube for respectively vertigo, tinnitus, hearing loss and aural fullness (respectively : 0.7 cm (SE 0.24), 0.7 cm (SE 0.27), –0.1 cm (SE 0.30) and 0.2 (SE 0.38). $P \leq 0.05$ was considered significant (related T-test for tinnitus, hearing and aural fullness; related MWU for vertigo).

Discussion
Intermittent middle ear pressure changes delivered by the *Meniett*™ (direct as well as for a three times a day regimen for a period of four weeks) do not have positive effects on hearing levels in the Menière's patients tested by us. A slight ($\approx$ 1 dB) positive direct therapy effect can be seen for 1000 Hz (figure 4) and for 4000 Hz after four weeks therapy (figure 6) compared with the control group, but this difference is not of statistical nor of clinical significance.
The VAS scores assessing the feeling of vertigo, tinnitus, hearing loss and aural fullness also did not differ significantly between groups and the average changes ranged between –1 and 1 cm. It can be seen in figure 5 that there is a slight improvement in both groups for tinnitus as well as for aural fullness with a slight beneficial therapeutic effect for tinnitus. After four weeks of therapy (figure 7) a slight improvement for the feeling of vertigo, tinnitus and hearing loss was found. For vertigo and tinnitus this was in contrast with the therapy group in which these feelings did not change on average. In the therapy group there was a relief in aural fullness which worsened in the control group. Intermittent middle ear pressure does

not seem to have a systematic beneficial effect on the feeling of hearing loss, vertigo, tinnitus and aural fullness.
Only nine of our patients did have measurable click evoked oto-acoustic emissions (figure 3). Oto-acoustic emissions are considered to be a product of the outer hair cells and absence or presence of the emissions are a projection of inner ear function (Probst et al. 1997). When hearing impairment is larger than approximately 30 dB (HL) CEOAEs are absent. Since hearing loss did not improve with intermittent middle ear pressure it is a logical consequence that CEOAEs did not recover nor that a systematically change was found.
The negative side effects of the tympanostomy tube in the present study were insignificantly small (see figure 8). Montandon et al. (1988) described a therapeutic effect of middle ear ventilation and 82% of their patients did find relief of vertigo or even complete remission. Our findings are more in accordance with the study of Maier et al. (1997), in which no systematic dysfunctioning Eustachian tube in Menière's patients was found.
Our results are in contrast with the results presented by Ödkvist et al. (2000) and Gates et al. (2004), who separately reported on a study with active Menière's disease. While significant improvement in hearing level and subjective parameters (VAS) after two weeks of therapy was noted in Ödkvist's therapy group (n=31), there was no improvement in the placebo group (n=25). No details are given on how the two groups were compared statistically. The results of Gates' four month randomized, multi-institution study (n=67) were also promising. Their study mainly focused on vertigo using symptom report cards and the effect of the *Meniett™* was striking for the first month interval. However, after four months the treatment effect disappeared almost entirely, perhaps due to the nature of the disease. Like in our present study no positive effect on hearing was found. The patients in the present report were not selected on disease activity but mainly wanted treatment for hearing loss. Especially the severity of vertigo is a measure for a typical Menière's attack and with a mean VAS score of 1.1 cm (see table 2) one can conclude that disease activity was low. Main complaints of he Menière's patients tested by us were tinnitus and hearing loss and to a lesser extent aural fullness (see VAS scores table 2). Given the negative results in this study it can not be ruled out that middle ear pressure therapy only has a role in active Menière's disease. To compare the results of our study with that of the studies that selected according to disease activity we selected the group of subjects with a typical Menière's attack within two months prior to the study. Ten subjects in the therapy group and thirteen in the control group subscribed to this criterion. In respectively figures 9 and 10 it can be seen that there is no systematic effect in the extent of hearing loss and in vertigo. Because groups are too small for sufficient statistical analysis no conclusions can be drawn but it can be expected that even for groups with a sufficient number of subjects changes probably will be insignificant.

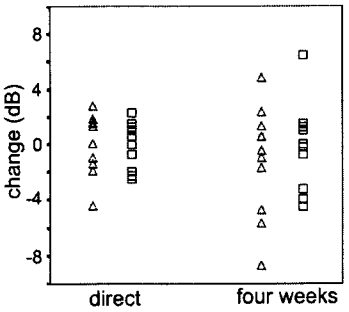

Figure 9. Change in Extended Fletcher Index (dB) respectively directly after therapy and after four weeks of therapy for a selection of patients with a typical attack within two months prior to the study. Triangles indicate the therapy group and squares the control group.

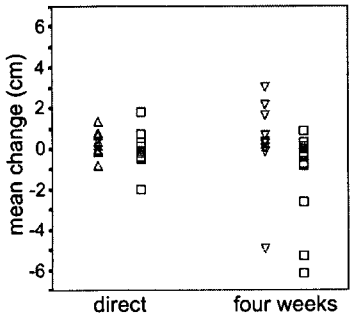

Figure 10. Change in the extent of vertigo VAS score (cm) respectively directly after therapy and for four weeks of therapy for a selection of patients with a typical attack within two months prior to the study. Triangles indicate the therapy group and squares the control group.

Middle ear pressure mainly has an effect on the round window membrane compared to the oval window because of its approximately five times greater compliance (Ivarsson and Pedersen 1977). So positive middle ear pressure produces an inward movement of the round window membrane (Wit et al. 2002). An inward movement of the round window membrane increases the resistance of the (guinea pig) cochlear aqueduct, which is the main pressure outlet of the inner ear (Feijen et al. 2004). If the same holds for humans (having a patent aqueduct (Gopen et al. 1997)) positive middle ear pressure, as delivered by the *Meniett*™, will temporary obstruct inner ear fluid pressure release. It can be hypothesized that

during this period the oscillating pressure component will have a beneficial effect on for instance the endolymphatic sac and/or duct (or other structures in the inner ear).

Chapter 8

Summary and conclusions

Summary and conclusions

The development of the *Meniett*™, a small pressure device for therapeutic use in Menière's disease, leaded to research described in this dissertation. The middle ear pressure of guinea pigs was changed with special emphasis on the inner ear pressure transfer properties. In a randomized clinical trial the efficacy of intermittent middle ear pressure for Menière's disease was assessed.

The *Meniett*™ pressure signal in the inner ear, when delivered to the external ear after perforating the tympanic membrane of guinea pigs, is described in chapter 2. The *Meniett*™ generates 3 periods of 12 positive pressure pulses. It was found that a single pressure pulse is the sum of a static positive component and a component oscillating with a frequency of approximately 6 Hz. The induced complex pressure signal in the middle ear cavity is transferred instantly and almost unchanged to the inner ear of guinea pigs. An average undershoot of –1.0 cm water with respect to the steady-state pressure is seen after application of a pressure pulse, that is released in a few seconds. A linear physical model was introduced to explain the results. The pressure change caused a transient flow out of the inner ear (most probably through the cochlear aqueduct according to the literature) and using the model it seemed that more inner ear fluid was pressed out of the inner ear than returned after the middle ear pressure change. However, the steady state inner ear pressure did not change after the middle ear pressure changes and it is unlikely that there is a net volume displacement.
It can be concluded that the linear model is too simple. The model assumes a constant inner ear compliance and a constant flow resistance of the cochlear aqueduct and the discrepancy can be solved when a directional dependent flow resistance is assumed, being higher when flow is directed towards the subarachnoid space.

In chapter 3 the inner ear fluid pressure of guinea pigs is described during square wave middle ear cavity pressure variation. Time constants were derived, a product of inner ear compliance and flow resistance, for the slopes of the inner ear pressure recovery curves after middle ear pressure change. A single exponential function did not fit well and therefore more complicated functions (found by trial and error) were used for this purpose. For middle ear pressure increasing from zero to a few centimeters of water, returning to zero again, larger time constants were found than for middle ear pressure decreasing from zero to minus a few centimeters of water and then returning to zero. The results could not be described with a linear model that assumes constant window membrane compliance and cochlear aqueduct flow resistance. It was found in the literature that the cochlear aqueduct has a function in equalizing inner ear pressure, despite the fact that the inner ear opening is filled with a meshwork of fibroblasts and loose connective tissue. It was also found that the round window membrane contributes most to the inner ear compliance and that

the internal orifice of the cochlear aqueduct is situated very close to the round window.
It can be concluded that the large difference in time constants for positive or negative middle ear pressure changes could be due to a dependence on aqueduct flow resistance or round window membrane position. It is possible that the aqueduct flow resistance depends on round window membrane position being higher when the membrane is moved towards the inner ear.

In order to derive the properties of the complicated shapes for inner ear pressure release curves, a consequence of the flow conducting properties of the aqueduct and of the compliance of the windows, representative results from two ears from the experiments in chapter 3 were selected for further analysis in chapter 4.
With a combination of results from studies by others and a theory given by us it was possible to estimate guinea pig round window membrane compliance (0.17 nl/Pa). It was found that the compliance only changes a few percent for the range of window pressure variation during an experiment. Inner ear fluid pressure was measured during 6.25 mHz square wave middle ear pressure manipulation, with a perforated tympanic membrane. After a negative-going middle ear pressure change the calculated flow resistance of the inner ear pressure release routes (mainly the cochlear aqueduct) was approximately constant, with a value of 12 Pa s/nl. After a positive-going middle ear pressure change it was found that the calculated flow resistance changes with round window position and with the pressure difference across the cochlear aqueduct. It reaches an average maximum value of 114 Pa s/nl.
It can be concluded that the change of flow resistance during inner ear pressure variation could be caused by a permeability change of the cochlear aqueduct entrance in scala tympani, caused by a change of structures filling the aqueduct. This study gives indications that aqueduct flow resistance does not depend on flow direction, in contrast with evidence from earlier studies.

In chapter 5 the resistance for fluid flow of the cochlear aqueduct was measured in guinea pigs for different positions of the round window membrane. These different positions were obtained by applying different constant pressures to the middle ear cavity. Fluid flow through the aqueduct was induced by small pressure steps (keeping inner ear ear volume almost constant) superimposed on these constant pressures. It was found that the inner ear equilibrium pressure depends on middle ear pressure and a model was given in which the cochlear aqueduct does not connect the inner ear with a cavity with constant pressure.
It can be concluded that the resistance for fluid flow through the aqueduct depends on round window position, but not on flow direction. The results can be explained by special fibrous structures that connect the round window with the entrance of the aqueduct.

In chapter 6 the influence of middle ear pressure on the transfer of periodic CSF pressure fluctuations to the inner ear is given. The CSF pressure of guinea pigs was modulated sinusoidally. Inner ear pressure changes were recorded while middle ear pressure was slowly changed. Frequency analysis of the inner ear pressure revealed two components: one at 0.33 Hz (caused by CSF pressure modulation) and one at 0.75 Hz (caused by artificial breathing). It was found that the amplitude of these components increased with decreasing middle ear pressure and decreased with increasing middle ear pressure. Although middle ear pressure was changed very slowly the inner ear pressure equilibrium value did not remain constant.
It can be concluded that middle ear pressure influences the flow resistance of the cochlear aqueduct by changing the position of the round window. How middle ear pressure also influences the inner ear pressure equilibrium value remains unclear and this finding is in contradiction with studies that inject fluid into the inner ear.

The efficacy of intermittent middle ear pressure for Menière's disease, delivered by the *Meniett*™, is evaluated in a prospective, randomized, double-blind, placebo-controlled clinical trial in chapter 7. A total of 57 patients with Menière's disease in one ear were included (confirmed by means of the Diagnostic Protocol Groningen) of which 28 patients were randomized for intermittent middle ear pressure and 29 for placebo therapy. Middle ear ventilation tubes were placed with no negative nor positive side effect. Hearing levels were evaluated with Von Bekesy audiometry at 500, 1000, 2000 and 4000 Hz and click evoked oto-acoustic emissions were measured. Patients were asked to grade hearing loss, vertigo, tinnitus and aural fullness using a standard visual analogue scale (VAS) and to register the number of Menière attacks during the four weeks of therapy. Evaluation of these parameters took place immediately after therapy once and after four weeks therapy three times daily. No significant difference was found between the therapy group and the control group in the change of hearing levels and VAS-scores. Neither a relevant change and/or difference was seen when a selection was made of patients who had a typical Menière attack within two weeks prior to the study (as an indication of disease activity) which is in contradiction with other studies. No difference was seen in the mean number of attacks during the four weeks of therapy between the therapy group and the placebo group. Only nine patients did have measurable click evoked oto-acoustic emissions which fits well to the individual degree of hearing loss and no significant change was found after intermittent middle ear pressure.
It can be concluded that intermittent middle ear pressure does not have a beneficial effect on hearing levels in Menière's disease and neither has a systemically beneficial effect on the feeling of hearing loss, vertigo, tinnitus and aural fullness. Intermittent middle ear pressure does not reduce the total number of Menière attacks.

Chapter 9

Samenvatting en conclusies

Inleiding

De ziekte van Menière is een invaliderende ziekte van het binnenoor, bestaande uit het gehoor- en evenwichtsorgaan. Deze ziekte wordt gekenmerkt door draaiduizeligheidsaanvallen, gehoorschade van het binnenoor (cochlea) en oorsuizen. Daarnaast gaat de ziekte vaak gepaard met een vol gevoel in het aangedane oor. Bij ongeveer 40% van de Menièrepatiënten komt de ziekte voor in beide oren. Het spontane beloop van de ziekte van Menière is niet eenduidig en voornamelijk de draaiduizeligheidsaanvallen verlopen grillig. In een klassiek geval neemt de tijd tussen de aanvallen in de loop van de tijd toe, zijn de draaiduizeligheidsaanvallen na ongeveer vijf tot tien jaar afwezig en houdt de patiënt ernstige, blijvende gehoorschade vaak in combinatie met hinderlijk oorsuizen. Tussen verschillende landen is er een groot verschil in het geschatte voorkomen van de ziekte en prevalentiecijfers variëren tussen 1-100 per 100.000. Meestal beginnen de eerste symptomen ergens tussen het 40-ste en 60-ste levensjaar. De ziekte komt iets vaker voor bij vrouwen dan bij mannen.
Hoewel de ziekte al meer dan 100 jaar geleden werd beschreven is er, ondanks wetenschappelijke inspanningen, nog steeds geen afdoende therapie voorhanden. Dit komt ondermeer doordat het onbekend is hoe de ziekte ontstaat. Uit postmortem studies is gebleken dat de ziekte van Menière gepaard gaat met een toename van het met endolymfe gevulde compartiment in het binnenoorcomplex (figuur 1).

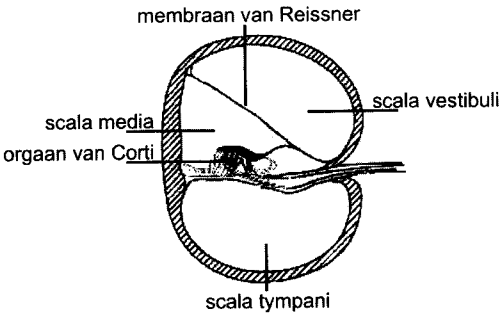

figuur 1. Dwardoorsnede door de cochlea. Scala vestibuli en scala tympani zijn gevuld met perilymfe. Scala media is gevuld met endolymfe. Bij endolymfatische hydrops rekt het membraan van Reissner uit ten koste van de perilymfatische ruimte.

Onduidelijk is hoe de zogenoemde endolymfatische hydrops ontstaat maar in cavia's kan dit worden opgewekt door de ductus en saccus endolymfaticus (figuur 2) te vernietigen. Vaak wordt gedacht dat endolymfatische hydrops synoniem is met een toegenomen druk in het endolymfatische compartiment ten opzichte van het perilymfatische compartiment hoewel dit met dierexperimentele drukmetingen niet kon worden aangetoond. Dat endolymfatische hydrops mogelijk een

bijkomend fenomeen is blijkt uit het gegeven dat een hydrops ook kan voorkomen bij personen die geen typische Menièresymptomen hebben gehad.

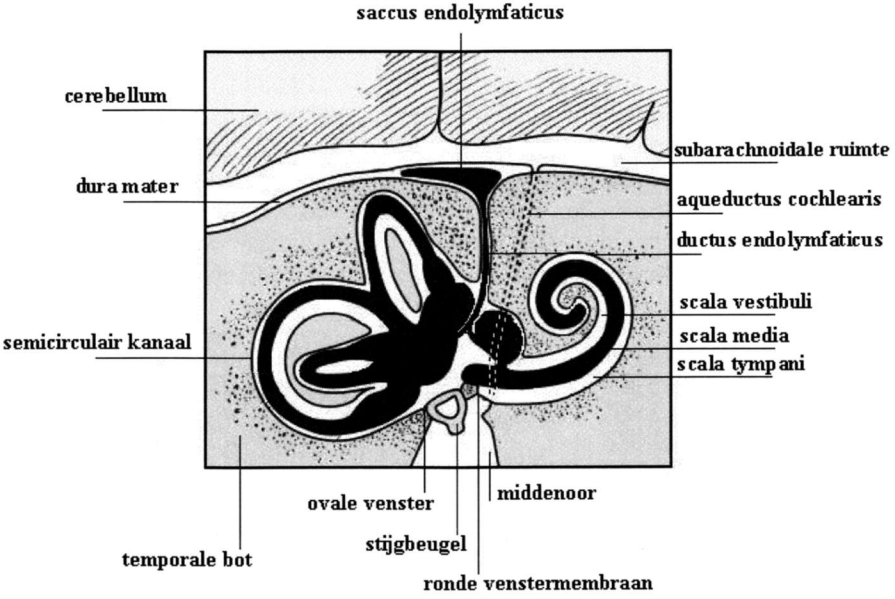

figuur 2. Schematische weergave van het binnenoorcomplex (labyrint) en de aangrenzend structuren. Het endolymfatische compartiment (zwart) wordt omgeven door perilymfe (wit). De aqueductus cochlearis (stippellijntjes) eindigt in de nabijheid van het ronde venstermembraan in het scala tympani.

Met de huidige medische techniek is het niet mogelijk endolymfatische hydrops tijdens het leven aan te tonen. Op de afdeling KNO-heelkunde van het Universitair Medisch Centrum Groningen wordt de diagnose ziekte van Menière gesteld of verworpen aan de hand van de zogenaamde "Definitie Menière Groningen". De vier criteria waaraan een patiënt met de ziekte van Menière moet voldoen zijn:

1) cochleair gehoorverlies (minstens bij één frequentie de gehoordrempel slechter dan 20 dB HL)
2) oorsuizen (nu of in het verleden)
3) duizeligheidsaanvallen (nu of in het verleden met een duur van 20 minuten of langer)
4) andere oorzaken uitgesloten door middel van het Diagnostisch Protocol Groningen.

De meeste therapievormen proberen aan te grijpen op een mogelijk toegenomen productie en/of afgenomen opname van endolymfe in het binnenoor, resulterend in een endolymfatische hydrops. Voorbeelden hiervan zijn: histaminergica, diuretica

("vochtafdrijvers"), zoutrestrictie, saccus endolymphaticuschirurgie en druktherapie. Vaak lijken deze therapievormen niet beter dan placebotherapie of rechtvaardigen de studies na grondige evaluatie geen eenduidige conclusies. Soms zijn de duizeligheidsklachten zo invaliderend en therapieresistent dat er wordt overgegaan tot het vernietigen (chemisch of chirurgisch) van het evenwichtsorgaan.
Na het aanbieden van multipele positieve drukpulsen aan het middenoor van Menièrepatiënten vonden Densert e.a. in 1997 normalisatie van objectieve electrofysiologische parameters van het binnenoor (met electrocochleografie). Deze interessante bevinding werd gedaan na uitgebreid klinisch en dierexperimenteel onderzoek. Dit leidde in 1999 tot de ontwikkeling van de *Meniett*™ (figuur 3) als druktherapie voor de ziekte van Menière.

figuur 3. De Meniett™ (Medtronic Xomed, Inc.; USA). Een flexibele slang, met hierop een passend oordopje, is verbonden met de drukgenerator.

Na het plaatsen van een trommelvliesbuisje kan de *Meniett*™, met behulp van een flexibele slang en een oordopje, op het oor worden aangesloten. Na het inschakelen genereert het apparaat enkele positieve drukpulsjes. Op deze manier neemt de middenoordruk van patiënten periodiek toe (voor een periode van 6 minuten). De in Zweden ontwikkelde handzame drukgenerator heeft als doel het terugdringen van een teveel aan binnenoorvocht bij Menièrepatiënten, maar de werking en het effect van de *Meniett*™ zijn onduidelijk. Gespeculeerd wordt over verschillende mechanismen die het binnenoor van Menièrepatiënten zouden kunnen beïnvloeden, zoals bijvoorbeeld het teweegbrengen van een stroom endolymfe uit het binnenoor of een verhoogde doorbloeding van binnenoorstructuren met als gevolg een verhoogde opname van endolymfe. Tot nu toe zijn er slechts enkele klinische studies gedaan naar het effect van de *Meniett*™, alle met een positief resultaat voor

zowel gehoorverlies als draaiduizeligheidsaanvallen. In hoofdstuk zeven wordt een door ons uitgevoerde klinische studie met Menièrepatiënten beschreven.
Een gedegen kennis van het hydrodynamische binnenoorsysteem kan helpen om de functionele eigenschappen van het binnenoor en de aangrenzende structuren beter te begrijpen. Het is bij mensen niet mogelijk om de vloeistofdruk van het binnenoorcomplex te meten zonder een aanzienlijke kans op blijvende schade. In het laboratorium van de afdeling KNO-heelkunde van het UMCG is het al meerdere jaren mogelijk de binnenoordruk en binnenoordrukveranderingen van cavia's meten. Bij deze meting wordt gebruik gemaakt van het *servo nulling* principe. Met deze methode is het mogelijk om met een micropipet drukken te meten in zeer kleine volumina zonder dat er een evidente verplaatsing van het vloeistofvolume plaatsvindt, met een minimale kans op schade aan vitale structuren en tevens met de mogelijkheid om elektrische potentialen te meten. Een schematische weergave van de basisproefopstelling voor de experimenten van dit proefschrift is te zien in figuur 4. Nadat het middenoor achter de oorschelp langs is geopend en er voorzichtig een gat in het trommelvlies is geprikt, wordt onder microscopisch zicht een puntig geslepen micropipet (met een puntdiameter van ongeveer 10 µm, gevuld met 2 M NaCl) door het ronde venstermembraan geprikt. De punt bevindt zich daarna in de met perilymfe gevulde scala tympani. Omdat gebleken is dat de perilymfatische druk gelijk is aan de endolymfatische druk is het niet noodzakelijk om verder te prikken naar de scala media.

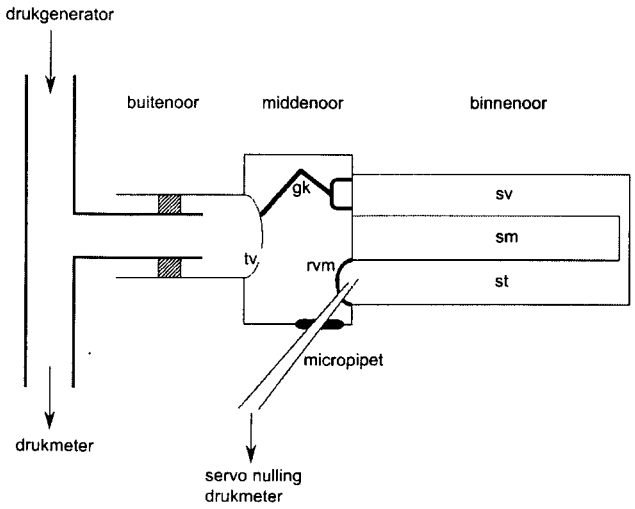

figuur 4. Schematische weergave van de proefopstelling. tv = geperforeerde trommelvlies; gk = gehoorbeenketen; rvm = ronde venstermembraan; sv = scala vestibuli (perilymfe); sm = scala media (endolymfe); st = scala tympani (perilymfe).

Hierna wordt het uitwendige defect (van het middenoor) rond de pipet gesloten met cement en kan de binnenoordruk worden gemeten. Elke drukverandering in de gehoorgang is zo een drukverandering van het middenoor. Het voordeel van het geperforeerde trommelvlies is dat dit niet meebeweegt met een drukverandering (evenals de gehoorbeenketen). Doel van de experimenten was om te meten en beschrijven hoe de binnenoordruk zou veranderen met het veranderen van de middenoordruk; de resultaten van deze experimenten zijn beschreven in de hoofdstukken 2 t/m 6 van dit proefschrift.

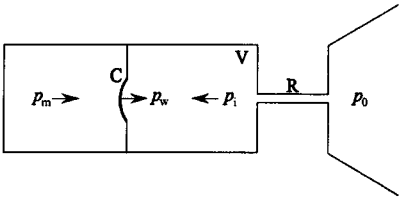

figuur 5. Een eenvoudig lineair model. p_m = middenoordruk; p_w = elastische kracht van ronde venstermembraan; p_i = binnenoordruk; p_0 = hersenvochtdruk; C = compliantie van membraan; V = volume van met vocht gevulde binnenoor; R= stromingsweerstand van aqueductus cochlearis. Aannames: het oor is volledig omgeven met bot; het middenoor wordt van het binnenoor gescheiden door een elastisch membraan met constante compliantie C; het binnenoor staat in open verbinding (aqueductus cochlearis) met de hersenvochtruimte via constante stromingsweerstand R; de hersenvochtruimte werkt als buffer voor drukveranderingen en heeft een constante druk p_0. In dat geval geldt: $p_m + p_w = p_i = p_0$. Bij een plotselinge, blijvende afname van de middenoordruk zal de binnenoordruk met dezelfde waarde afnemen. Doordat p_0 constant is wordt deze hoger dan p_i en dit leidt tot een vloeistofstroom door R richting het binnenoor. Deze volumetoename leidt tot het verder uitbollen van het venster C richting het middenoor. Dit leidt tot een toename van de elastische kracht van het membraan totdat weer geldt $p_m + p_w = p_i = p_0$ (waarbij p_i weer de uitgangswaarde heeft gekregen, p_m is afgenomen en p_w is toegenomen). Dit betekent dat bij een afname van de middenoordruk het ronde venstermembraan zal uitbollen richting het middenoor en dat het bij een toename zal uitbollen richting het binnenoor met in beide omstandigheden een gelijkblijvende binnenoordruk.

Hoe het binnenoorcomplex omgaat met drukveranderingen hangt voornamelijk af van de stijfheid van het systeem (is omgekeerd evenredig met de compliantie) en van de stromingsweerstand van de open verbindingen met aangrenzende ruimten. De compliantie van het systeem is de som van de elasticiteit van het ronde venstermembraan en het ovale venster, de elasticiteit van de bloedvaten en de elasticiteit van het weefsel rond de zenuwen. Uit studies is gebleken dat het ronde venstermembraan verreweg het meest bijdraagt aan de compliantie van het

binnenoorcomplex (oftewel dit is het minst stijf). In de in onze studie gepresenteerde modellen (figuur 5 en figuur 6) wordt er dan ook vanuit gegaan dat voornamelijk de stand van het ronde venstermembraan wordt beïnvloed met drukveranderingen. De oppervlakte van het ronde venstermembraan van een cavia bedraagt ongeveer 1,2 mm^2 en het membraan scheidt de scala tympani van het middenoor (zie figuur 2).

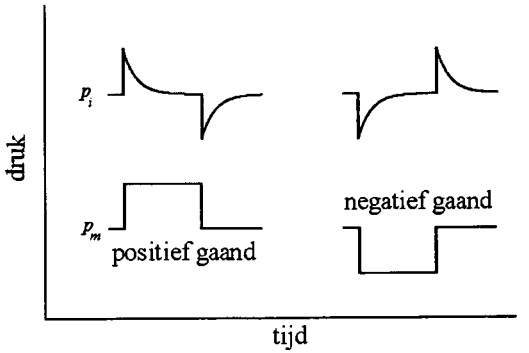

figuur 6. Voorspelde profiel van de binnenoordruk (p_i) geïnduceerd door rechthoekvormige veranderingen van de middenoordruk (p_m), bij een constante compliance C en stromingsweerstand R.

De aqueductus cochlearis is een min of meer open verbinding tussen de scala tympani (perilymfe) met de subarachnoidale ruimte (gevuld met hersenvocht). De aqueductus cochlearis heeft een kelkachtige vorm en de inwendige opening ligt dicht bij het ronde venstermembraan. De stromingsweerstand van de aqueductus cochlearis is vrij groot omdat het kanaal is gevuld met een zeer los netwerk van bindweefsel dat dichter wordt nabij de scala tympani. Het bindweefsel gaat bij de scala tympani over in het ronde venstermembraan. De lengte van de aqueductus in cavia's is ongeveer 2 mm met een kleinste diameter van ongeveer 0.14 mm. Het wordt algemeen aangenomen dat de aqueductus cochlearis een functie heeft in het constant houden van de binnenoordruk in zowel proefdieren als mensen. Met een toename van de binnenoordruk zal er perilymfe stromen in de richting van de subarachnoidale ruimte en andersom bij drukafname.

Samenvatting en conclusies

De door de *Meniett*™ veroorzaakte drukveranderingen in het binnenoor, na aanbieding van het signaal uit het apparaat aan het middenoor van cavia's, werd beschreven in hoofdstuk 2. De *Meniett*™ genereerde 3 periodes van 12 positieve drukpulsen. Een enkele drukpuls bestond uit de som van een statische positieve component en een oscillerende component met een frequentie van ongeveer 6 Hz.

Het opgewekte complexe druksignaal in het middenoor werd direct en bijna onveranderd doorgegeven aan het binnenoor van cavia's. Een onderdruk van gemiddeld 1,0 cm water (ten opzichte van de rustdruk van het binnenoor) werd gezien direct na de overdracht van een drukpuls, waarna de druk binnen enkele seconden weer toenam tot de rustdruk. Om de resultaten te verklaren werd een eenvoudig lineair model gepresenteerd. De drukverandering veroorzaakte een tijdelijke vloeistofstroom vanuit het binnenoor (volgens de geraadpleegde literatuur het meest waarschijnlijk door de aqueductus cochlearis). Aan de hand van het model leek het alsof er meer vloeistof het binnenoor uit werd geduwd tijdens een drukpuls dan dat er weer terugvloeide na een verandering van de middenoordruk. Echter, de rustdruk van het binnenoor veranderde niet na de aan het middenoor aangeboden drukpulsen en een netto volumeverplaatsing van binnenoorvloeistof werd daardoor onwaarschijnlijk geacht.
Concluderend kan worden gesteld dat het gepresenteerde model te eenvoudig is. Het model veronderstelt een constante compliantie van het binnenoor en een constante stromingsweerstand van de aqueductus cochlearis. De discrepantie kan worden opgelost als wordt verondersteld dat de stromingsweerstand van de aqueductus cochlearis afhangt van de stroomrichting, waarbij de weerstand hoger is als de vloeistof stroomt van het binnenoor naar de subarachnoidale ruimte.

In hoofdstuk 3 werd de vloeistofdruk van het binnenoor van cavia's beschreven tijdens een rechthoekvormige drukvariatie van het middenoor. Tijdconstantes, een product van de compliantie van het binnenoor en de stromingsweerstand van voornamelijk de aqueductus cochlearis, werden berekend aan de hand van de helling van de herstelcurves van de binnenoordruk na een drukverandering van het middenoor. Het bleek dat een enkelvoudige exponentiële functie de gemeten drukverandering niet goed beschreef en daarom werden voor dit doel meervoudige exponentiële functies gebruikt. Langere tijdconstantes werden gemeten wanneer de druk van het middenoor toenam van nul tot enkele centimeters, weer terugkerend naar nul, in vergelijking met een afname van de middenoordruk van nul naar minus enkele centimeters water, weer terugkerend naar nul. De resultaten konden niet worden beschreven met een lineair model dat een constante compliantie en een constante stromingsweerstand veronderstelt. Uit de literatuur werd gevonden dat de aqueductus cochlearis een functie heeft in het gelijk houden van de druk van het binnenoor. Dit ondanks dat de opening van de aqueductus aan de binnenoorzijde gevuld is met een netwerk van fibroblasten en los bindweefsel. Verder werd gevonden dat het ronde venstermembraan het meest bijdraagt aan de compliantie van het binnenoor en dat het venster zeer dicht bij de opening van de aqueductus cochlearis is gesitueerd.
Concluderend kan worden gesteld dat het grote verschil in tijdconstantes tussen positieve en negatieve veranderingen van de middenoordruk zou kunnen worden veroorzaakt door een afhankelijkheid van deze "constantes" van de

stromingsweerstand of de stand van het ronde venstermembraan. Het is mogelijk dat de stromingsweerstand van de aqueductus cochlearis afhangt van de stand van het ronde venstermembraan, die hoger is wanneer het venstermembraan zich heeft bewogen in de richting van het binnenoor.

In hoofdstuk 4 werden twee representatieve resultaten van experimenten in hoofdstuk 3 geanalyseerd om de eigenschappen van de complexe vormen van de herstelcurves van de binnenoorduk te verkrijgen. De herstelcurves zijn een resultaat van de stromingseigenschappen van de aqueductus cochlearis en de compliantie van de vensters. Op basis van een door ons geformuleerde hypothese in combinatie met de resultaten van studies uitgevoerd door anderen werd het mogelijk de compliantie van het ronde venstermembraan van de cavia te schatten (0,17 nl/Pa). Er werd geschat dat gedurende een experiment de compliantie slechts enkele procenten varieerde tijdens de gemeten verandering van de vensterdruk. De druk van de binnenoorvloeistof werd gemeten tijdens een 6,25 mHz rechthoekige drukverandering van het middenoor, met een geperforeerd trommelvlies. De berekende stromingsweerstand van de drukuitlaatroutes van het binnenoor (voornamelijk de aqueductus cochlearis), na een negatieve drukverandering van het middenoor, was ongeveer constant met een waarde van 12 Pa s/nl. Na een positieve drukverandering van het middenoor bleek de berekende stromingsweerstand van de drukuitlaatroutes van het binnenoor te veranderen met de stand van het ronde venstermembraan en met het drukverschil over de aqueductus cochlearis. De weerstand bereikte een gemiddelde maximumwaarde van 114 Pa s/nl.
Concluderend kan worden gesteld dat de verandering van de stromingsweerstand tijdens een verandering van de binnenoordruk zou kunnen worden veroorzaakt door een verandering in permeabiliteit van de opening van de aqueductus cochlearis in scala tympani als resultaat van een veranderde structuur van het weefsel in de aqueductus. Deze studie geeft aanwijzingen dat de stromingsweerstand van de aqueductus cochlearis niet afhangt van de stroomrichting, dit in tegenstelling tot de veronderstelling op grond van eerdere studies.

In hoofdstuk 5 werd de stromingsweerstand van de aqueductus cochlearis in cavia's gemeten bij verschillende standen van het ronde venstermembraan. De verschillende standen werden verkregen door verschillende constante drukken aan het middenoor aan te bieden. Bovenop de al aanwezige constante druk werden kleine drukstapjes aangeboden (de druk in het binnenoor dus bijna constant houdend), en zo werd een vloeistofstroom door de aqueductus cochlearis geïnduceerd. Een nevenuitkomst van de metingen was dat de evenwichtsdruk in het binnenoor afhing van de middenoordruk en een model werd geïntroduceerd waarbij de aqueductus cochlearis niet in verbinding stond met een ruimte met een constante druk.

Concluderend kan worden gesteld dat de stromingsweerstand door de aqueductus cochlearis primair afhangt van de stand van het ronde venstermembraan maar niet van de stromingsrichting. De resultaten kunnen worden verklaard door speciale fibreuze structuren die het ronde venstermembraan verbinden met de ingang van de aqueductus.

In hoofdstuk 6 werd de invloed van de druk van het middenoor op het doorgeven van periodieke variaties van de druk van het hersenvocht aan het binnenoor bestudeerd. De druk van het hersenvocht werd sinusvormig gemoduleerd. Bovendien werd de middenoordruk zeer langzaam gevarieerd en werd de binnenoordruk gemeten. Frequentieanalyse van de binnenoordruk liet twee componenten zien: een bij 0,33 Hz (veroorzaakt door de modulatie van druk van het hersenvocht) en een bij 0,75 Hz (veroorzaakt door de kunstmatige beademing). Het bleek dat de amplitude van deze twee componenten toenam met een afname van de middenoordruk en afnam met een toename van de middenoordruk. Ook werd gevonden dat de evenwichtsdruk van het binnenoor niet constant bleef ondanks een zeer langzaam veranderende middenoordruk.
Concluderend kan worden gesteld dat de stromingsweerstand van de aqueductus cochlearis afhangt van de middenoordruk doordat deze de stand van het ronde venstermembraan beïnvloedt. Hoe de middenoordruk ook de evenwichtsdruk van het binnenoor kan beïnvloeden blijft onduidelijk. Deze bevinding is niet in overeenstemming met de resultaten van studies waarbij vloeistof in het binnenoor wordt geïnjecteerd.

In hoofdstuk 7 werd de werking van intermitterende drukveranderingen van het middenoor bij Menièrepatiënten, gegenereerd door de *Meniett*™, geëvalueerd in een prospectieve, gerandomiseerde, dubbelblinde, placebo-gecontroleerde klinische studie. In totaal 57 patiënten met de ziekte van Menière in één oor werden geïncludeerd (bevestigd aan de hand van het Diagnostische Protocol Groningen), waarvan 28 patiënten werden gerandomiseerd voor intermitterende middenoordruk en 29 voor placebotherapie. Patiënten kregen een trommelvliesbuisje zonder positieve of negatieve bijeffecten. Gehoordrempels werden bepaald met Von Bekesy audiometrie voor de frequenties 500, 1000, 2000 en 4000 Hz en tevens werden door clicks opgewekte oto-acoustische emissies gemeten. De ernst van de subjectieve parameters gehoorverlies, duizeligheid, oorsuizen en een vol gevoel in het oor werd bepaald met behulp van een visuele analoge schaal (VAS). Gevraagd werd om het aantal typische aanvallen te registreren tijdens de vier weken therapie. Evaluatie van de parameters vond plaats direct na één keer therapie en na gebruik drie maal daags van de *Meniett*™ voor een periode van vier weken. Geen significante verschillen werden gevonden tussen de therapiegroep en de placebogroep voor wat betreft de verandering in gehoordrempels en subjectieve klachten (VAS). Ook wanneer een selectie werd gemaakt van patiënten die binnen

twee maanden voorafgaand aan de studie een typische Menièreaanval hadden gehad (als een indicatie voor ziekteactiviteit) werd geen verschil gezien tussen de twee groepen, dit in tegenstelling tot de resultaten van andere studies. Tijdens de therapieperiode werd tussen de twee groepen geen verschil waargenomen in het aantal Menièreaanvallen. Slechts negen patiënten hadden meetbare oto-acoustische emissies (wat goed past bij de individuele ernst van het gehoorverlies) en geen significante veranderingen werden waargenomen na positieve intermitterende middenoordruk.

Concluderend kan worden gesteld dat positieve intermitterende middenoordruk, gegenereerd door de *Meniett*™, binnen de onderzochte patiëntenpopulatie geen positief effect heeft op de gehoordrempels van Menièrepatiënten en ook geen systematisch positief effect heeft op het gevoel van gehoorverlies, duizeligheid, oorsuizen en volheid in het oor. Intermitterende middenoordruk reduceert het totale aantal typische Menière-aanvallen niet.

Dankwoord
Dit voor mij belangrijke project was niet mogelijk geweest zonder hulp.
Enkele personen ben ik speciale dank verschuldigd.
Professor Albers, niet snel zal ik vergeten hoe enthousiast ik altijd was, of weer werd, na een wetenschapsbespreking met u. Hierdoor ben ik nooit gaan twijfelen aan een goede afloop. Ik wil u bedanken voor het gestelde vertrouwen en voor uw nimmer aflatende begeleiding.
Professor Wit, beste Hero, altijd weer was jij beschikbaar voor uitleg als de materie te ingewikkeld dreigde te worden. Jij gaf richting en inhoud aan de experimenten en je deed dit op een voor mij heldere manier. Samenwerken met jou heb ik als bijzonder prettig ervaren.
H. Segenhout, beste Hans, jij was van onschatbare waarde voor de uitvoering van de minutieuze experimenten. Niet snel zal ik de uren vergeten die we samen doorbrachten in het laboratorium. Deze uren zijn door je kundigheid en humor nooit gaan vervelen.
Beoordelingscommissie, hartelijk dank voor uw tijd en moeite.
Paranimfen, Albert en Emile, dank voor jullie vriendschap en ondersteuning.
Mijn ouders, lieve papa en mama, als jullie zeggen trots op mij te zijn dan gloei ik van binnen.
Sjouke en Hilly, bedankt dat jullie altijd voor ons klaar staan.
Lieve Esther, zonder jou had ik me niet kunnen ontwikkelen tot wat ik nu ben. Erg blij en zielsgelukkig ben ik dat ik dit alles met jou mag meemaken ♥.
Casper, grote vriend, samen met jou wil ik de wereld ontdekken.
Esther en Casper, jullie zijn mijn alles!

Curriculum vitae

Robert Feijen werd op 2 oktober van het jaar 1971 geboren te Coevorden. Na de lagere school ging hij naar de CSG Jan van Arkel in Hardenberg waar hij in 1990 zijn VWO-examen behaalde. Hierna werd hij twee keer uitgeloot voor de studie Geneeskunde. In die twee jaar heeft hij een jaar Rechten gestudeerd aan de RU te Utrecht en heeft hij een jaar zijn land gediend als dienstplichtig huzaar met als standplaats Het Harde. In 1992 startte hij met de studie Geneeskunde aan de RU Groningen. Na in 1996 zijn doctoraalfase te hebben beëindigd liep hij zijn co-assistentschap te Zwolle. In 1999 behaalde hij zijn artsexamen. Al tijdens de studie Geneeskunde werd zijn aandacht getrokken naar de KNO-heelkunde en in 1999 startte hij in Groningen met promotieonderzoek op deze afdeling. In 2001 begon hij met de klinische opleiding tot KNO-arts in het Universitair Medisch Centrum Groningen. Op de middelbare school ontmoette hij Esther, zijn huidige echtgenote. In 2002 kregen zij samen een zoon, Casper.

Bibliography

Allen GW. Fluid flow in the cochlear aqueduct and cochleahydrodynamic considerations in perilymph fistula, stapes gusher, and secondary endolymphatic hydrops. Am J Otol 1987; 8:319-322.

Andrews JC, Böhmer A, Hoffman LF. The measurement and manipulation of intralabyrinthine pressure in experimental endolymphatic hydrops. Laryngoscope 1991; 101:661-668.

Beentjes BI. The cochlear aqueduct and the pressure of cerebrospinal and endolabyrinthine fluids. Acta Otolaryngol (Stockh) 1972; 73:112-120.

Bergmann K, Haupt H, Scheibe F, Rogge I. Blockage of cochlear aqueduct for examination of perilymph (guinea pig) Arch Otolaryngol 1979; 224:257-265.

Carlborg B, Densert B, Densert O. Functional patency of the cochlear aqueduct. Ann Otol Rhinol Laryngol 1982; 91:209-215.

Carlborg BI, Farmer-JC J. Transmission of cerebrospinal fluid pressure via the cochlear aqueduct and endolymphatic sac. Am J Otolaryngol 1983; 4:273-282.

Claes J, Van-de-Heyning PH. Medical treatment of Menière's disease: a review of literature. Acta Otolaryngol (Stockh) 1997; Suppl 526:37-42.

Committee on Hearing and Equilibrium guidelines for the diagnosis and evaluation of therapy in Menière's disease. American Academy of Otolaryngology-Head and Neck Foundation, Inc [see comments]. Otolaryngol Head.Neck Surg 1995; 113:181-185.

Décory L, Franke RB, Dancer AL. Measurement of the middle ear transfer function in cat, chinchilla and guinea pig. In: Dallos P, Geisler CD, Matthews JW, Ruggero MA, Steele CR (Eds.) The Mechanics and Biophysics of Hearing. Springer, Berlin 1990; pp. 270-277.

Deelen van GW, Huizing EH. Use of a diuretic (Dyazide) in the treatment of Menière's disease. A double-blind cross-over placebo-controlled study. ORL J Otorhinolaryngol Relat Spec 1986; 48:287-292.

Deelen van GW, Hulk J, Huizing EH. The use of the underpressure chamber in the treatment of patients with Menière's disease. J Laryngol Otol 1987; 101:229-235.

Densert B, Densert O, Arlinger S, Sass K, Ödkvist L. Immediate effects of middle ear pressure changes on the elctrocochleographic recordings in patients with Menière's disease: a clinical placebo-controlled study. Am J Otol 1997; 18:726-733.

Densert B, Densert O, Erlandsson B, Sheppard H. Transmission of complex pressure waves through the perilymphatic fluid in cats. Acta Otolaryngol (Stockh) 1986; 102:403-409.

Densert B, Densert O, Erlandsson B, Sheppard H. Transmission of square wave pressure pulses through the perilymphatic fluid in cats. Acta Otolaryngol (Stockh) 1986; 102:186-193.

Densert B, Sass K, Arlinger S. Short term effects of induced middle ear pressure changes on the electrocochleogram in Menière's disease. Acta Otolaryngol (Stockh) 1995; 115:732-737.

Densert O, Carlborg B, Stagg J. Pressure-regulating mechanisms in the inner ear. ORL J Otorhinolaryngol Relat Spec 1979; 40:319-324.

Densert O, Carlborg B, Stagg J. Transmission of low frequency pressure steps to the perilymphatic fluid. Acta Otolaryngol (Stockh) 1981; 91:55-64.

Densert O, Ingelstedt S, Ivarsson A, Pedersen K. Immediate restoration of basal sensorineural hearing (Mb Menière) using a pressure chamber. Acta Otolaryngol (Stockh) 1975; 80:93-100.

Duckert L. The morphology of the cochlear aqueduct and periotic duct of the guinea pig - a light and electron microscopic study. Trans Am Acad Ophtalmol Otolaryngol 1974; 78: ORL, 21-48.

Dunnebier EA, Segenhout JM, Wit HP, Albers FWJ. Two-phase endolymphatic hydrops: a new dynamic guinea pig model. Acta Otolaryngol (Stockh) 1997; 117:13-19

Feijen RA, Segenhout JM, Albers FW, Wit HP. Cochlear aqueduct flow resistance depends on round window membrane position in guinea pigs. J Assoc Res Otolaryngol 2004; 5:404-410.

Feijen RA, Segenhout JM, Albers FWJ, Wit HP. Change of guinea pig inner ear pressure by square wave middle ear cavity pressure variation. Acta Otolaryngol (Stockh) 2002; 122:138-145.

Feijen RA, Segenhout JM, Wit HP, Albers FWJ. Monitoring inner ear pressure changes in normal guinea pigs induced by the Meniett20. Acta Otolaryngol (Stockh) 2000; 120:804-809.

Fernández C. Dimensions of the cochlea (guinea pig) J Acoust Soc Am 1952; 24:519-523.

Friberg U, Stahle J, Svedberg A. The natural course of Menière's disease. Acta Otolaryngol (Stockh) 1984; Suppl 406:72-77.

Galic M, Giebel W. Scanning electron microscopy studies of the structure of tissue in the cochlear opening of the cochlear aqueduct. Laryngol Rhinol Otol Stuttg 1987; 66:1-5.

Gates GA, Green JD Jr, Tucci DL, Telian SA. The effects of transtympanic micropressure treatment in people with unilateral Menière's disease. Arch Otolaryngol Head Neck Surg 2004; 130:718-25.

Ghiz AF, Salt AN, DeMott JE, Henson MM, Henson OW, Gewalt SL. Quantitative anatomy of the round window and cochlear aqueduct in guinea pigs. Hear Res 2001; 162:105-112.

Gibson WP, Arenberg IK. Pathophysiologic theories in the etiology of Menière's disease. Otolaryngol Clin N Am 1997; 30:961-967.

Gopen Q, Rosowski JJ, Merchant SN. Anatomy of the normal human cochlear aqueduct with functional implications. Hear Res 1997; 107:9-22.

Gyo K, Nishihara S, Yanagihara N. Pressure transmission properties from the external ear canal to the inner ear. An experimental study using guinea pigs. Acta Otolaryngol (Stockh) 1988; Suppl 456:87-91.

Hallpike CS, Cairns H. Observations on the pathology of Menière's syndrom. J Laryngol Otol 1938; 53:625-655.

Huang TS. Three new surgeries for treatment of intractable Menière's disease. Am J Otol 1999; 20:233-237.

Ingelstedt S, Ivarsson A, Tjernstrom O. Immediate relief of symptoms during acute attacks of Menière's disease, using a pressure chamber. Acta Otolaryngol (Stockh) 1976; 82:368-78.

Ivarsson A, Pedersen K. Volume-pressure properties of round and oval windows. A quantitative study on human temporal bone. Acta Otolaryngol (Stockh) 1977; 84:38-43.

Kimura RS, Schuknecht HF. Membranous hydrops in the inner ear of the guinea pig after obliteration of the endolymphatic sac. Pract Otolaryngol 1965; 27:343-354

Konradsson KS, Carlborg B, Grenner J, Tjernstrom O. Electrocochleographic and audiometric evaluation of hypobaric effect in Menière's disease. Laryngoscope 1999; 109:59-64.

Krukowski B, Carlborg B, Densert O. Nonlinear aspects of infrasonic pressure transfer into the perilymph. Hear Res 1980; 2:207-212.

Larsen HC, Angelborg C, Klockhoff I, Stahle J. Hearing in patients with Menière's disease after exposure to low ambient pressure and after ingestion of glycerol and urea. Adv Otorhinolaryngol 1988; 42:144-147.

Lutman ME. Reliable identification of click-evoked otoacoustic emissions using signal-processing techniques. Br J Audiol 1993; 27:103-8.

Maier W, Ross U, Fradis M, Richter B. Middle ear pressure and dysfunction of the labyrinth: is there a relationship? Ann Otol Rhinol Laryngol 1997; 106:478-82.

Mateijsen DJ, Van Hengel PW, Krikke AP, Van Huffelen WM, Wit HP, Albers FW. Three-dimensional Fourier transformation constructive interference in steady state magnetic resonance imaging of the inner ear in patients with unilateral and bilateral Menière's disease. Otol Neurotol 2002; 23:208-13.

Menière P. Memoire sur des lésions de l'oreille interne donnant lieu à des symptômes de congestion cérébrale apoplectiforme. (A report on lesions of the inner ear giving rise to symptoms of cerebral congestion of apoplectic type.) Gazette Medicale de Paris 1861; 16:597-601.

Merchant SN, Adams JC, Nadol JB Jr. Pathophysiology of Menière's syndrome: Are symptoms caused by endolymphatic hydrops? Otol Neurotol 2005; 26:74-81.

Merchant SN, Rauch SD, Nadol JB Jr. Menière's disease. Eur Arch Otorhinolaryngol 1995; 252:63-75.

Minor LB, Schessel DA, Carey JP. Menière's disease. Curr Opin Neurol 2004; 17:9-16.

Moffat DA. Endolymphatic mastoid shunt surgery in unilateral Menière's disease. Ear Nose Throat J 1997; 76:642-8,650.

Montandon P, Guillemin P, Hausler R. Prevention of vertigo in Menière's syndrome by means of transtympanic ventilation tubes. ORL J Otorhinolaryngol Relat Spec 1988; 50:377-81.

Nishihara S, Gyo K, Yanagihara N. Transmission of change in the atmospheric pressure of the external ear to the perilymph. Am J Otol 1992; 13:364-368.

Nishimura S, Yanagita N, Inafuku S, et al. A scanning electron microscopic study of the guinea pig cochlear aqueduct with emphasis on fracture preparation. ORL J Otorhinolaryngol Relat Spec 1981; 43:79-88.

Ödkvist LM, Arlinger S, Billermark E, Densert B, Lindholm S, Wallqvist J. Effects of middle ear pressure changes on clinical symptoms in patients with Menière's disease - a clinical multicentre placebo-controlled study. Acta Otolaryngol (Stockh) 2000; Suppl 543:99-101.

Okuno T, Sando I. Localization, frequency, and severity of endolymphatic hydrops and the pathology of the labyrinthine membrane in Menière's disease. Ann OtolRhinolLaryngol 1987; 96:438-445.

Oosterveld WJ. [Menière's disease: a study of 457 patients]. Ned Tijdschr Geneeskd 1981; 125:582-585.

Paparella MM. Pathogenesis and pathophysiology of Menière's disease. Acta Otolaryngol (Stockh) 1991; Suppl 485:26-35.

Probst R, Lonsbury-Martin BL, Martin GK. A review of otoacoustic emissions. J Acoust Soc Am 1991; 89:2027-67.

Rapport PN, Lim DJ, Weiss HS. Surface-active agent in Eustachian tube function. Arch Otolaryngol 1975; 101:305-311.

Rauch SD, Merchant SN, Thedinger BA. Menière's syndrome and endolymphatic hydrops. Double-blind temporal bone study. Ann Otol Rhinol Laryngol 1989; 98:873-883.

Ruckenstein MJ, Rutka JA, Hawke M. The treatment of Menière's disease: Torok revisited. Laryngoscope 1991; 101:211-218

Salt AN, DeMott JE. Longitudinal endolymph movements induced by perilymphatic injections. Hear Res 1998; 123:137-147.

Sperling NM, Paparella MM, Yoon TH, Zelterman D. Symptomatic versus asymptomatic endolymphatic hydrops: a histopathologic comparison. Laryngoscope 1993; 103:277-285.

Suzuki M, Kitahara M, Kitano H. The influence of middle ear pressure changes on the primary vestibular neurons in guinea pigs. Acta Otolaryngol (Stockh) 1994a; Suppl 510:9-15.

Suzuki M, Kitahara M, Kitano H. The influence of vestibular and cochlear aqueducts on vestibular response to middle ear pressure changes in guinea pigs. Acta Otolaryngol (Stockh) 1994b; Suppl 510:16-19.

Suzuki M, Kitano H, Yazawa Y, Kitajima K. Involvement of round and oval windows in the vestibular response to pressure changes in the middle ear of guinea pigs. Acta Otolaryngol (Stockh) 1998; 118:712-716.

Svane-Knudsen V. Resorption of the cerebrospinal fluid in guinea pig. Acta Otolaryngol (Stockh) 1958; 49:240-251.

Takeuchi S, Takeda T, Saito H. Pressure relation between perilymph and endolymph associated with endolymphatic infusion. Ann Otol Rhinol Laryngol 1991; 100:244-248.

Takeuchi S, Takeda T, Saito H. Pressure relationship between perilymph and endolymph associated with endolymphatic infusion. Ann Otol Rhinol Laryngol 1991; 100:244-248.

Thalen E, Wit H, Segenhout H, Albers F. Inner ear pressure changes following square wave intracranial or ear canal pressure manipulation in the same guinea pig. Eur Arch Otorhinolaryngol 2002; 259:174-179.

Thalen EO, Wit HP, Segenhout JM, Albers FWJ. Direct measurement of the flow resistance of the cochlear aqueduct in the guinea pig. Acta Otolaryngol (Stockh) 2004; 124:1-5.

Thalen EO, Wit HP, Segenhout JM, Albers FWJ. Dynamics of inner ear pressure change caused by intracranial pressure manipulation in the guinea pig. Acta Otolaryngol (Stockh) 2001; 121:470-476.

Tjernstrom O, Casselbrant M, Harris S, Ivarsson. A. Current status of pressure chamber treatment. Otolaryngol Clin North Am 1980; 13:723-729.

Tomsen J, Sass K, Ödkvist L, Arlinger S. Local overpressure treatment reduces vestibular symptoms in patients with Menière's disease: a clinical, randomized, multicenter, double-blind, placebo-controlled study. Oltol Neurotol 2005; 26:68-73.

Toriya R, Arima T, Kuraoka A, Uemura T. Ultrastructure of the guinea pig cochlear aqueduct. Acta Otolaryngol (Stockh) 1991a; 111:699-706.

Toriya R, Arima T, Kuraoka A, Uemura T. Computeraided three-dimensional reconstruction of guinea pig cochlear aqueduct. Acta Otolaryngol (Stockh) 1991b; 111:917-920.

Waltner JG. Barrier membrane of the cochlear aqueduct. Histologic studies on the patency of the cochlear aqueduct. Acta Otolaryngol (Stockh) 1947; 47:656-669.

Warmerdam TJ, Schröder FH, Wit HP, Albers FW. Perilymphatic and endolymphatic pressure in the normal guinea pig. ORL J Otorhinolaryngol Relat Spec 1999; 61:71-73.

Wiederhielm CA, Woodburry JW, Kirk S, Rushmer RF. Pulsatile pressures in the microcirculation of frog's mesentery. Am J Physiol 1964; 207:173-176.

Wit HP, Feijen RA, Albers FW. Cochlear aqueduct flow resistance is not constant during evoked inner ear pressure change in the guinea pig. Hear Res 2003; 175:190-9.

Wit HP, Thalen EO, Albers FWJ. Dynamics of inner ear pressure release, measured with a double-barreled micropipette in the guinea pig. Hear Res 1999; 132:131-139.

Wit HP, Warmerdam TJ, Albers FWJ. Measurement of the mechanical compliance of the endolymphatic compartments in the guinea pig. Hear Res 2000; 145:82-90.

Younger R, Longridge NS, Mekjavic I. Effect of reduced atmospheric pressure on patients with fluctuating hearing loss due to Menière's disease. J Otolaryngol 1984; 13:76-82.